INTRODUCTION TO BIOPHOTONICS

Csilla GERGELY

Bionanophotonics
Laboratoire Charles Coulomb
UMR 5221 CNRS - Université Montpellier 2

OUTLINE

1
- Biophotonics – definition
- Interaction of light with biological material
- Natural photonic materials

2
- Lasers in health care
- Bioimaging: functional and spectroscopic microscopy

3
- Light for biosensing
- Towards hybrid photonic devices

Biophotonics – definition

Photonics for Life Science and Health → Biophotonics

« the study of the interaction of light with biological material »

"light" includes all forms of radiant energy whose quantum unit is the photon

Biophotonics utilizes light-based technologies to solve problems in medecine and the life sciences

- **Light measures contact-free**
- **Light measures fast**
- **Light measures precisely**

photon energies « matches » molecular energy levels
wavelengths "measure" cell, tissue micro-structures

→ Photonic tools are capable to manipulate molecules and living cells

Biophotonics investigates, gathers and enables (1):

- Photo-physics; Photochemistry; Photo-biology
- Photosynthesis in plants and bacteriae
- The vision, our eyes
- Therapy (photodynamic, photothermal, photomechanical ablation)
- Natural photonic crystals (feathers, eyes, optically active biomolecules)

Biophotonics investigates, gathers and enables (2):

- Lasers for medecine
- Non-invasive medical imaging modalities assuring good contrasts for imaging:
    - a great variety of colors (λ-dependent absorption contrast)
    - other contrast mechanisms (fluorescence, Raman, polarization, phase)
    - high spatial and color resolution, wide dynamic range
    - eliminating light scattering in mammalian tissues via optical solutions (confocal, 2-photon, OCT, polarization)
- Biosensing via plasmonics, photonic resonance, evanescent waves, bioluminescence

Interaction of light with biological material

Light (laser) tissue interaction

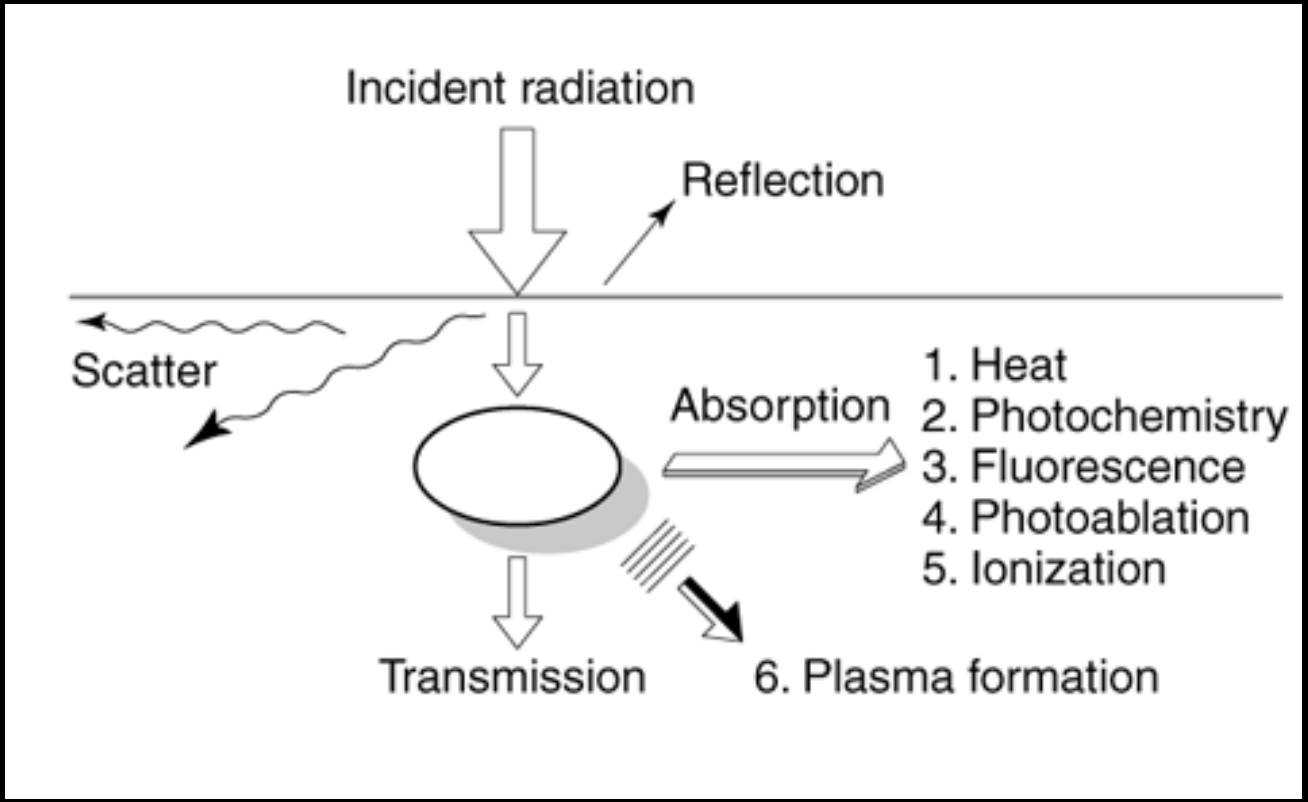

- The tissue molecules that absorb light = " pigments" : hemoglobin , water, melanin
- Light causes molecular vibration, which in turn produces heat
- Photochemistry: the presence of these photosensitizers in certain cells makes the cells vulnerable to light of an appropriate wavelength and intensity
- Photon energy might be dissipated as the re-emission of light within 10^{-6} seconds after absorption → fluorescence.
- Photoablation: the tissue absorbs the high energy ultraviolet photons that are produced by an excimer laser

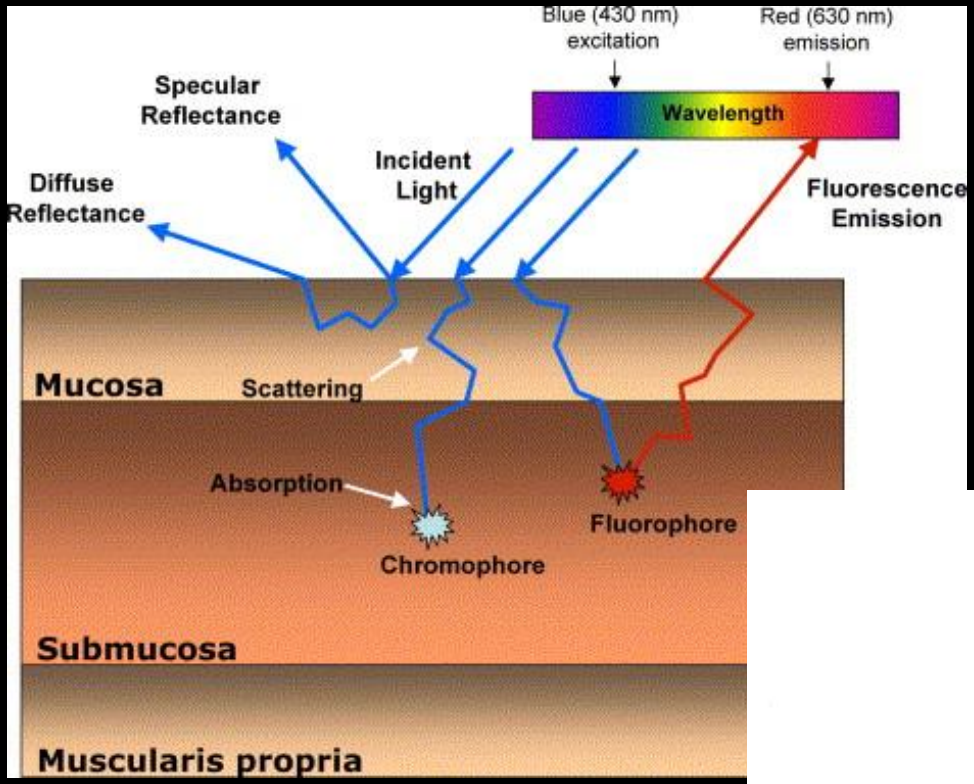

Light path in tissue is very complex

R. DaCosta et al. Best Practice & Research Clinical Gastroenterology, 2006

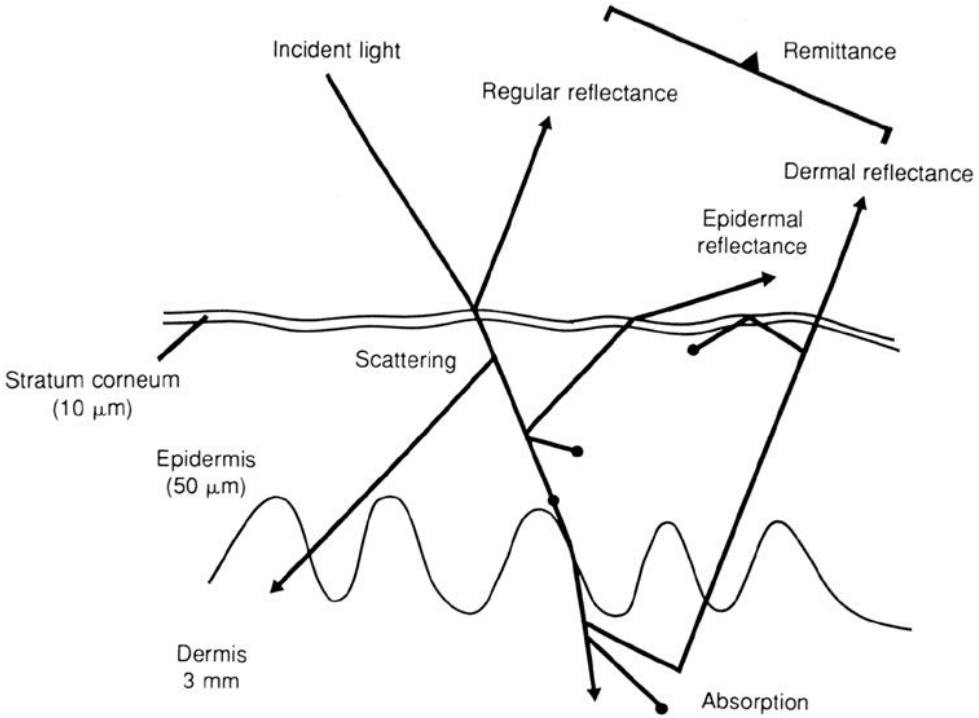

FIGURE 13.1 Schematic representation of optical pathways in human skin. Adapted from Kochevar *et al.* (1993) in "Dermatology in General Medicine" (T. B. Fitzpatrick *et al.*, eds.). With permission of McGraw-Hill, New York.

Absorption spectra of tissue chromophores

(water, oxy- and deoxyhemoglobin and melanin)

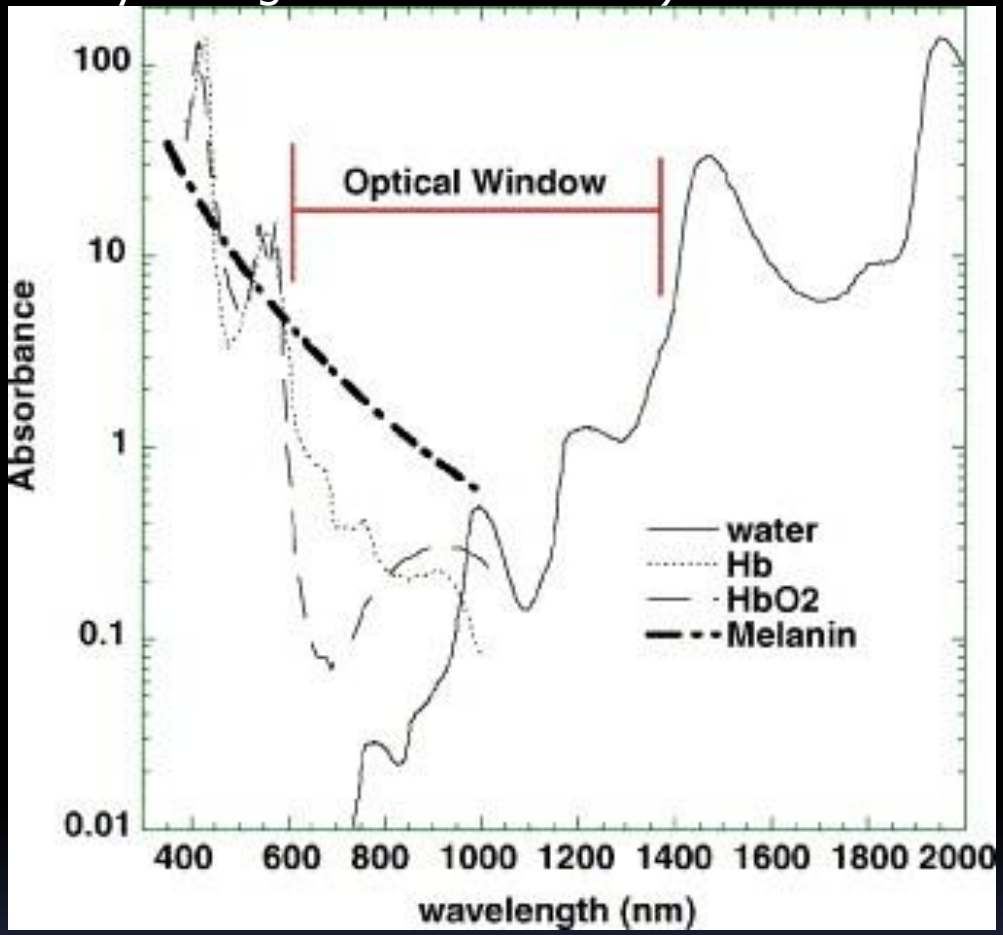

Hemoglobin has a very high absorption in the violet and blue/green

→ use of argon laser, which emits blue/green light for treating hemoglobin containing lesions

Water is absorbed maximally in the far infrared (IR) regions of the spectrum.

→ Use of CO_2 laser that removes cell layer by cell layer by volatilizing the water

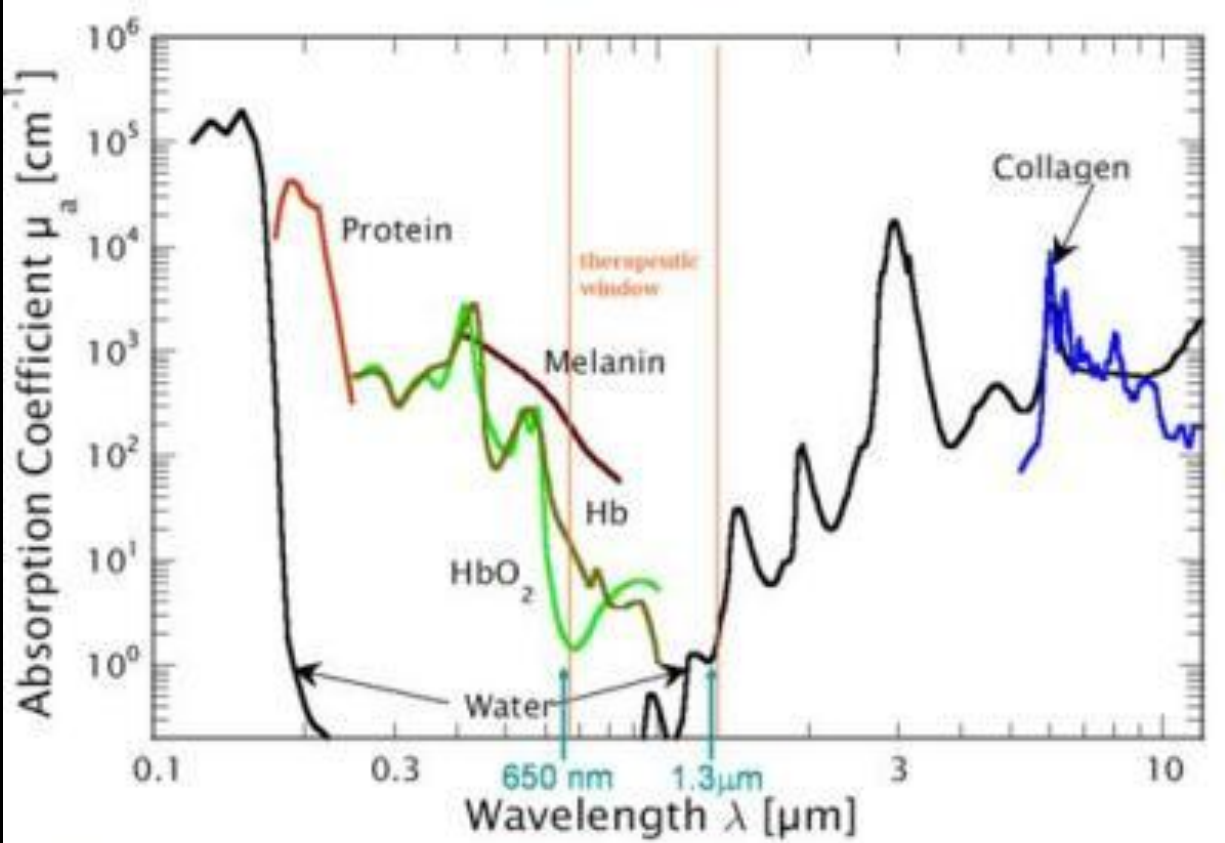

Figure 1. Optical absorption spectra of various tissue components in the ultraviolet to infrared frequency range.

Optical absorption window: tissue has minimum absorption in the NIR range from 650nm-1300nm → most optical imaging applications are centered in this window. Non-linear imaging window in IR…

http://www.chem.duke.edu/~wwarren/tissueimaging.php

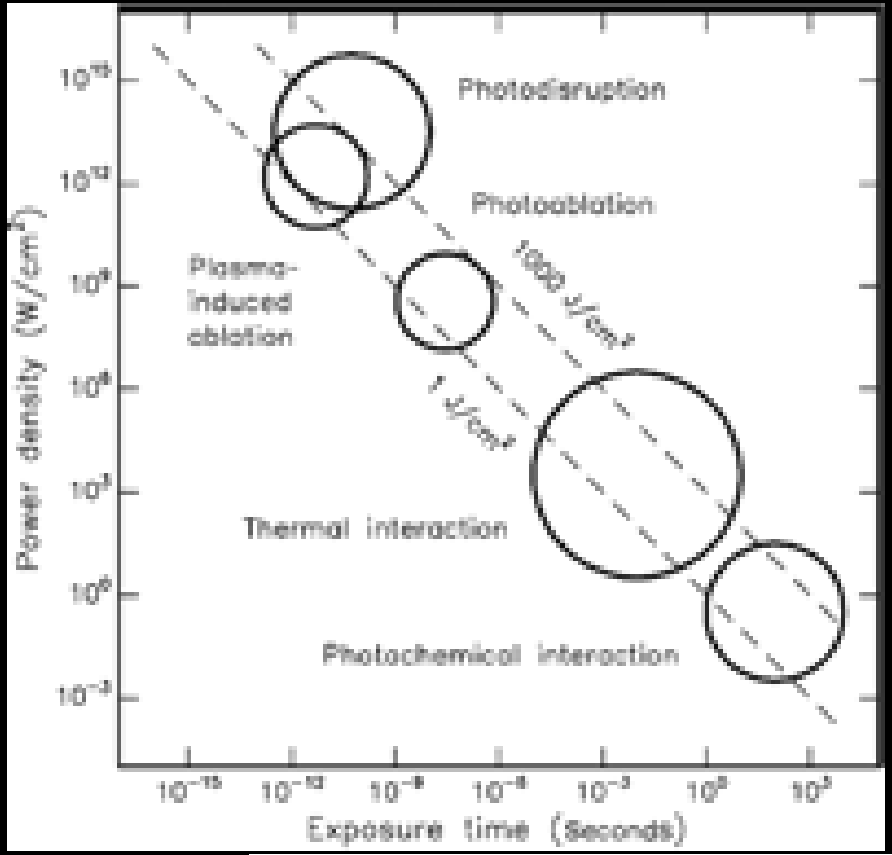

Laser action: combination of color, power and exposure time

Each type of tissue has its specific absorption characteristics depending on its specific components

E. D. Felice, Phlebology, 2010

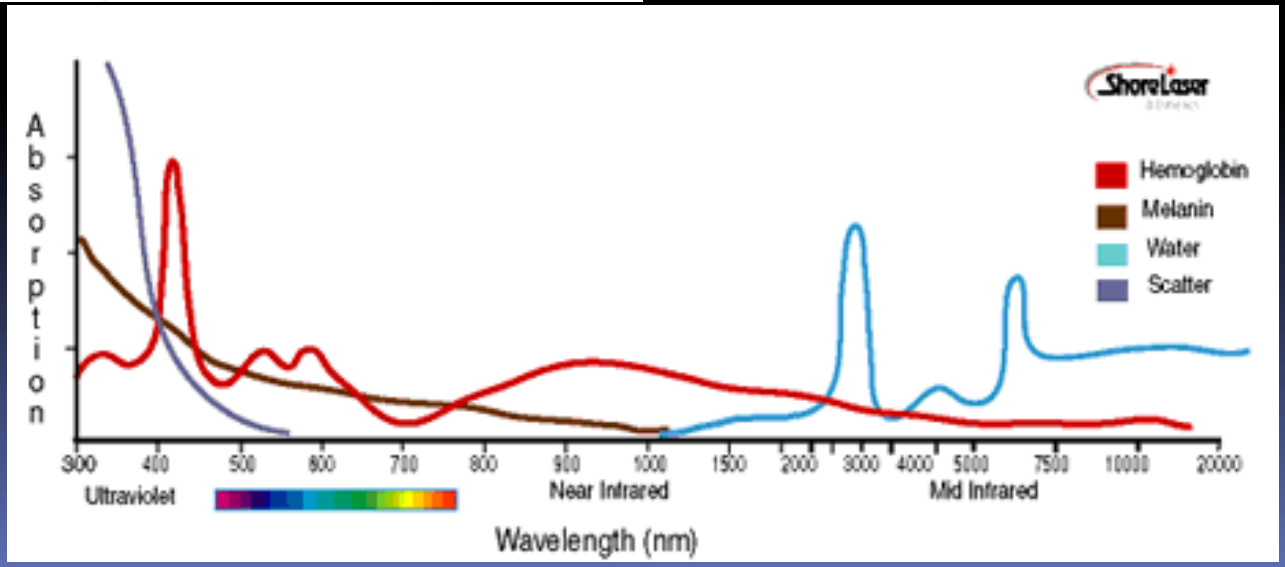

Photochemistry

Photochemistry is the underlying mechanism for photobiology.
When a molecule absorbs a photon, its electronic structure changes, and it reacts differently with other molecules. The energy that is absorbed from light can result in photochemical changes in the absorbing molecule, or in an adjacent molecule.

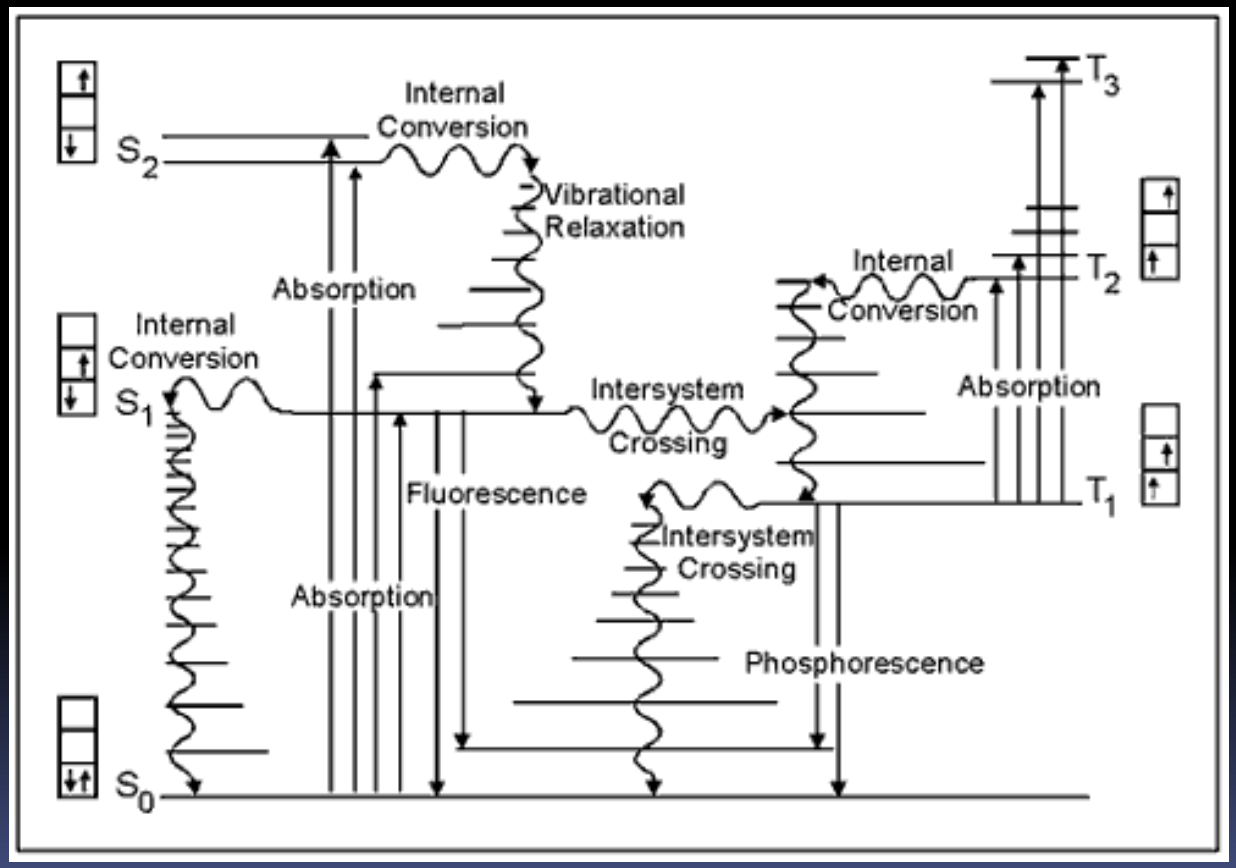

Jablonski diagram illustrating the principal photophysical radiative and non-radiative processes displayed by organic molecules in solution

A photochemical reaction

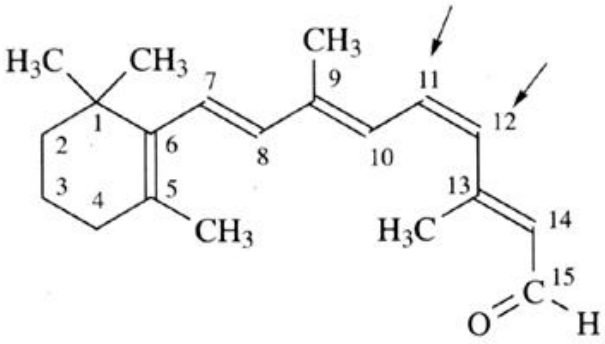

11-*cis*-Retinal

light

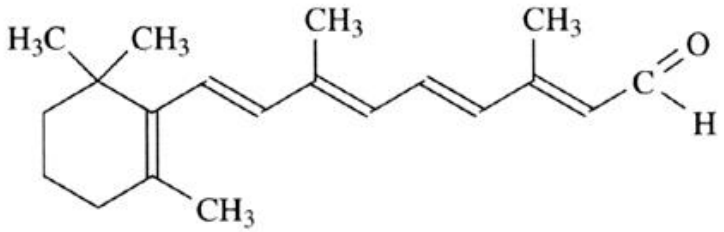

All-*trans*-Retinal

Figure 6.7. Retinal isomerization under light exposure.

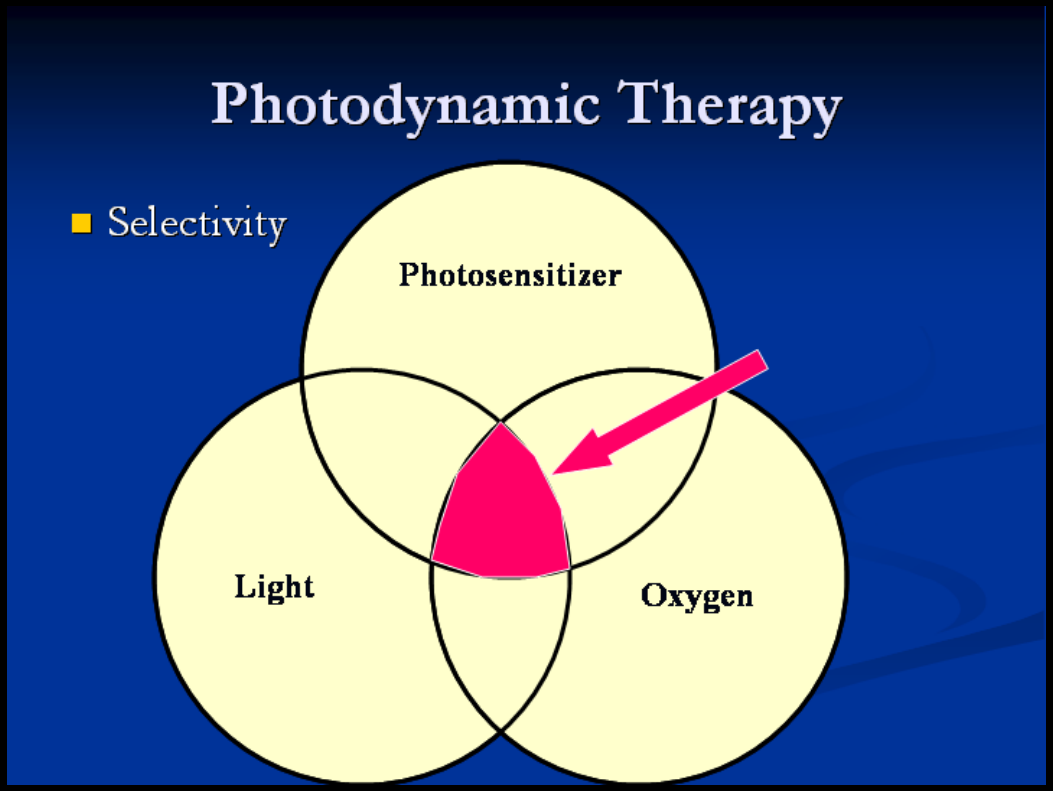

Photodynamic therapy (PDT) is a treatment that uses a drug,
called a photosensitizer or photosensitizing agent, and a particular type of light

When photosensitizers are exposed to a specific wavelength of light, they produce a form of oxygen (singlet O) that kills nearby cells

Each photosensitizer is activated by light of a specific wavelength

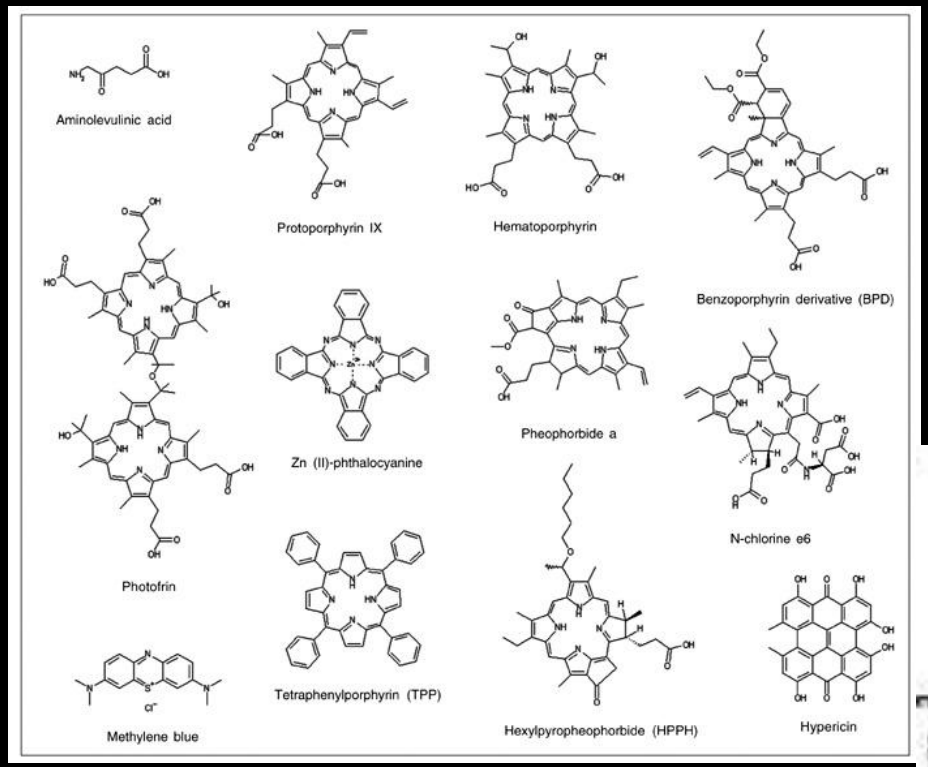

Structure of some photosensitizers used in photodynamic therapy studies

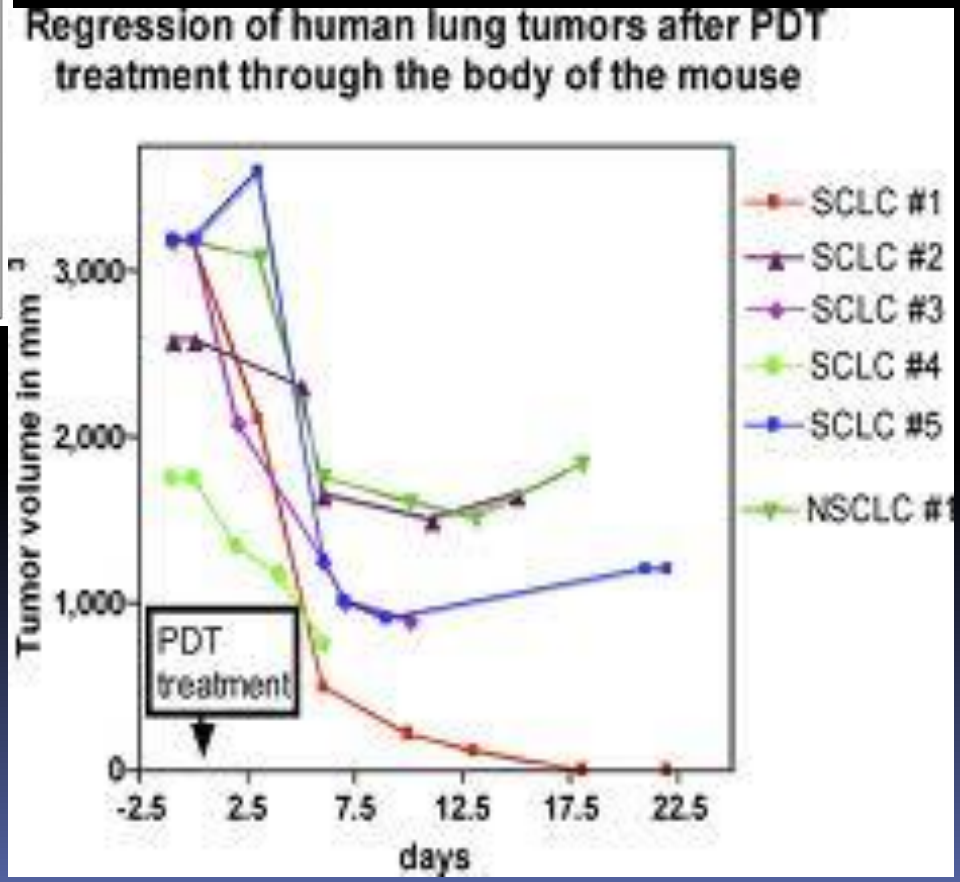

C. Spangler, Biomedical Optics & Medical Imaging, 2008

A great example of photo-biology

Energy transduction in *Halobacterium salinarium*

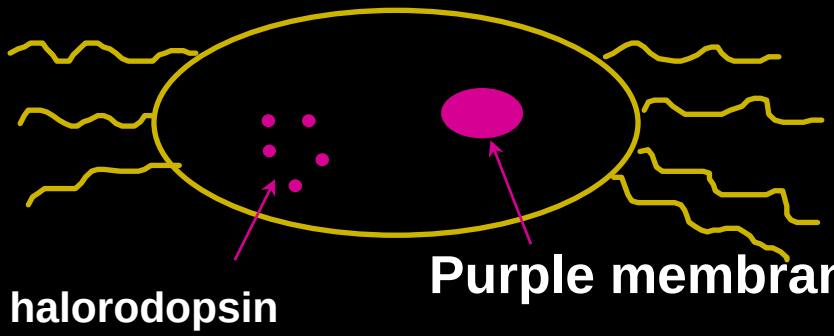

The purple membrane = (BR + lipids)

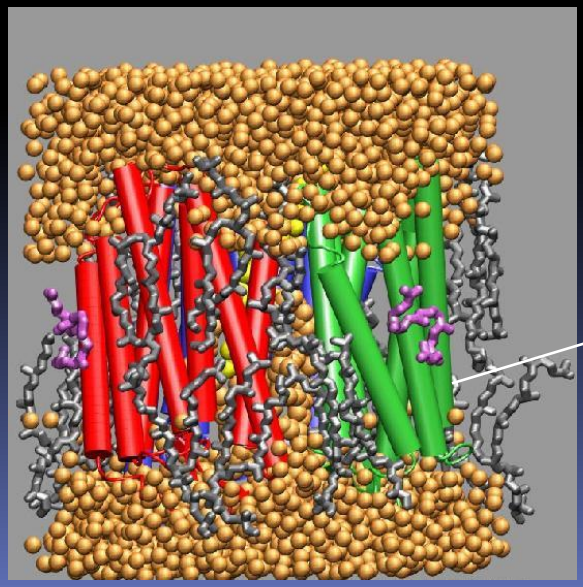

Bacteriorhodopsin
BR

Photoactivable membrane protein and protonpump

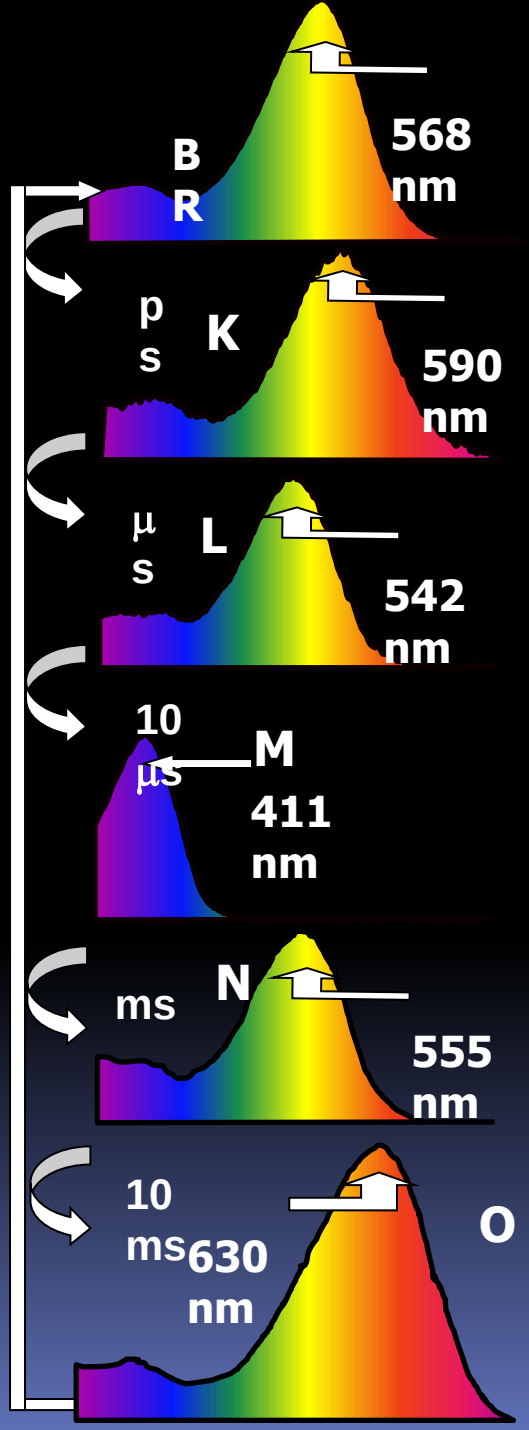

1st step of photoactivation: isomerization of retinal chromophore in BR

Light adapted BR contains all-trans retinal. Its transition dipole makes an angle of 67º with the membrane normal.

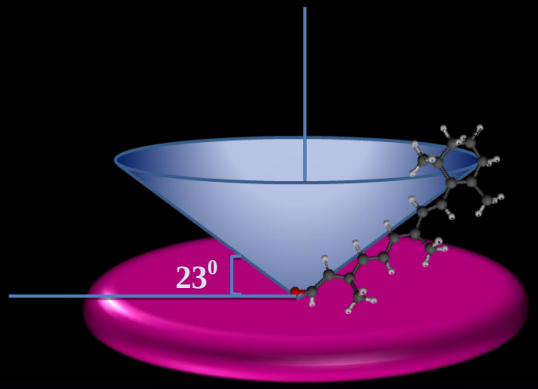

Light absorption results in isomerization to 13-cis. The direction of the transition dipole hardly changes (to 65º), but the lysine residue and the middle of the retinal is displaced.

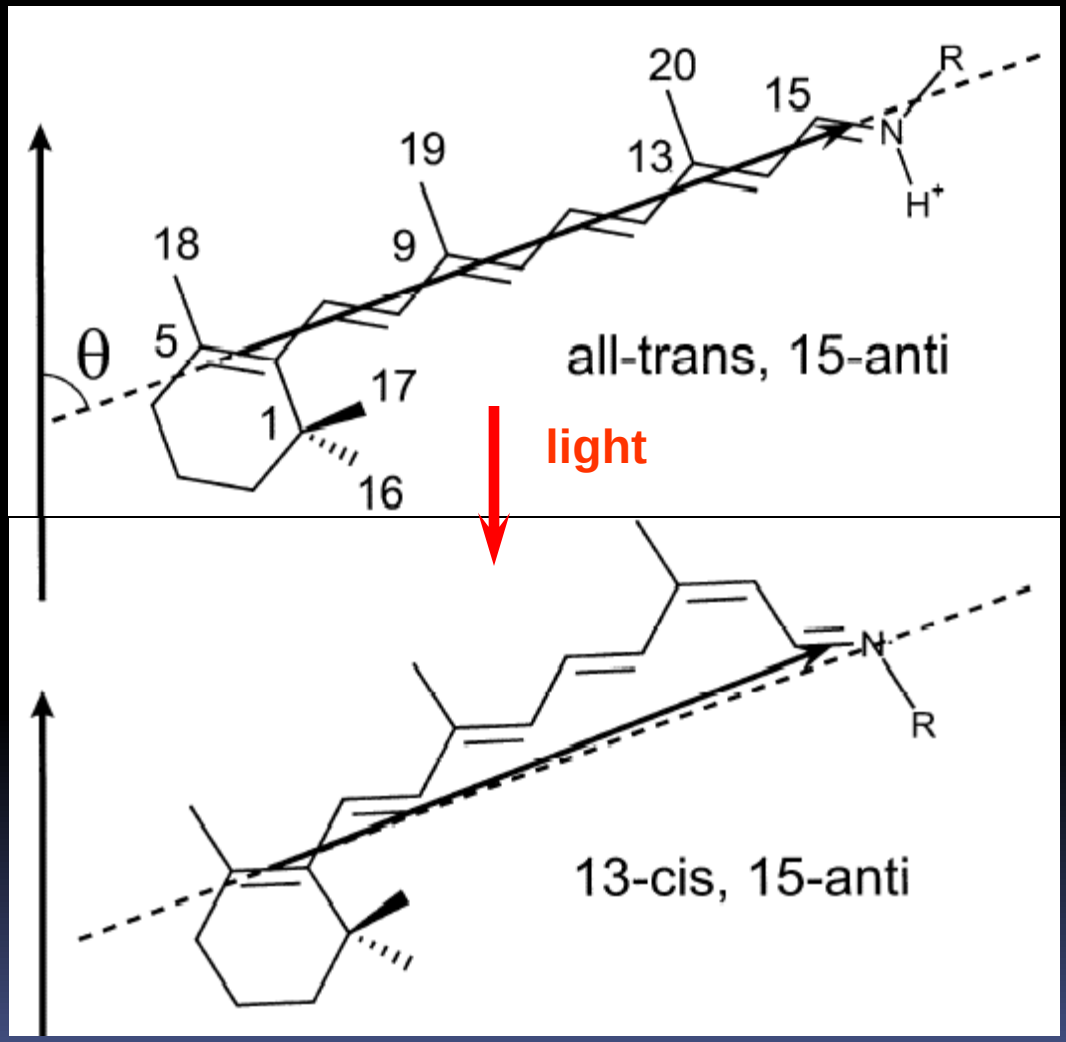

Heyn et al., BBA 1460, 60-74, 2000

2nd step: the photocycle of bacteriorhodopsin

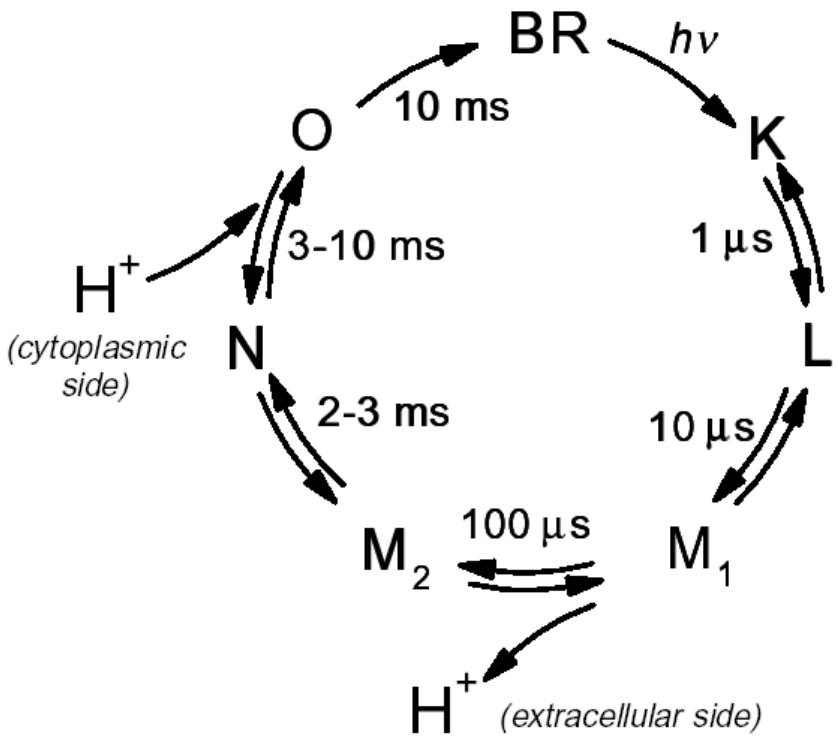

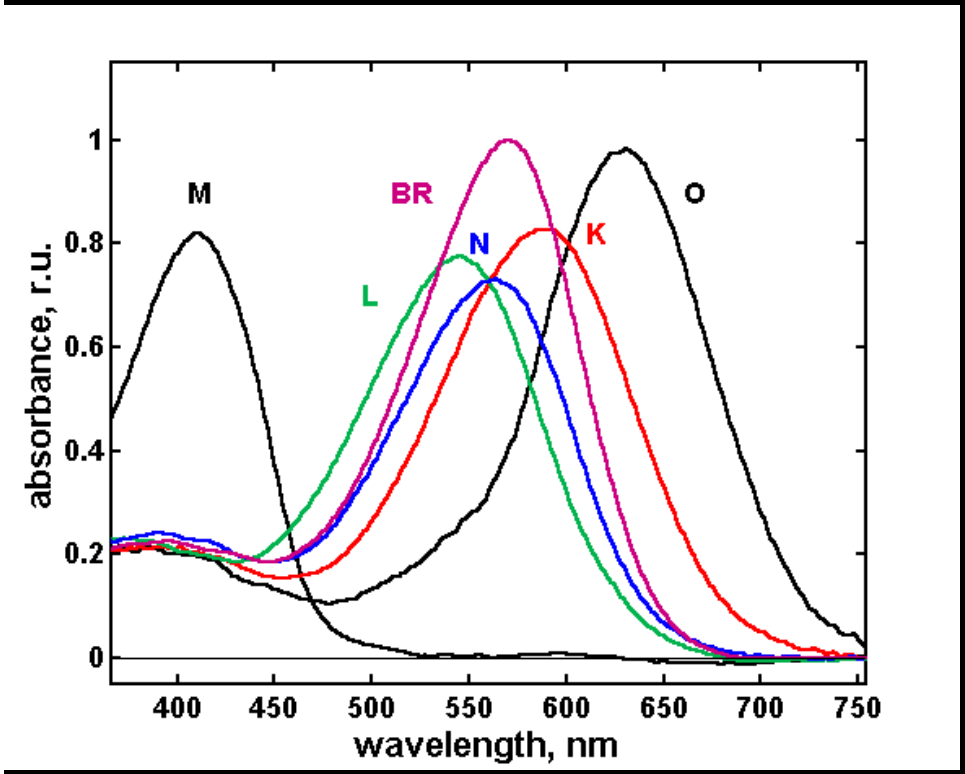

The spectrally distinct intermediates (K, L, M, N, O) and their characteristic lifetimes were identified decades ago by kinetic absorption spectroscopy.

Substates (M_1, M_2) were introduced for kinetic reasons.

The proton release ($M_1 \rightarrow M_2$) and uptake ($N \rightarrow 0$) were measured with pH sensitive dyes.

The time evolution (kinetics) of the photocycle intermediates

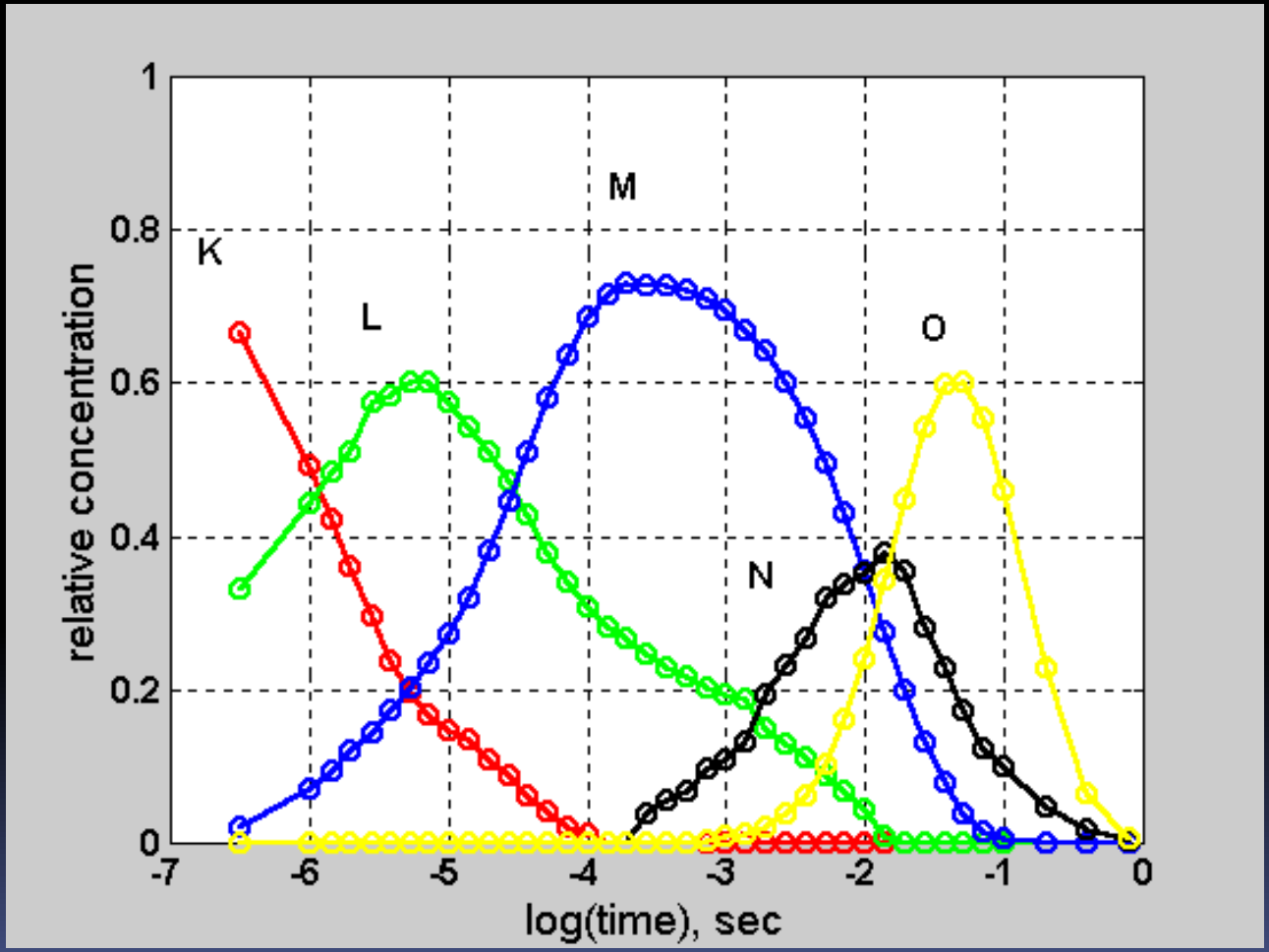

The proton pumping cycle

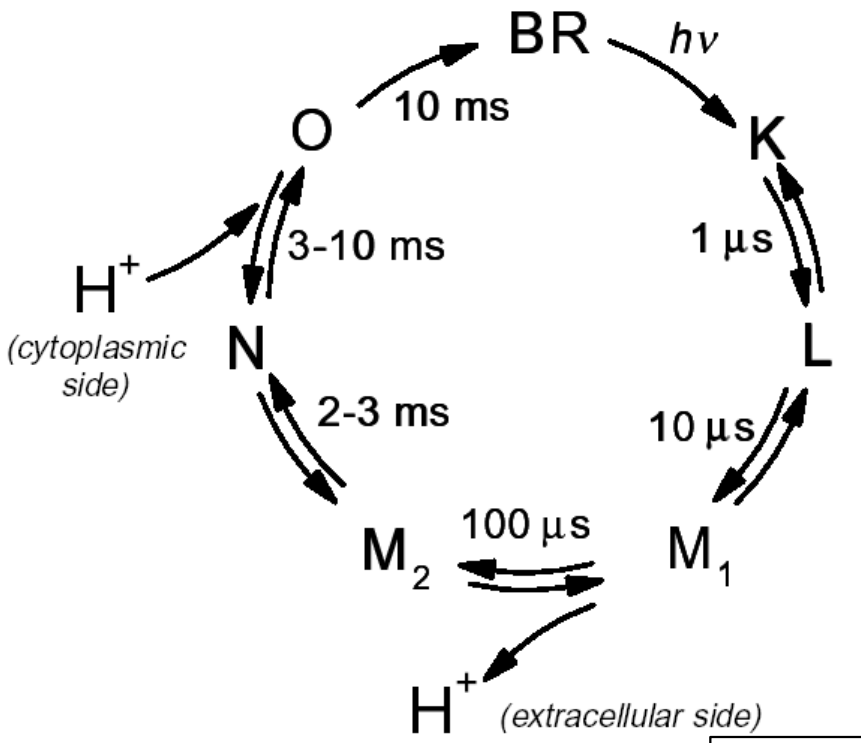

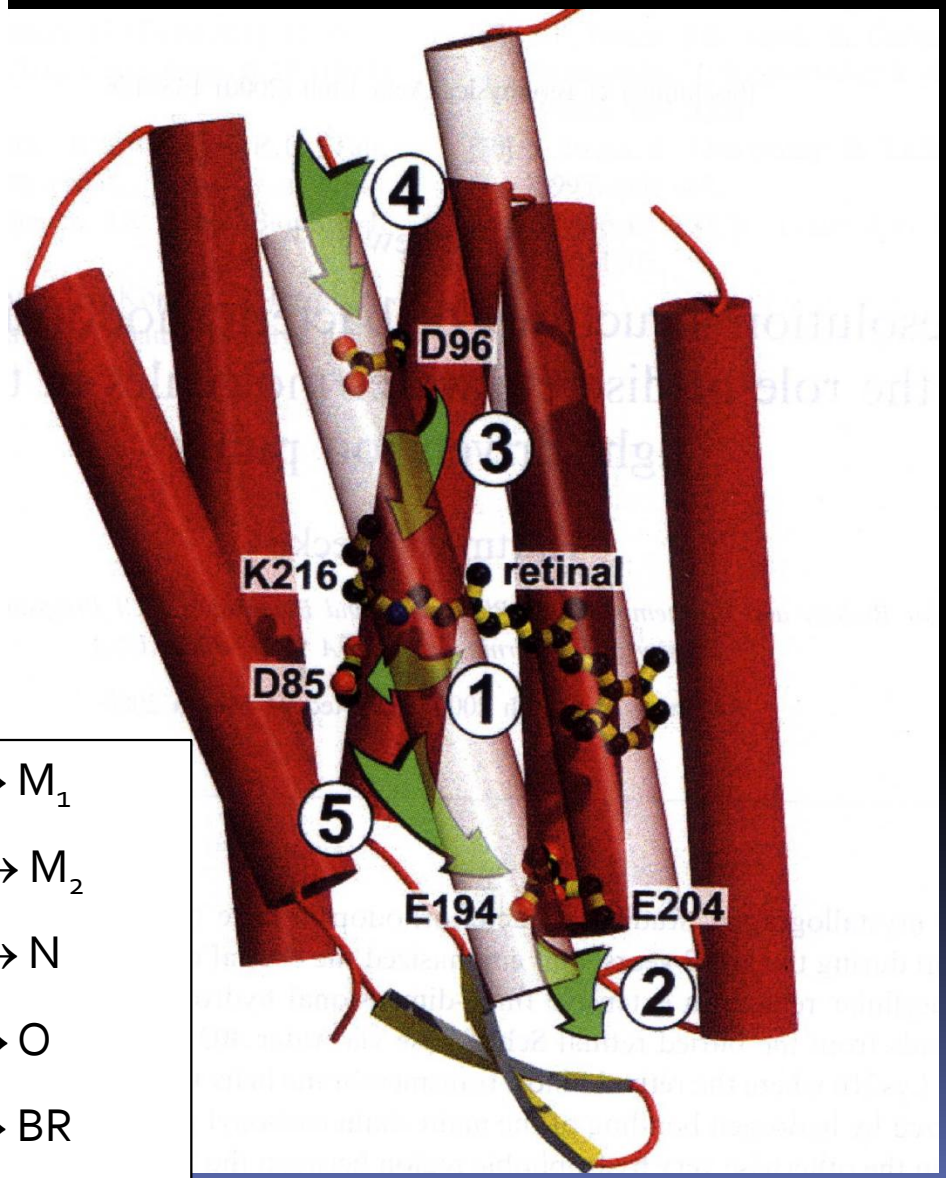

Groups involved in sequential protonation/reprotonation steps were identified by kinetic FTIR spectroscopy and site directed mutagenesis.

1: $L \rightarrow M_1$

2: $M_1 \rightarrow M_2$

3: $M_2 \rightarrow N$

4: $N \rightarrow O$

5: $O \rightarrow BR$

Luecke, BBA 1460, 133-156, 2000

Use of light activated rhodopsins

Matrix photostimulation, multi-site optical excitation of neurons

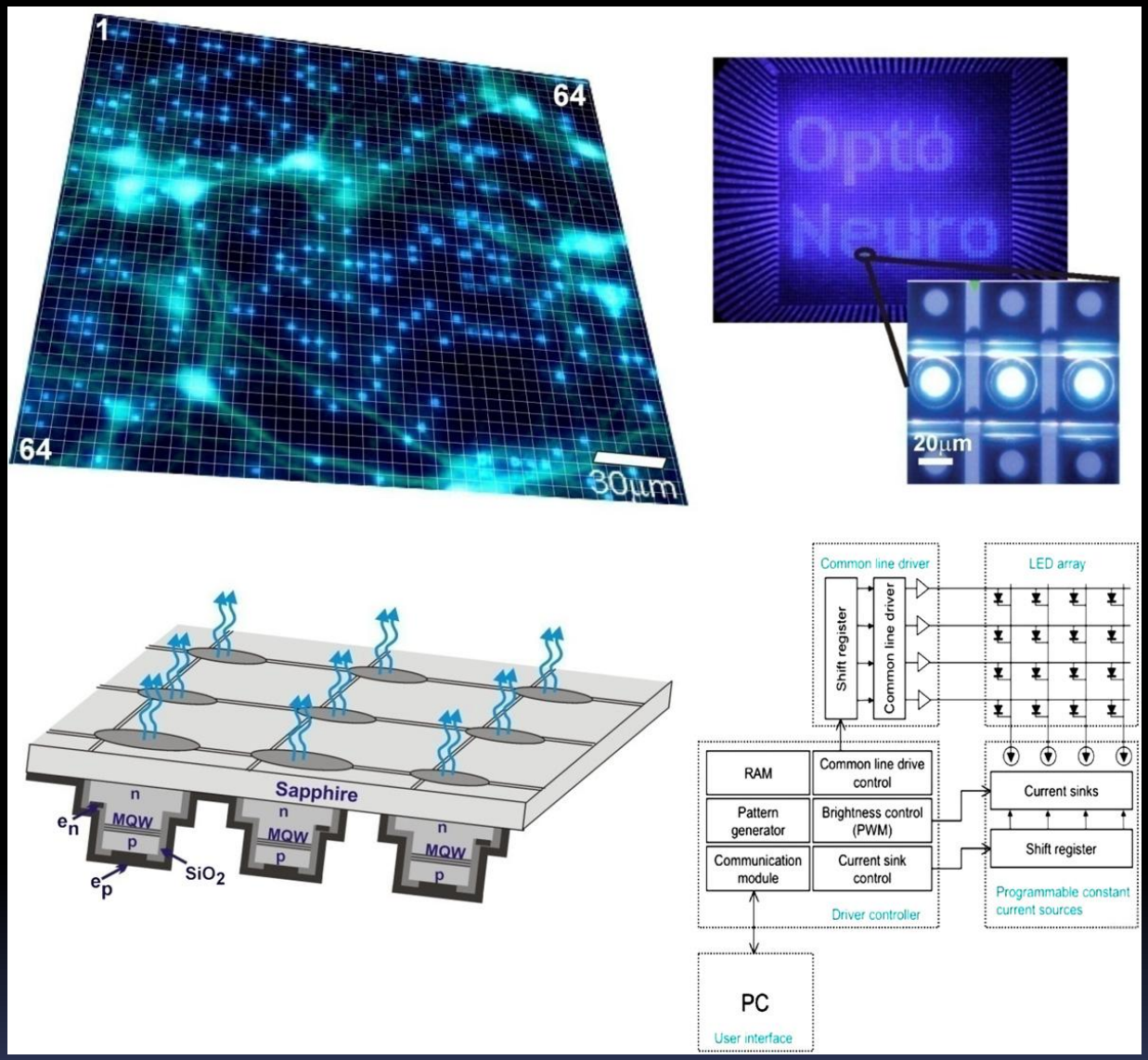

Neural cells expressing channelrhodopsin are covered by the 64 × 64 matrix of bright small light spots, with individual control of their intensity and timing via a micro-LED array (Grossman, J. Neur . Eng. 2010)

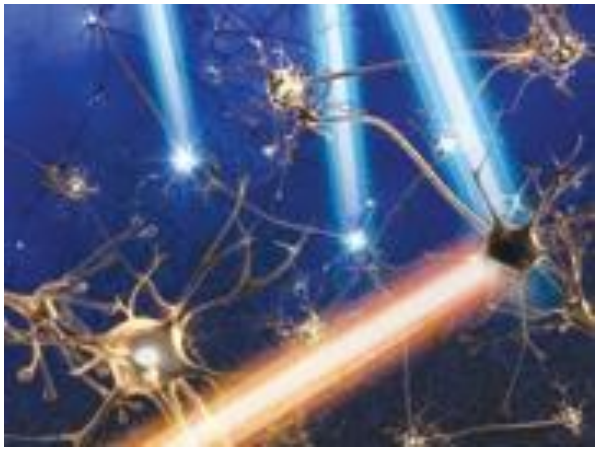

Optogenetics

Karl Deisseroth

Optogenetics is a technology that allows targeted, fast control of precisely defined events in biological systems as complex as freely moving mammals. By delivering optical control at the speed (millisecond-scale) and with the precision (cell type–specific) required for biological processing, optogenetic approaches have opened new landscapes for the study of biology, both in health and disease.

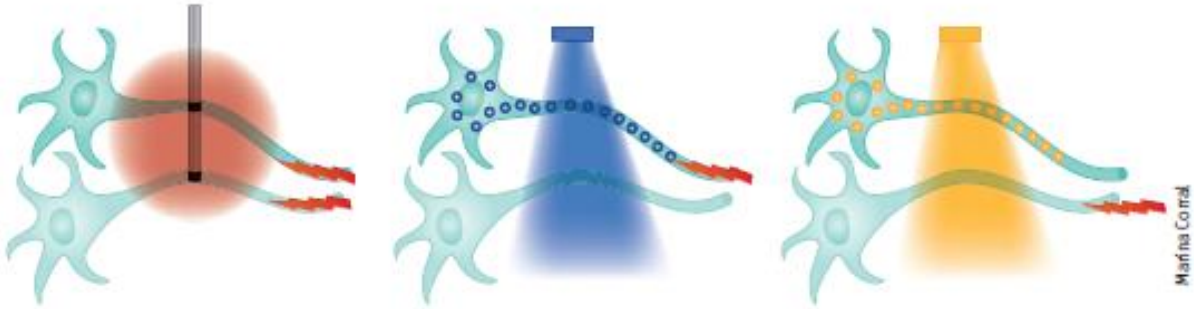

Figure 2 | Principle of optogenetics in neuroscience. Targeted excitation (as with a blue light–activated channelrhodopsin) or inhibition (as with a yellow light–activated halorhodopsin), conferring cellular specificity and even projection specificity not feasible with electrodes while maintaining high temporal (action-potential scale) precision.

light-sensitive brain activated with light

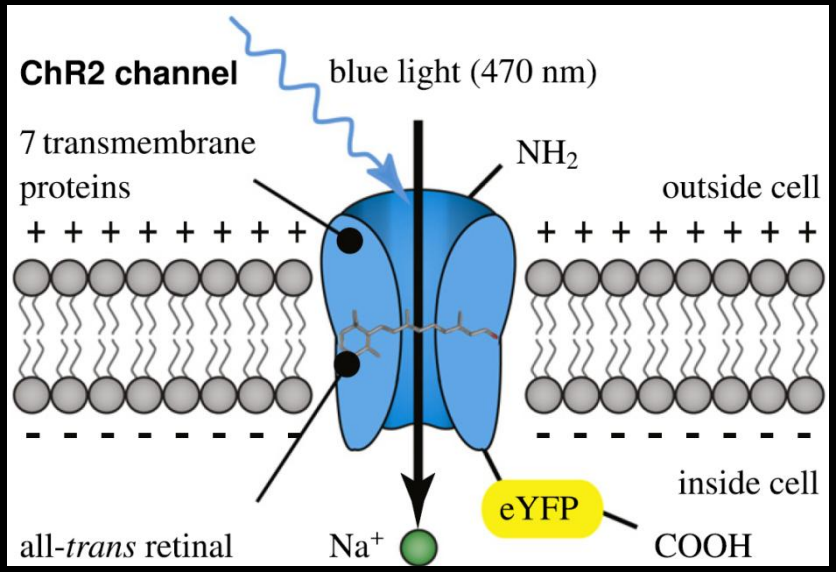

Channelrhodopsin-2 is a gated light-sensitive cation channel that uses a molecule of all-*trans* retinal to absorb photons.

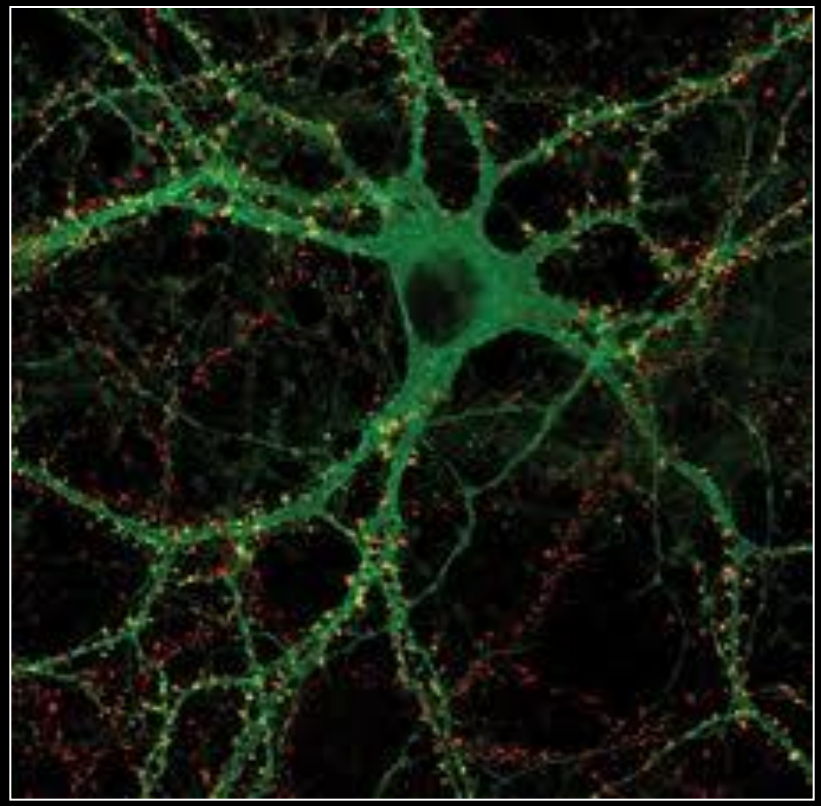

Neurons labeled with ChR2 (in green) and synapses (in red)

Channelrhodopsin-2 was expressed in hippocampal neurons in the mouse brain then shone blue light on the region
→ the cells with ChR2 responded to the light stimulation, opening the channel and initiating the flow of ions, which resulted in an action potential in those neurons

Vision

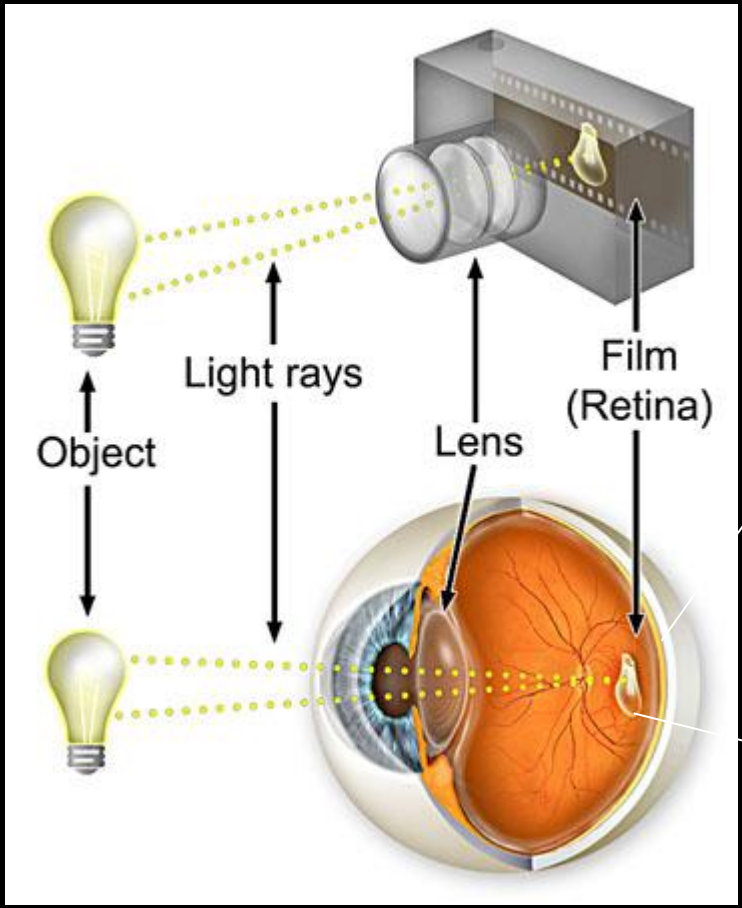

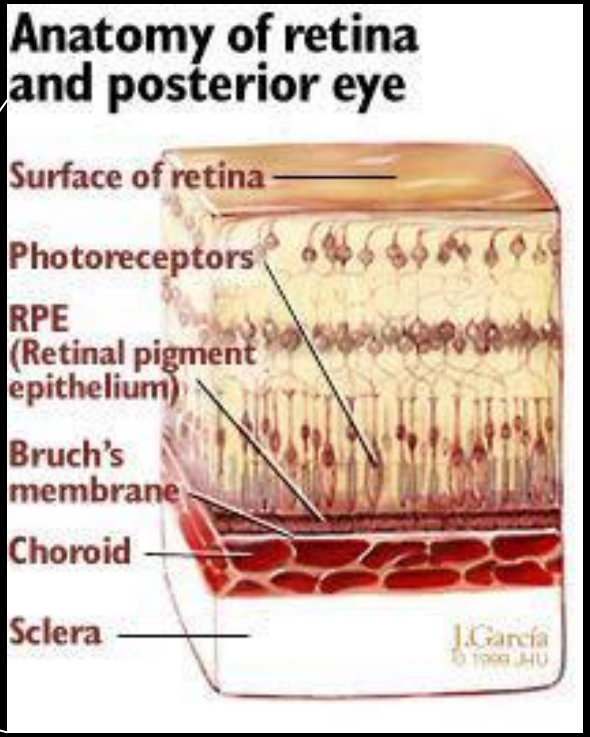

The light rays from the object pass through the conjuctiva, cornea, aqueous humour, lens and vitreous humour. All these structures refract the light such that it falls on the retina = focussing. Maximum focussing is done by the cornea and the lens. The light then falls on the retina.

When light strikes the retina, a photon interacts with 1-cis-retinal, rearranging within picoseconds to trans-retinal which forces a change in the shape of rhodopsin to which retinal is bound.

Light → Photosynthesis → produce energy (ATP)

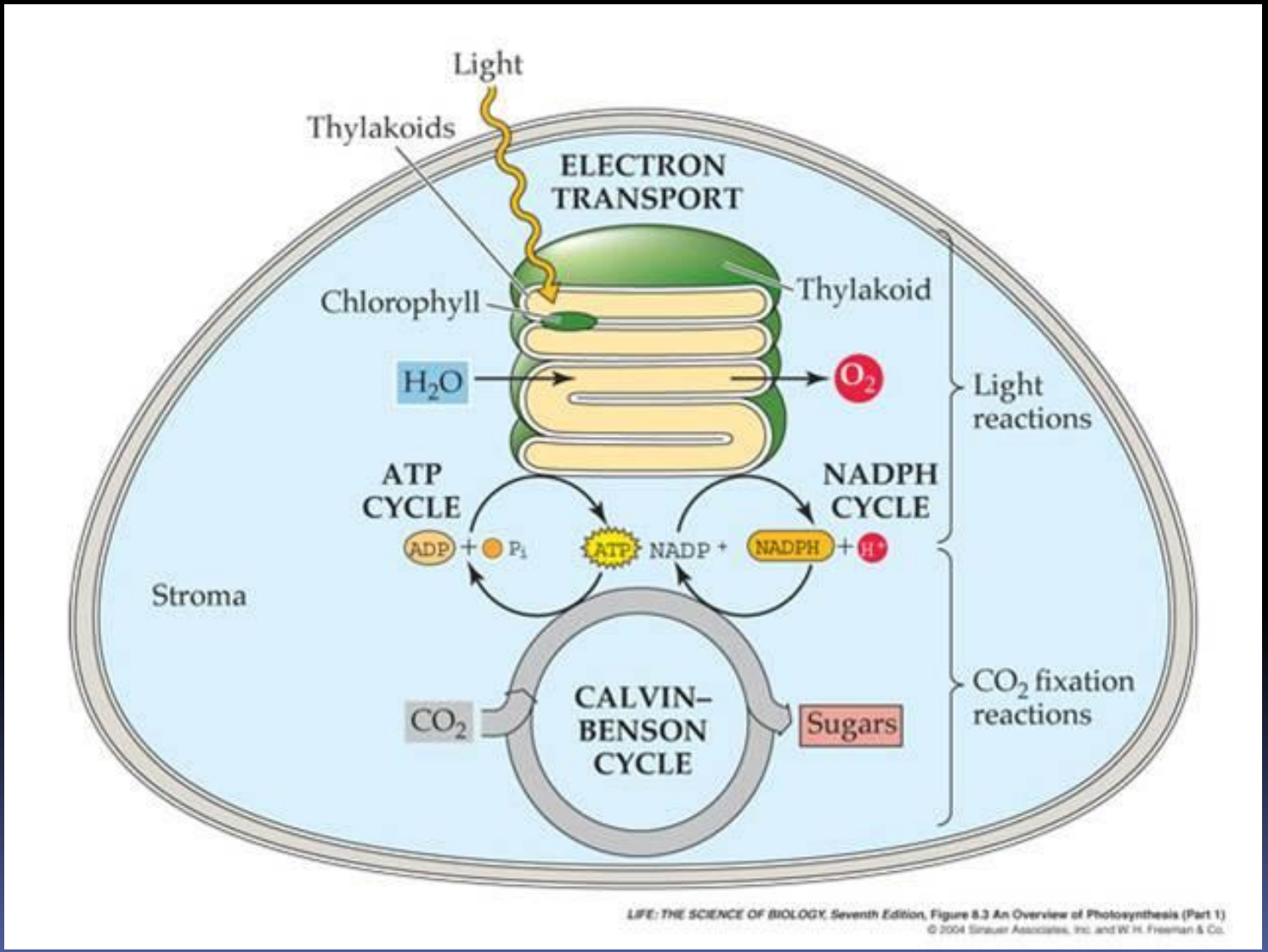

Use of exogenous labels for in vivo imaging

Luciferin is a chemical substance found in the cells of various bioluminescent organisms.

When luciferin is oxidized under the catalytic effects of luciferase and ATP, a bluish-green light is produced.

As the reaction is dependent on ATP, it allows to determine the presence of energy or life.

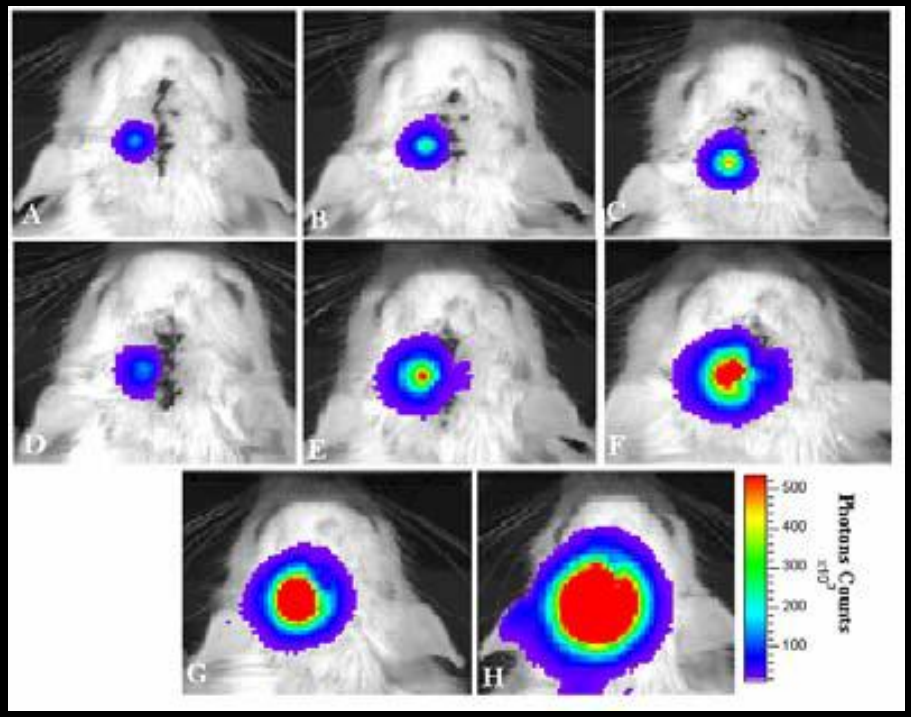

Monitoring of
- nr. of transfected cell
- O2
- ATP
- Depth of cells
- Metabolizing cells

Quantum dots : semiconductor nanoparticles:as biolabels

- they can simultaneously reveal the fine details of many cell structures

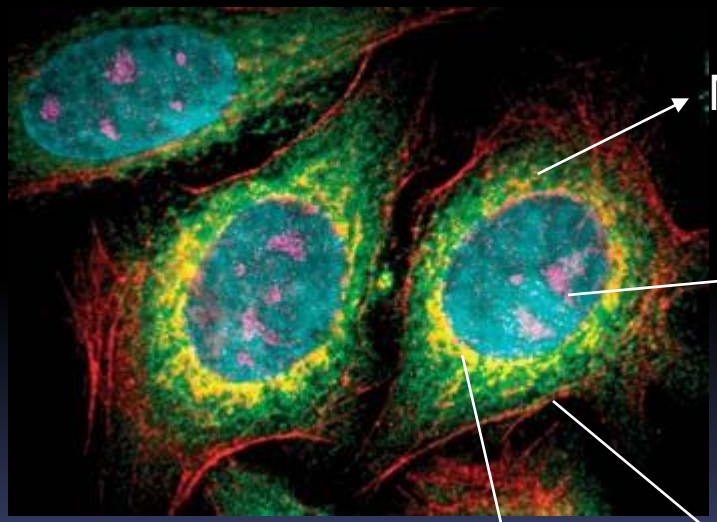

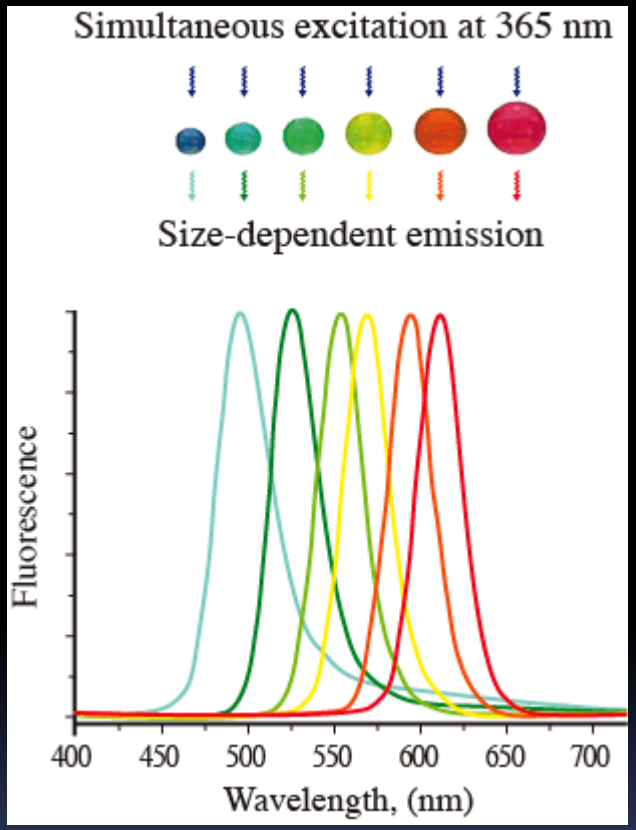

QUANTUM DOT CORP., HAYWARD, CA

Natural photonic crystals

insight review articles

Photonic structures in biology

Pete Vukusic and J. Roy Sambles

Thin Film Photonics, School of Physics, Exeter U

Millions of years before we began t
systems were using nanometre-sca
of natural photonic structures exists
collect light, *Morpho* butterflies use
some insects use arrays of element
Natural photonic structures are prov

Natural Photonic Crystals

Chrysochroa vittata

Morpho didius

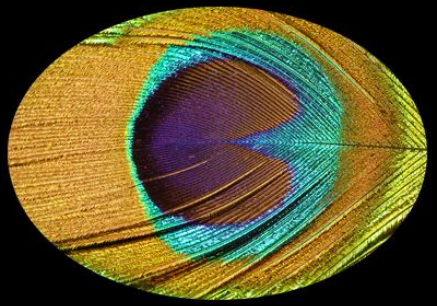

Pavo cristatus (feather)

Chrysina resplendens

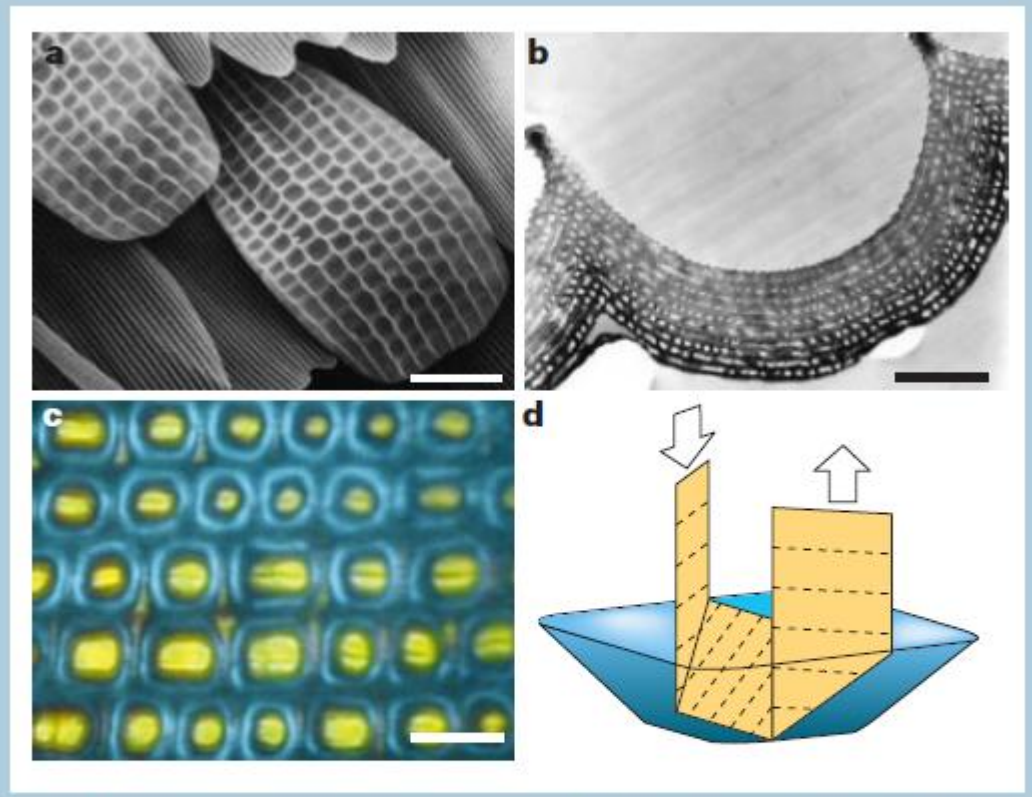

Figure 4 Iridiscence in *Papilo palinurus*. **a**, SEM of an iridescent scale showing its array of concavities, each with a section that exhibits the curved multilayering shown by transmission electron micrography in **b**. This structure produces two simultaneous structural colours **c**, yellow and blue . **d**, The blue annulus is created by a double reflection from opposite and perpendicular concavity sides. **d** also schematically illustrates the way in which incident linearly polarized blue light has its e-vector (dotted lines) rotated by this double reflection. Bars, **a**, 15 μm; **b**, 1 μm; **c**, 6 μm.

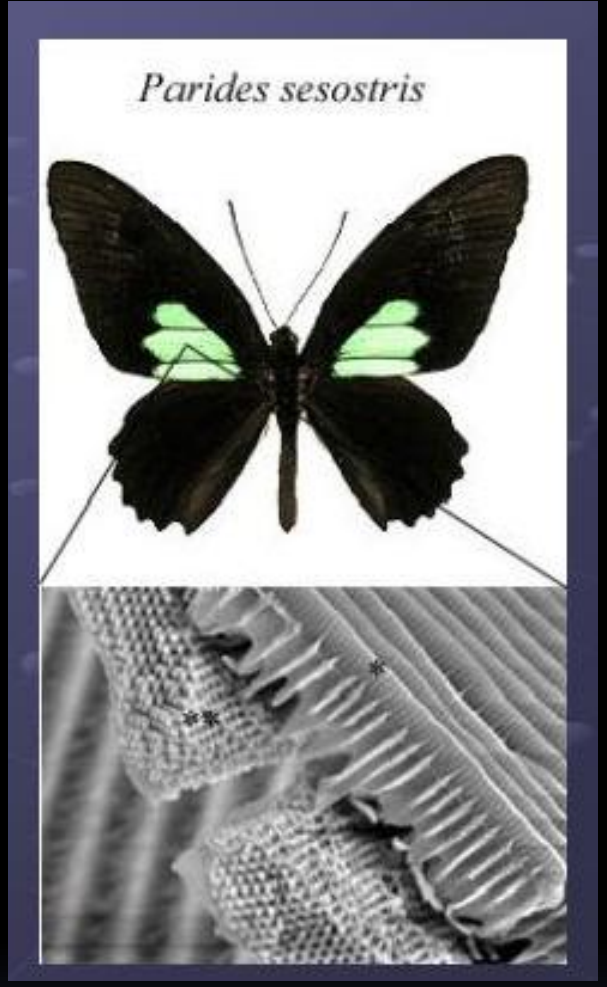

Nanometric two-dimensional structures found in eyes of some insects

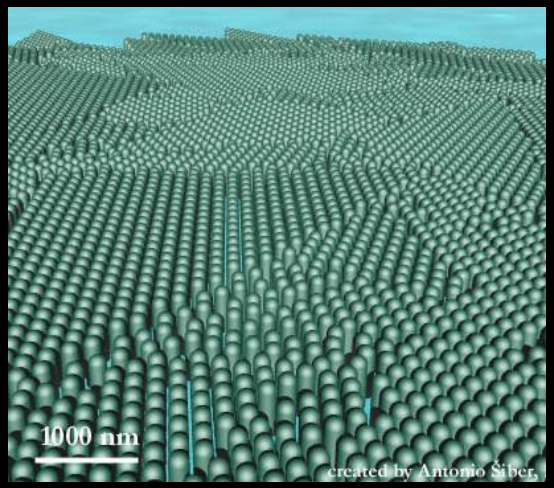

The brown in the feathers of male peacocks arise from natural photonic crystals.

The microstructure in the wings of some butterflies causes their remarkable iridescent colours. They reflect electromagnetic radiation as propagation through them is prohibited. The periodicity of the crystal plays a very important role in the formation of a useful band gap. The width of this band gap depends on the geometry, feature size, spacing and the materials which make up the crystal.

Science at the shine Dome 2004
Michael Shake/Dreamstime.com; P. Vukusic Nature, 2003

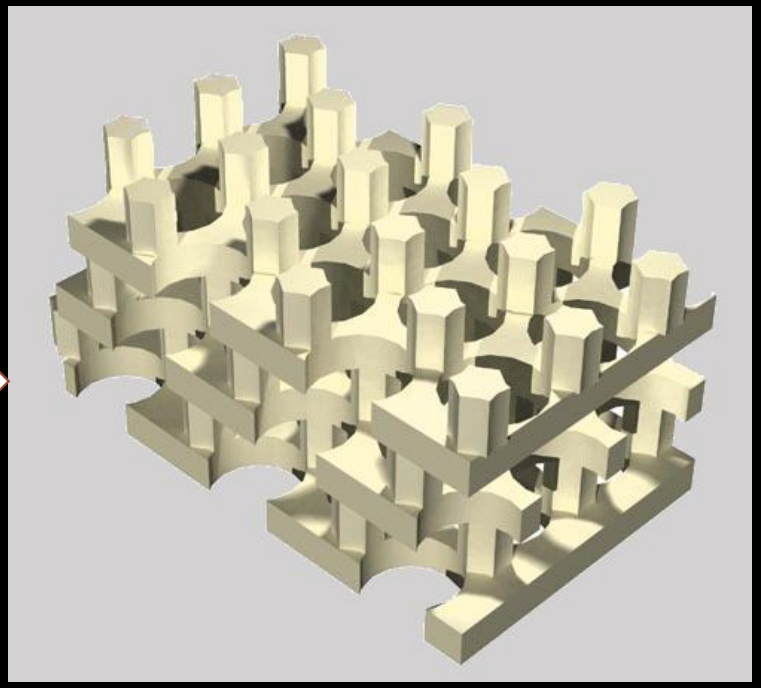

An example of natural band gap: butterfly wings

-→ proposed a new structure for achieving a full three-dimensional band gap

S. G. Johnson and J. D. Joannopoulos, APL 77, 3490-3492

Butterflies and beetles have developed various cuticular exoskeleton photonic crystal structures

→ a variety of optical effects throughout the visible range of the electromagnetic spectrum.

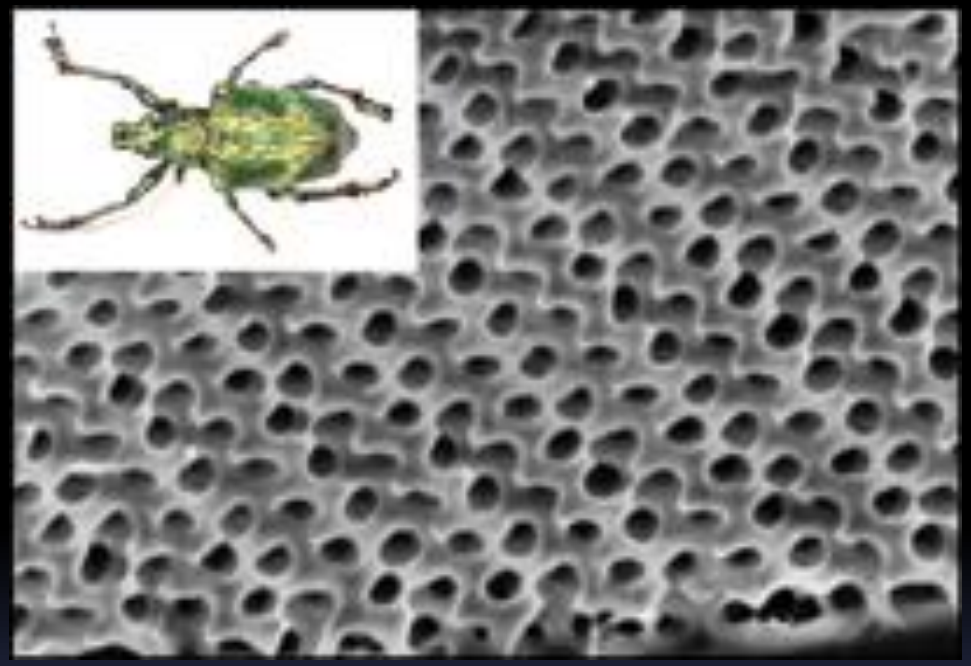

Cuticular exoskeleton photonic crystal structure of the weevil Lamprocyphus augustus.

http://www.chem.utah.edu/directory/faculty/bartl.html

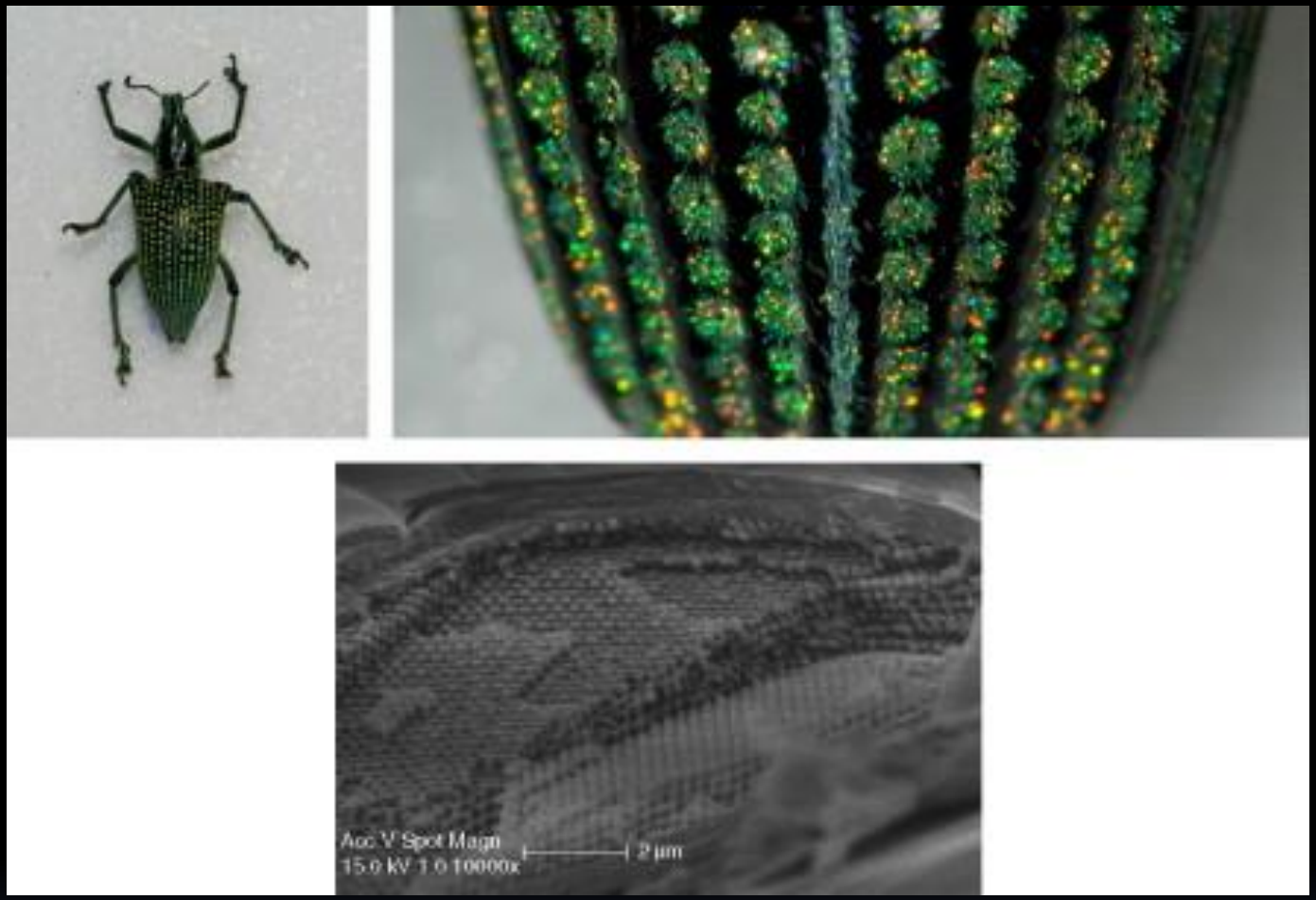

Entimus imperialis shows one of the most perfect three-dimensional photonic crystals in nature. The insect bears transparent scales that scatter white light as many different colours, ranging from deep blue to red. The origin of this coloration is the diffraction by the structure shown in the lower panel, occurring inside each scale. The scale itself is about 100 μm long, and contains one or two large grains of photonic crystal.

J. P. Vigneron, Adv. in Insect Physiology, 38, 2010

Nonlinearity in materials

Strong enhancement of second-harmonic generation (SHG) response through multi-chiral centers and metal-coordination (Ye et al. Dalt Trans 2005)

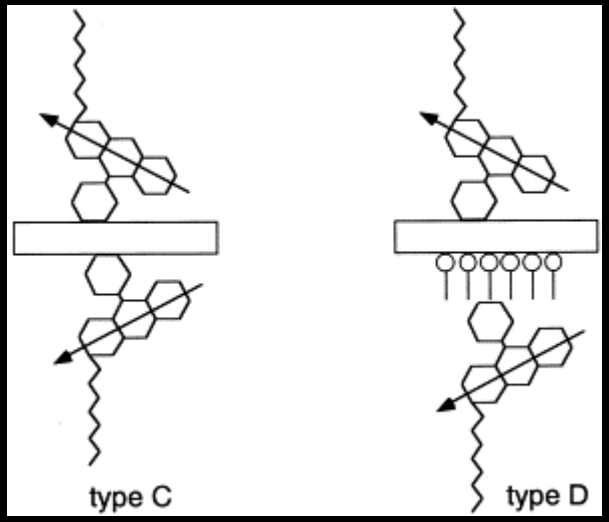

SHG interferometry allows the characterization of Rhodamine B derivative (dipoles) in Langmuir Blodget films (Ishibashi, J. Elec.anal. Chem, 1999)

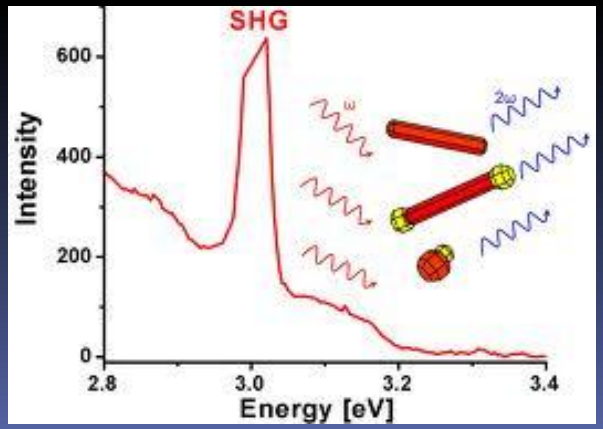

Second order non-linear optical properties and SHG in semiconductor nanocrystals and nanorods depends of their size, shape and composition.
http://chem.ch.huji.ac.il/~nano/Research.html

Second Harmonic generation in biological systems

with non-centrosymmetry , with polarisable electrons

Ex: chromophores, FAD, NADH, collagen, microtubules, sarcomeres

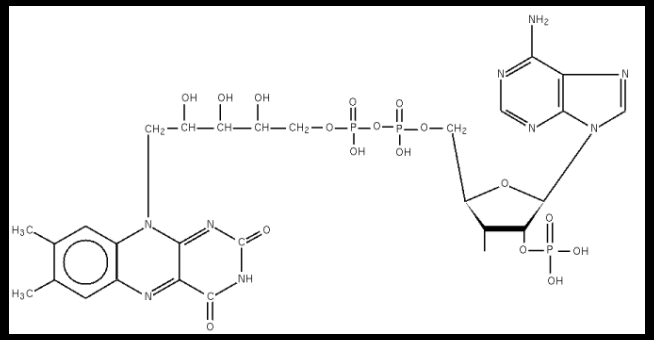

Flavin adenine dinucleotid
(in oxido-reductive enzymes)

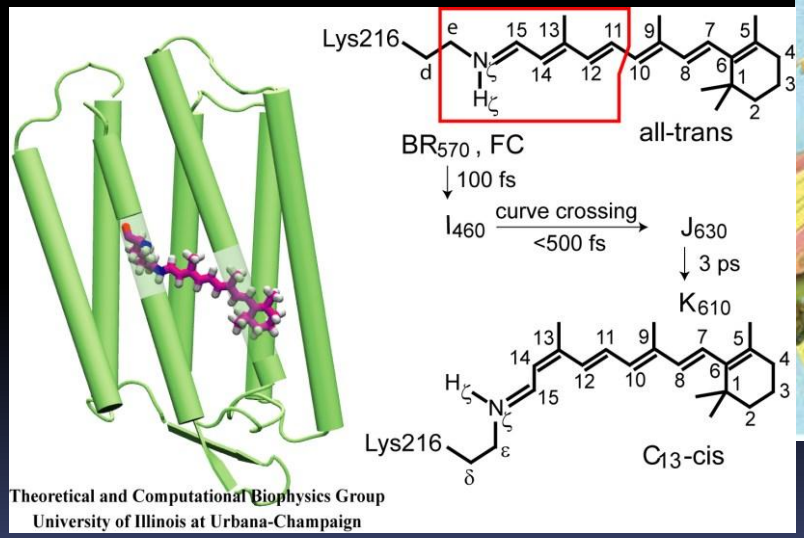

Chromophores
(in chromo/retinal proteins)

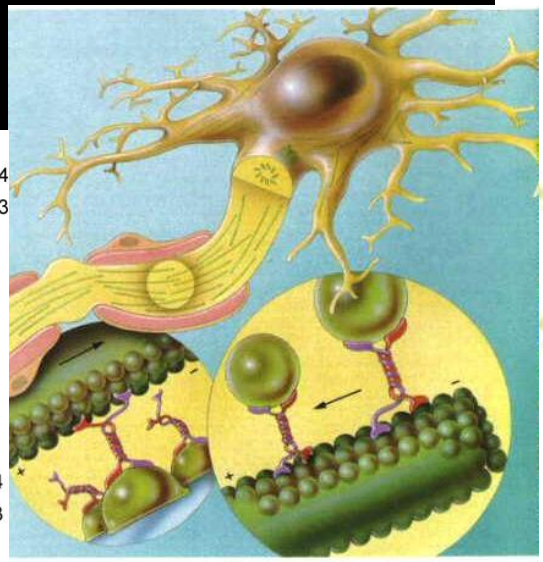

Microtubules
= target of chimio-therapeutic treatment in cancer

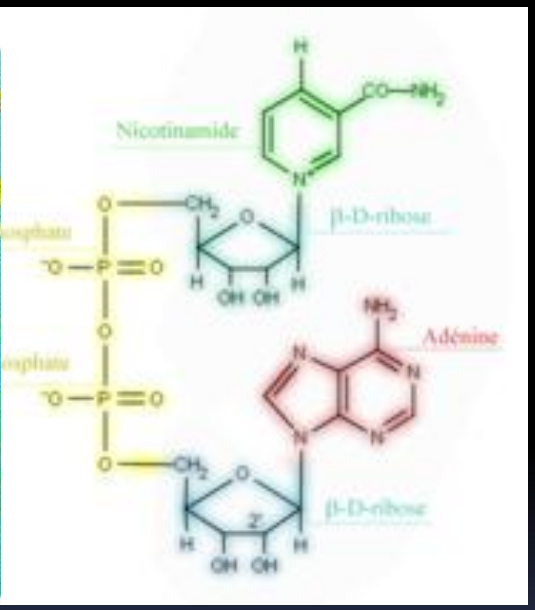

NAD, NADH
in mytochondries

Bacteriorhodopsin (BR): natural photonic crystal

Salt lake

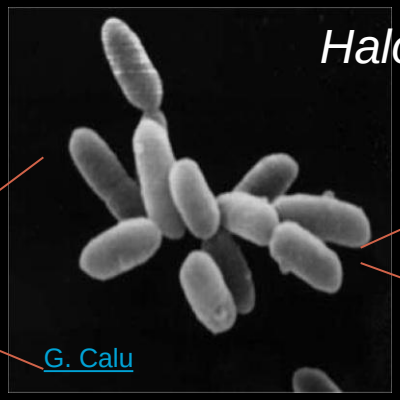

Halobacterium Salinarium

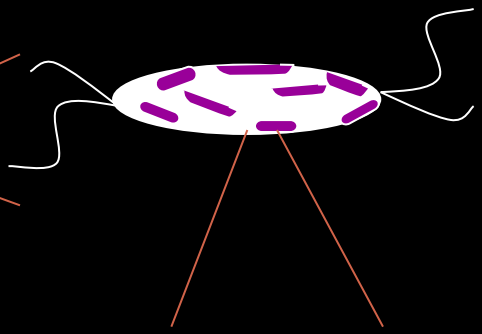

Cromophore retinal within the 7 helices of the protein

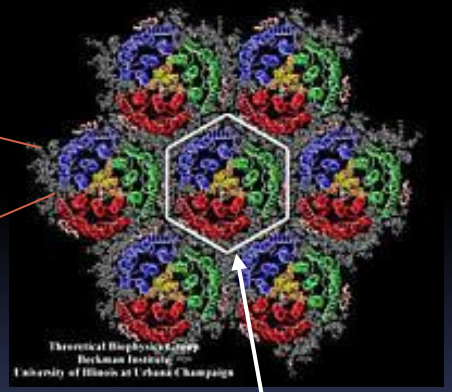

Hexagonal arrangement of BR trimers within the purple membrane

Bacteriorhodopsin → SHG

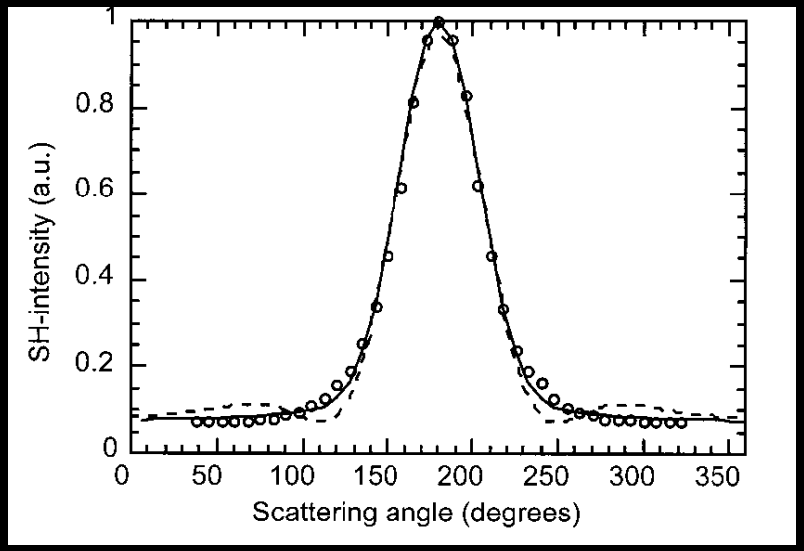

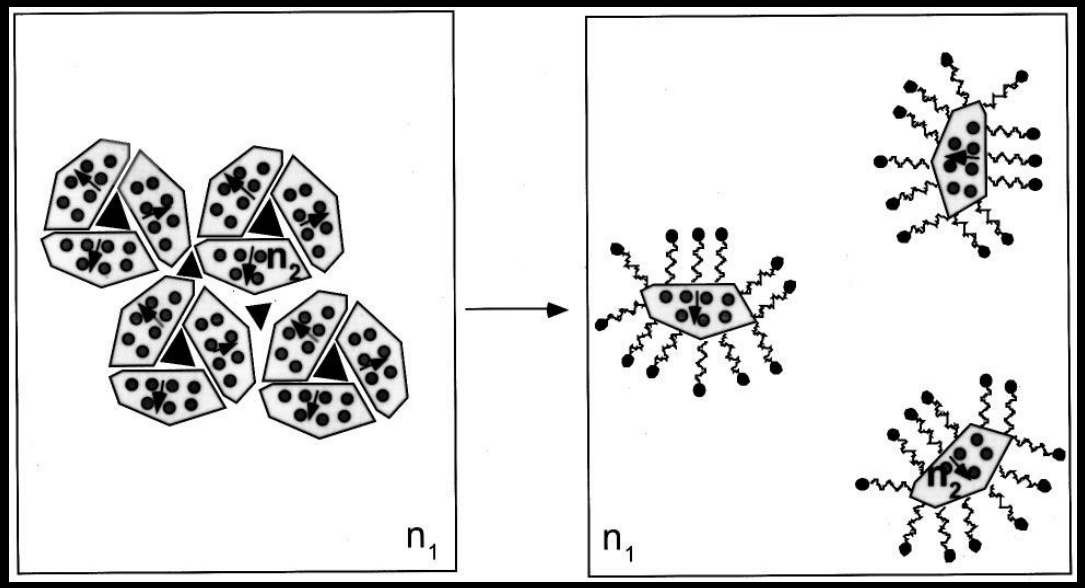

Solubilization of purple membrane patches (left) to individual bacteriorhodopsin protein molecules (right) with the embedded dipolar nonlinear chromophore, i.e., retinal (dipoles indicated by arrows) and solubilized by the surfactant (indicated by amphiphilic icons). **Solubilization makes dissapearing SHG**

The protein matrix has a linear refractive index *n*1 .
Only the retinal has a second-order optical nonlinearity β
and a higher linear refractive index *n*2 .

J. Clays et al; J. Opt Soc Am. 2001

Orientation of BR containing purple membranes in electric field

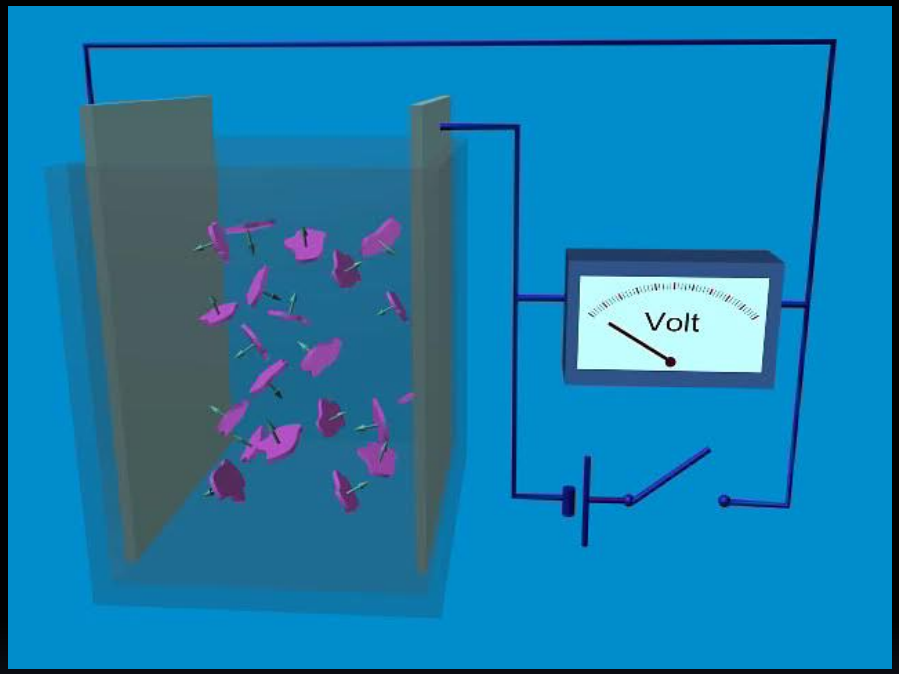

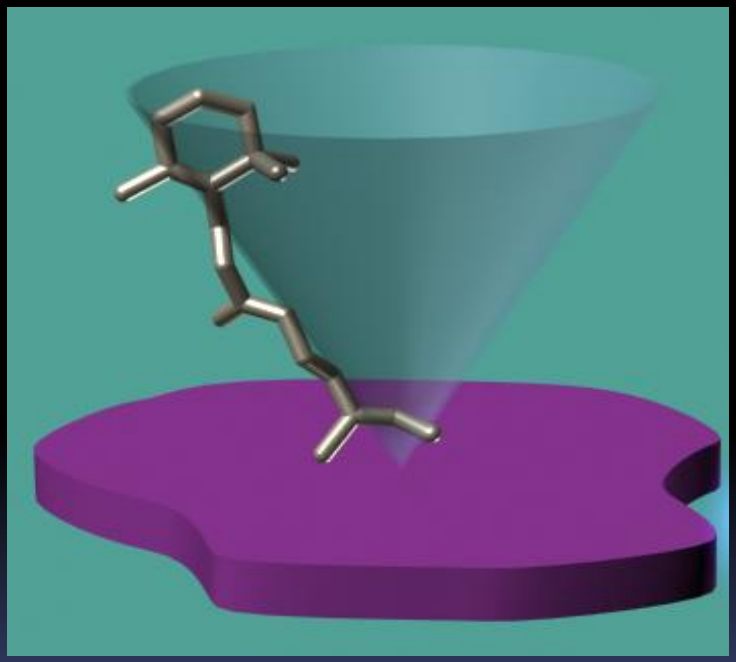

Electrophoretic deposition of BR
→ 4 µm thick oriented BR film onto a ITO substrate -> BR film composed by ~800 purple membrane layers (5 nm each).

G. Váró Acta Biol. Acad. Sci. Hung.(1981)

Structure and composition of the BR containing purple membrane = crystal

Purple membrane = a crystal

trimers of BR form hexagonal 2D crystalline lattice

- Unit cell size d = 63 Å

- The unit cell contains 3 BR molecules + 12-14 lipid molecules

The symmetry structure of BR arises by consecutive stacking of the naturally hexagonal lattice represented by the membrane sheets showing P3 symmetry.
The resulting point group symmetry 6mm is **noncentrosymmetric and its second order susceptibility tensor has three nonvanishing components.**

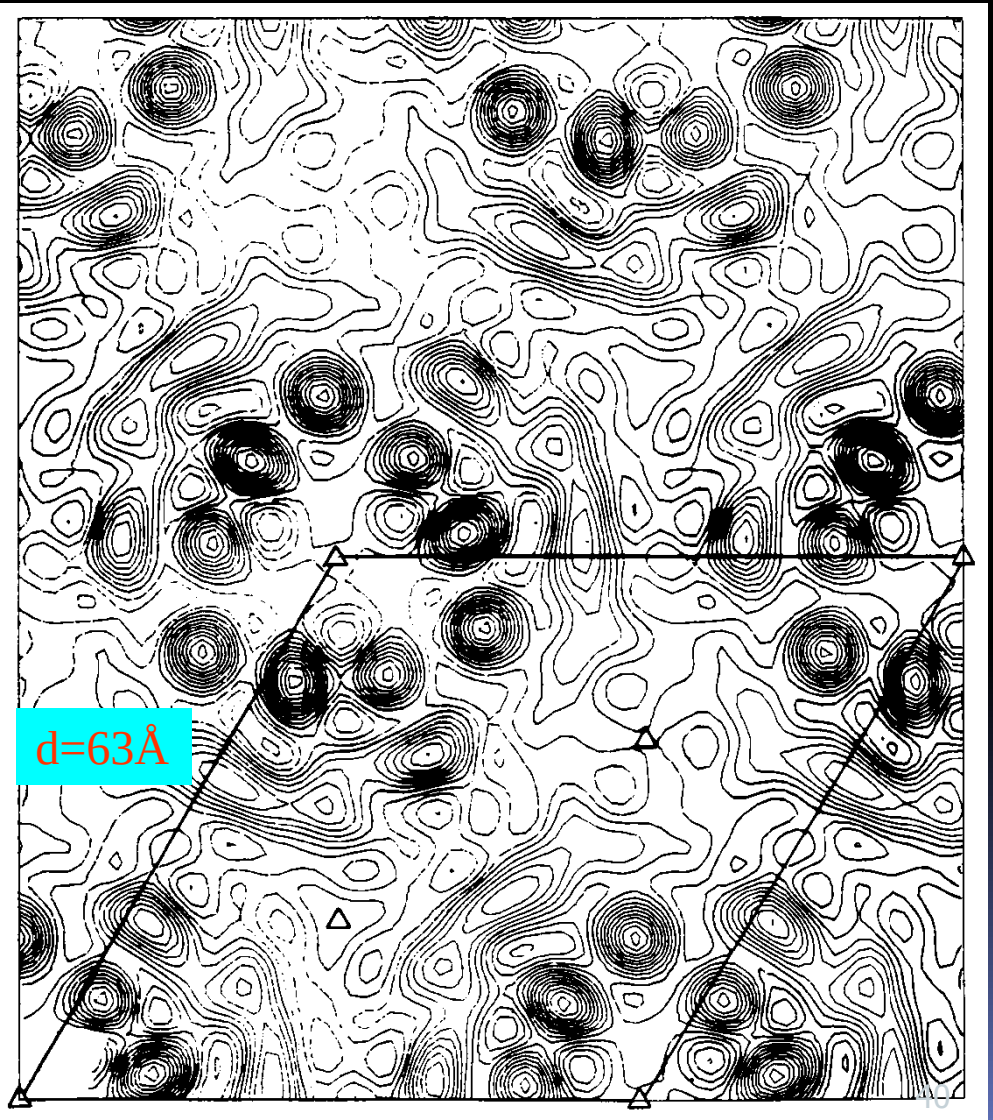

APPLIED PHYSICS LETTERS 96, 221108 (2010)

Optical chirality of bacteriorhodopsin films via second harmonic Maker's fringes measurements

M. C. Larciprete,[1,a)] A. Belardini,[1] C. Sibilia,[1] M.-b. Saab,[2] G. Váró,[3] and C. Gergely[2]
[1]*Dipartimento di Energetica, Università di Roma "La Sapienza," Via A. Scarpa 16, 00161 Roma, Italy*
[2]*Groupe d'Etudes des Semiconducteurs, UMR 5650 CNRS, Université Montpellier 2, 34095 Montpellier Cedex 5, France*
[3]*Institute of Biophysics, Biological Research Center of the Hungarian Academy of Sciences, H-6701 Szeged, Hungary*

(Received 22 February 2010; accepted 28 April 2010; published online 3 June 2010)

We experimentally investigated second harmonic generation from an oriented multilayer film of bacteriorhodopsin protein, deposited onto a charged surface. The generated signal is obtained as a function of incidence angle, at different polarization state of both fundamental and generated beams. We show that the measurements, together with the analytical curves, allow to retrieve the nonvanishing elements of the nonlinear optical tensor, including the ones introduced by optical chirality. © *2010 American Institute of Physics*. [doi:10.1063/1.3442503]

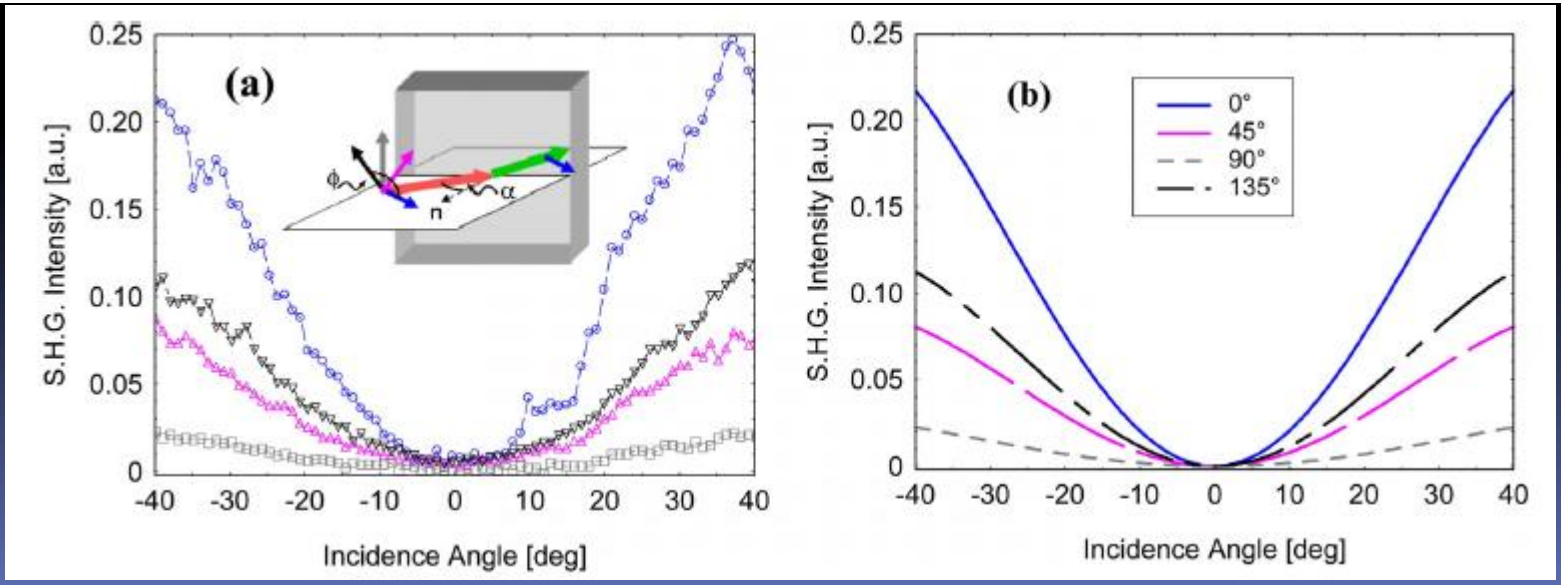

Evidence of multipolar response of Bacteriorhodopsin by noncollinear second harmonic generation

F. A. Bovino,[1,*] M. C. Larciprete,[2] C. Sibilia,[2] G. Váró,[3] and C. Gergely[4,5]

[1]*Quantum Optics Lab., Selex-SI Via Puccini 2 Genova, Italy*
[2]*Dipartimento SBAI, Università di Roma La sapienza, Via A.Scarpa 16 00161 Roma, Italy*
[3]*Institute of Biophysics, Biological Research Center of the Hungarian Academy of Sciences, H-6701 Szeged, Hungary*
[4]*Université Montpellier 2, Laboratoire Charles Coulomb UMR 5221, F-34095, Montpellier, France*
[5]*CNRS, Laboratoire Charles Coulomb UMR 5221, F-34095, Montpellier, France*
[*]*fbovino@selex-si.com*

Abstract: Noncollinear second harmonic generation from a Bacteriorhodopsin (BR) oriented multilayer film was systematically investigated by varying the polarization state of both fundamental beams. Both experimental results and theoretical simulations, show that the resulting polarization mapping is an useful tool to put in evidence the optical chirality of the investigated film as well as the corresponding multipolar contributions to the nonlinear.

→ **magnetic-dipole contributions to the quadratic nonlinear response in BR**

3350 Biophysical Journal Volume 77 December 1999 3350–3355

Second Harmonic Generation of Glucose Oxidase at the Air/Water Interface

J. Rinuy, P. F. Brevet, and H. H. Girault
Laboratoire d'Electrochimie, Ecole Polytechnique Fédérale de Lausanne, CH-1015 Lausanne, Switzerland

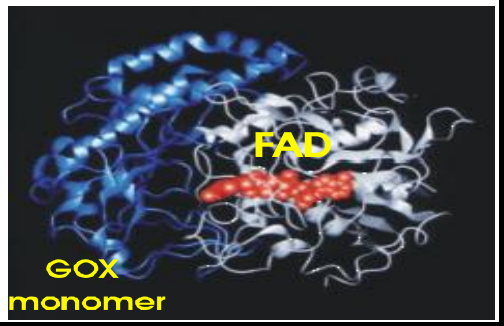

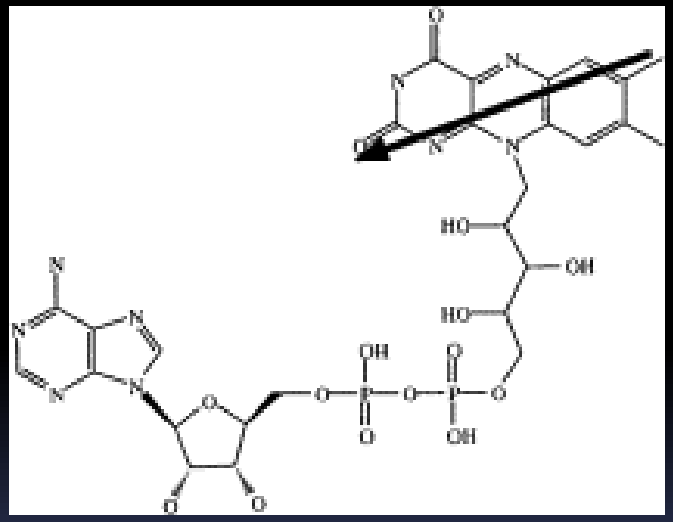

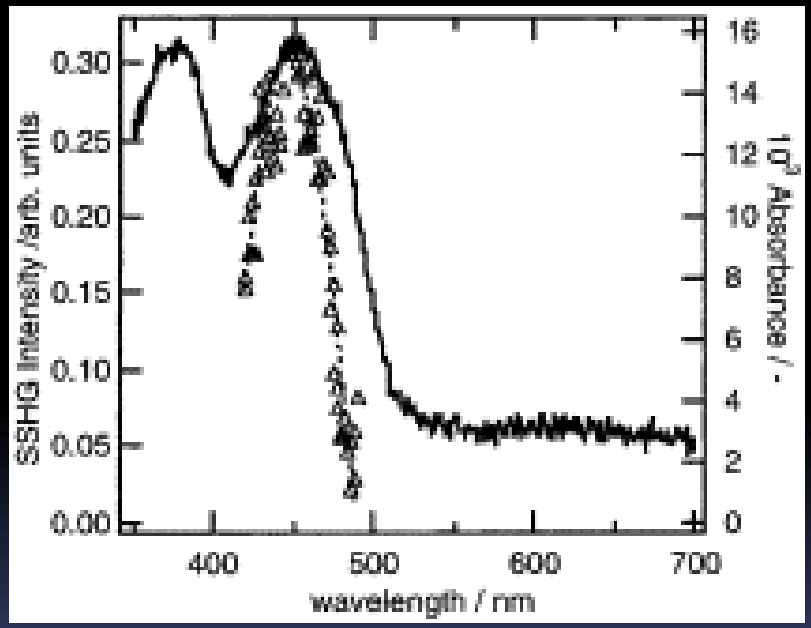

Structure of the FAD chromophore. The π-π^* transition moment probed by SHG has an angle of orientation of ~35° with respect to the axis of the three cycles of the isoalloxazine ring

Lasers in health care

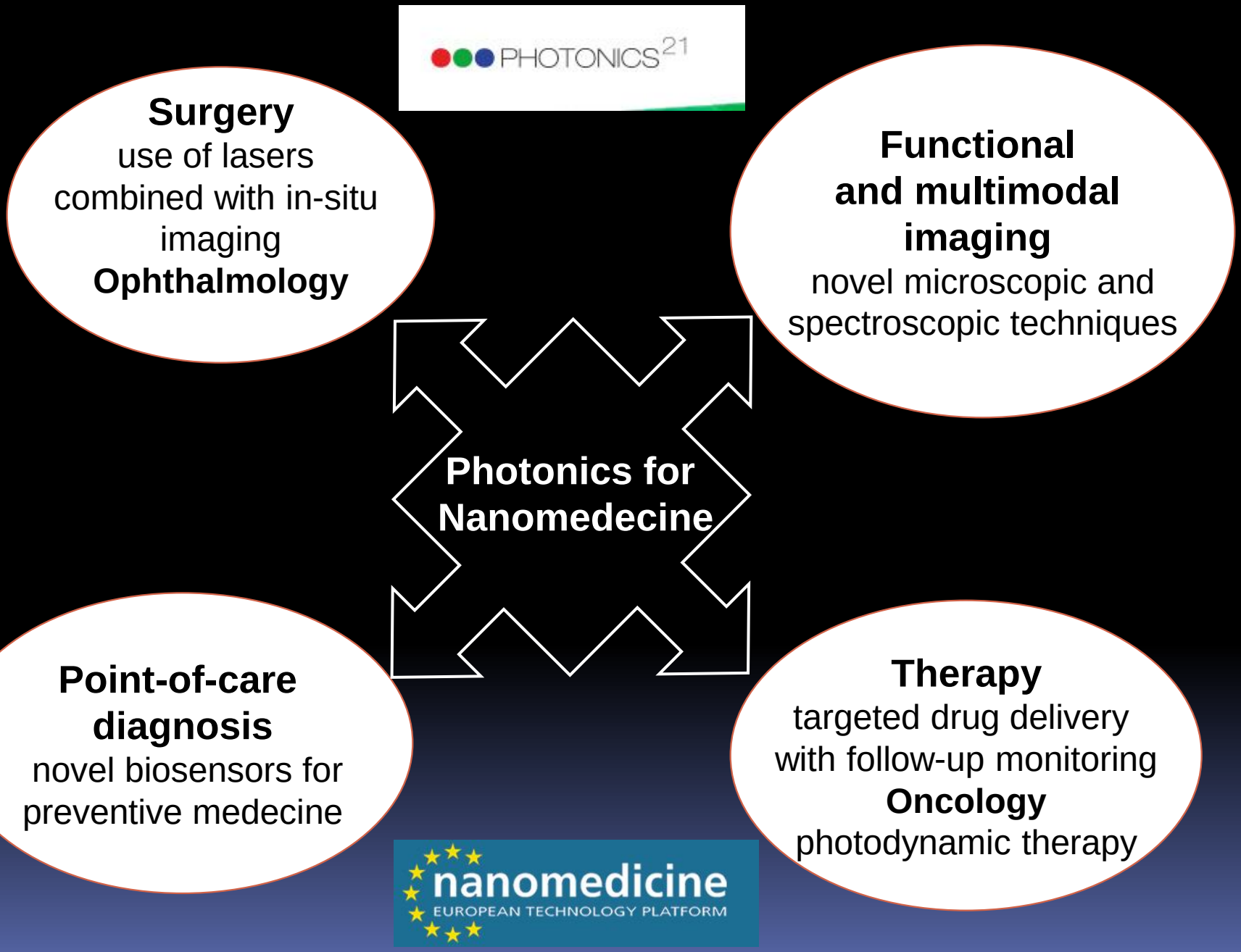
PHOTONICS21
Surgery
use of lasers
combined with in-situ
imaging
Ophthalmology
Functional
and multimodal
imaging
novel microscopic and
spectroscopic techniques
Photonics for
Nanomedecine
Point-of-care
diagnosis
novel biosensors for
preventive medecine
Therapy
targeted drug delivery
with follow-up monitoring
Oncology
photodynamic therapy
nanomedicine
EUROPEAN TECHNOLOGY PLATFORM

Lasers in medecine

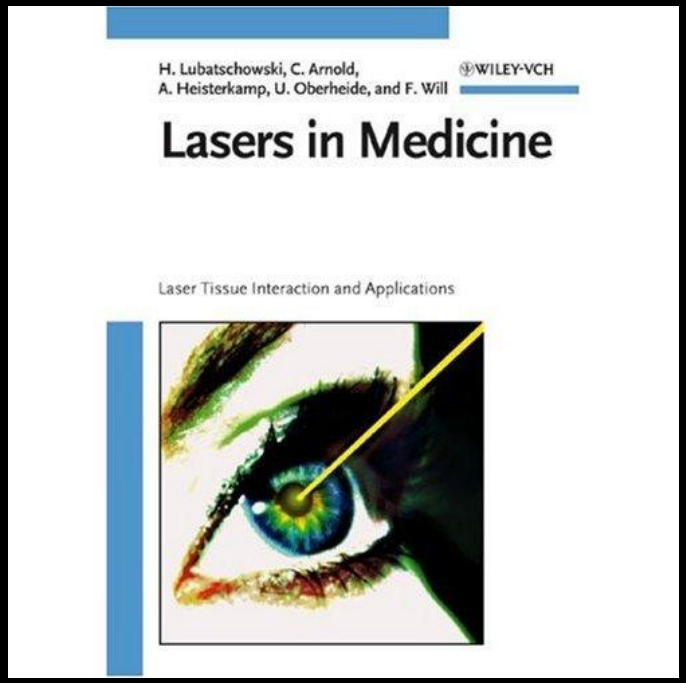

CO_2 laser → Photoablation removing cell layer by cell layer by volatilizing the water (ads. in IR)

Argon laser → emits blue/green light for treating hemoglobin and hemosiderin-containing lesions (Hb. ads in violet and blue/green)

Excimer laser → Photoablation: the tissue absorbs the high energy ultraviolet photons that are produced

Q-switched (nanosecond) and short-pulsed (picosecond) lasers generate very high power densities (GW cm^{-2}) in focal spots of 25-50mm → creation of a plasma and intense acoustical shock wave in the medium due to the sudden production of an electrical field in 10^{-9} to 10^{-12} seconds

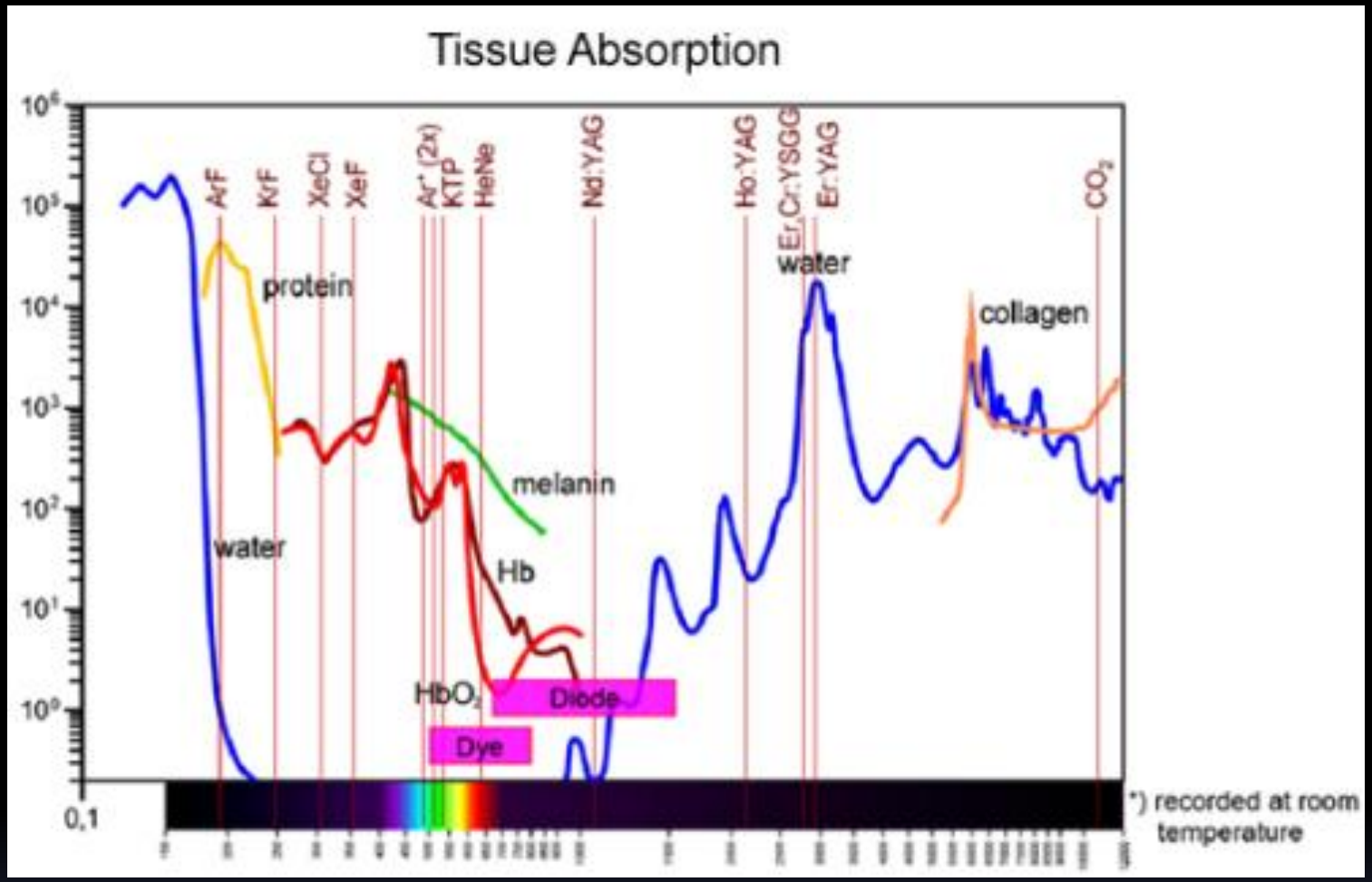

Each wavelength has its own specific absorption rate on different types of tissues containing hemoglobin, water, melanin, hydroxyapatite (if dental tissue).

For each tissue part there are absorption curves that can be used to determine the ideal wavelength to be used.

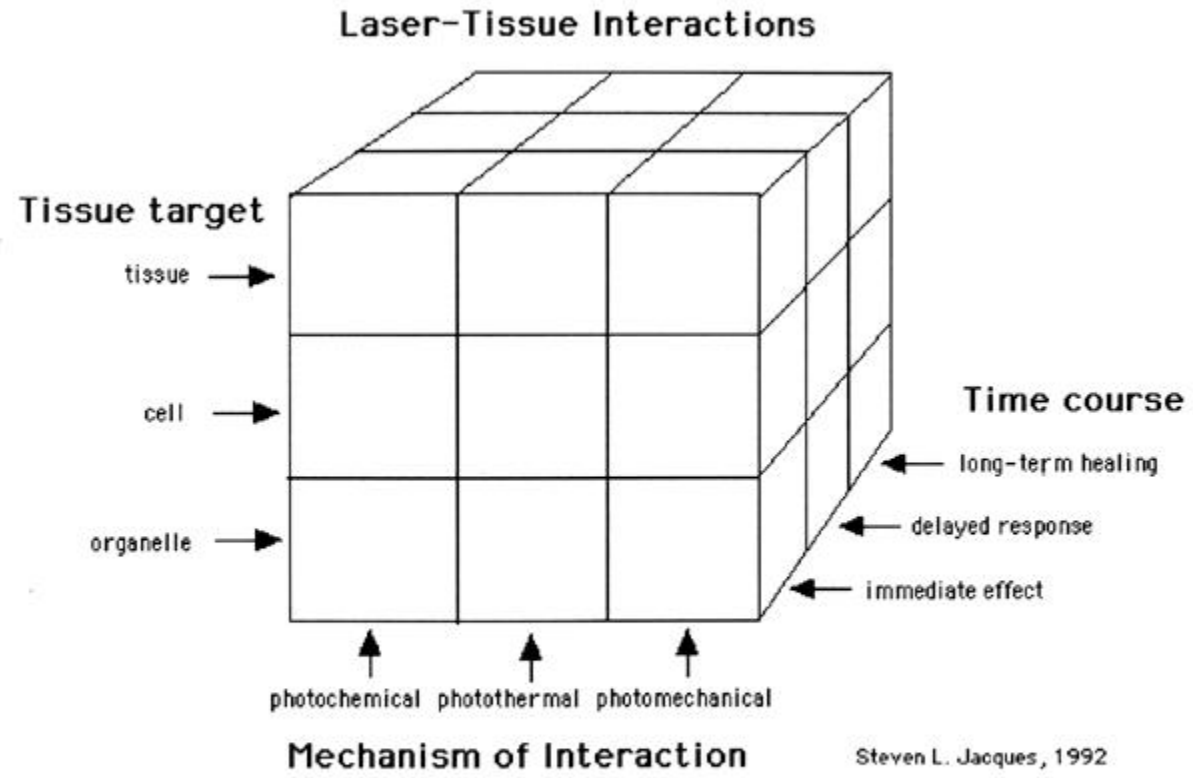

Figure D3.1.17. Cube of laser–tissue interactions. A laser–tissue interaction can involve various mechanisms of interaction, time courses and tissue targets. (Adapted from Jacques 1992 *Surgical Clinics* 72:531–558.)

Controlling tissue heating is an important consideration for the laser surgeon
At 37-60°C, tissue retracts
Above 60°C, there is protein denaturation and coagulation
At 90-100°C, carbonization and tissue burning occur
Above 100°C, the tissue is vaporized and ablated

Typical tissue optical penetration depths

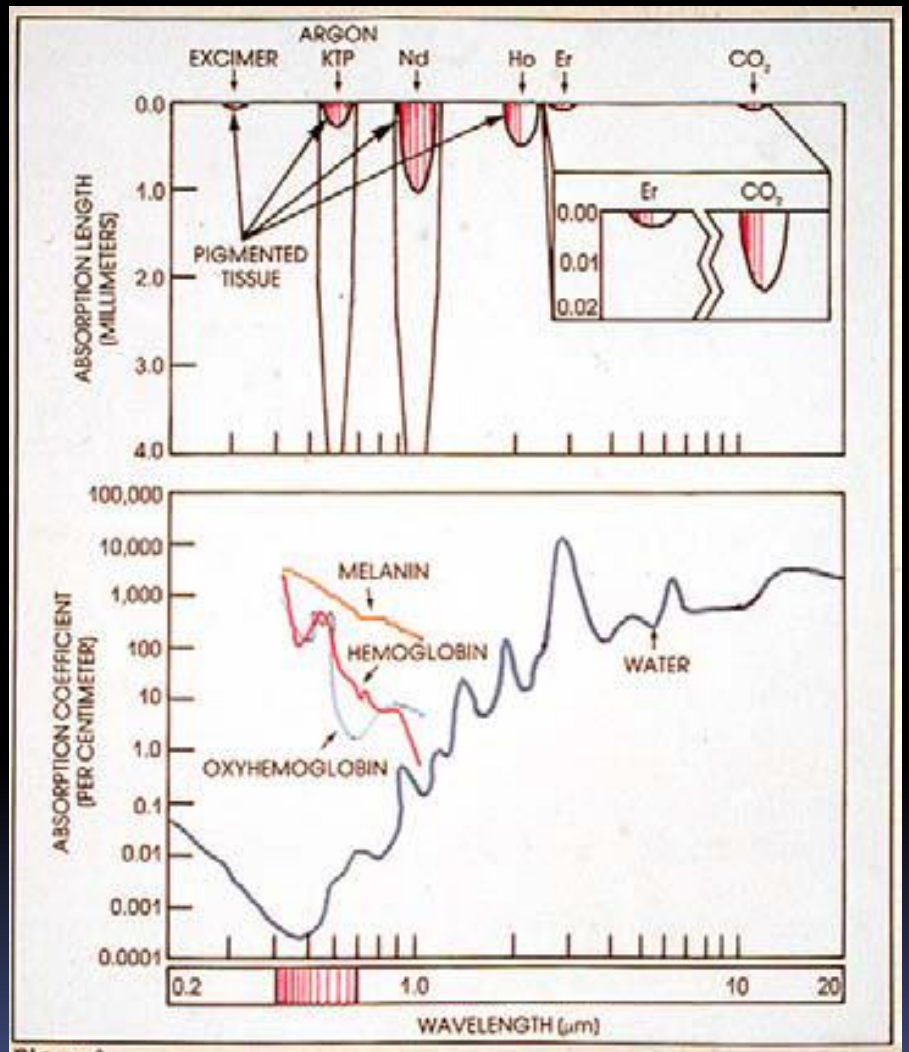

Figure 2.
Laser absorption and tissue penetration.

The main absorbing components, or chromophores, of tissue are:
- Hemoglobin in blood
- Melanin in skin, hair, moles, etc.
- Water (present in all biologic tissue)
- Protein or "Scatter" (covalent bonds present in tissue)

Tissue interaction terms:
Electromechanical : dielectric breakdown in tissue caused by shock wave plasma expansion resulting in localized mechanical rupture
Photoablative : photodissociation or breaking of the molecular bonds in tissue
Photothermal converts light energy into heat energy; tissue heat up and vaporize
Photochemical: target cells start light-induced chemical reactions

Guided surgery with ultra-short pulsed laser light

Plasma-mediated ablation of biological tissue with ultra-short laser pulses

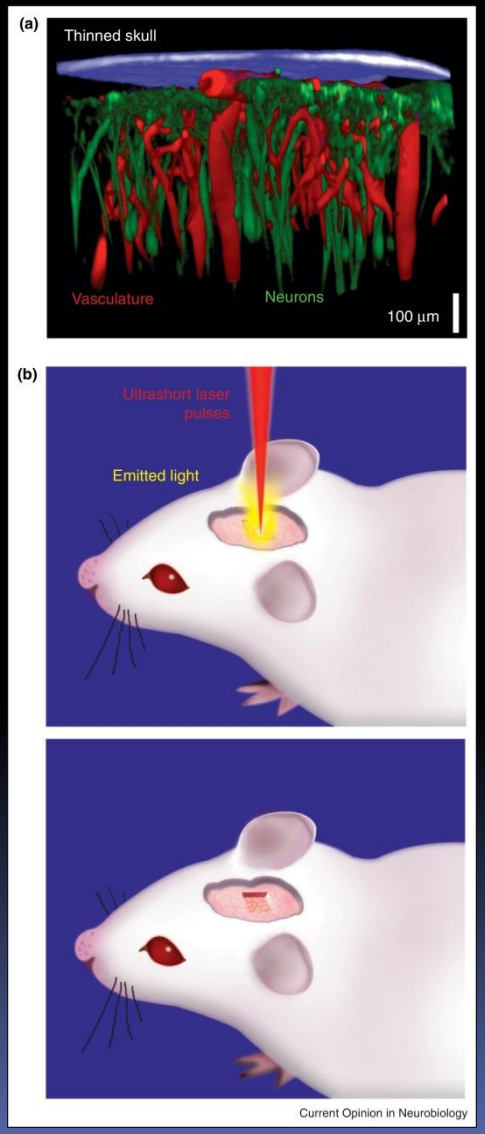

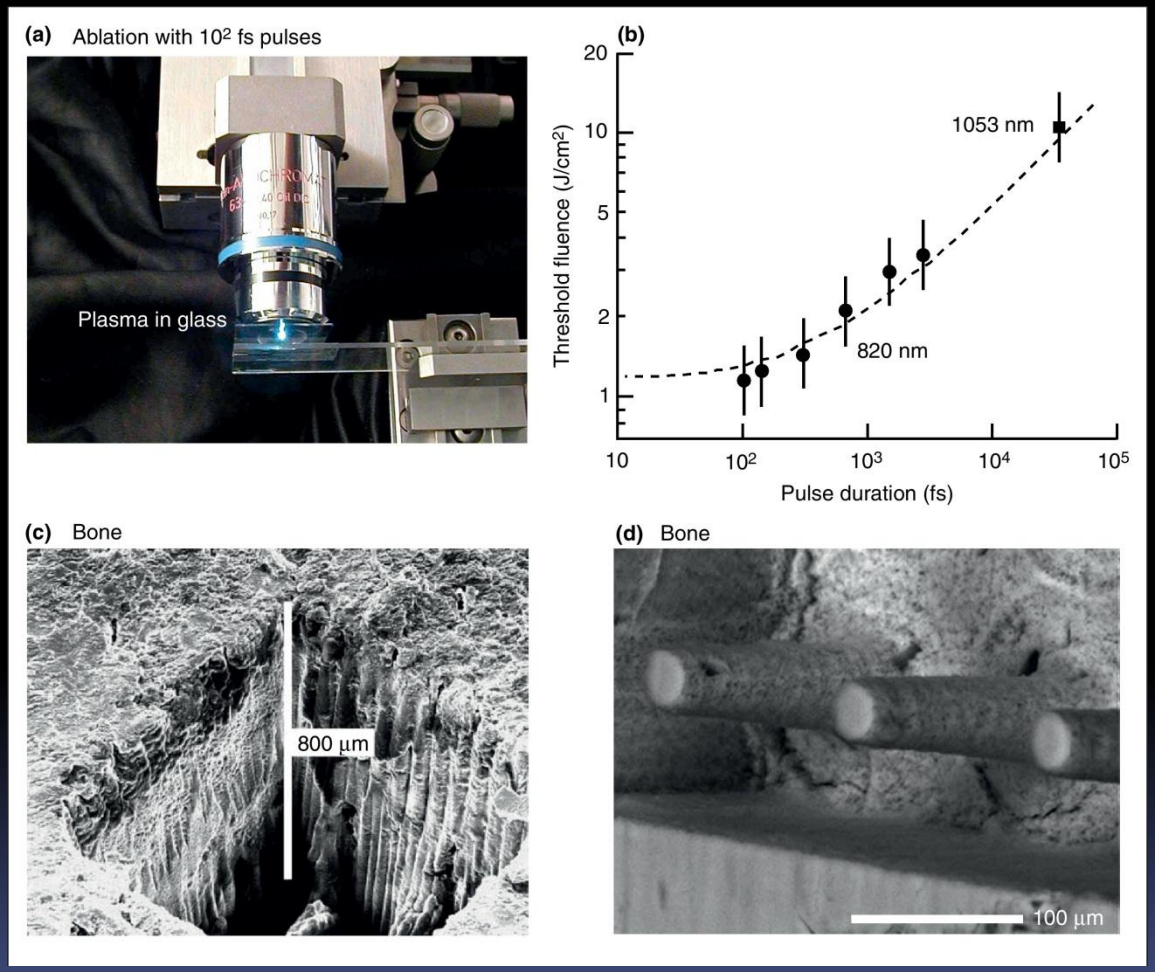

Scanning electron micrograph of a porcine long bone and a patterned bone cut in air.

D. Jeong et al. Curr. Opp. Neurobiol. 22, 2012

The physics of plasma-mediated ablation for cutting tissue

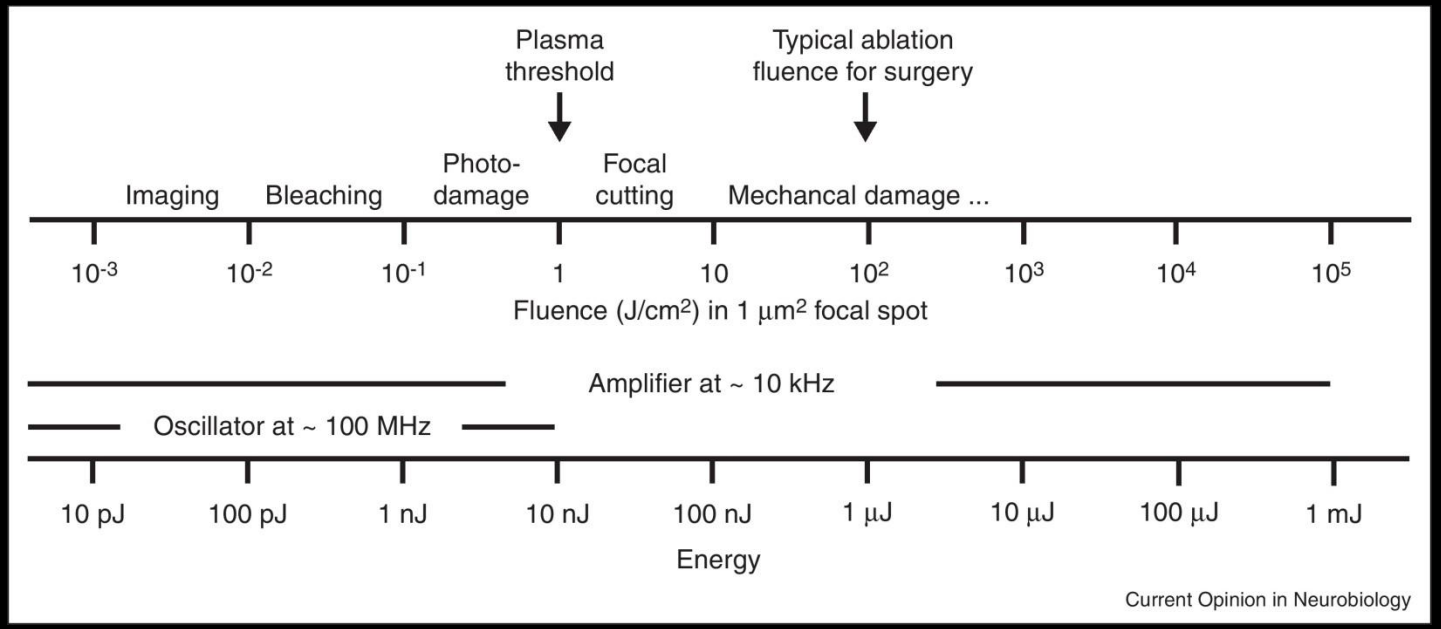

Energy fluence = the energy per unit area in the pulse

EX:

A 10-nJ, 100-fs pulse focused to an 1 μm^2 area yields a fluence of 1 J/cm^2 or an intensity of 10 TW/cm^2.

This is equivalent to an electric field of $\sim 10^8$ V/cm or ~1 V/Å, which approaches the ~10 V/Å Coulomb field seen by valence electrons in atoms and molecules and leads to significant electron tunneling that frees bound electrons from their molecular orbitals **to form a plasma.**

Laser Surgery: conventional and novel

A minimal invasive corneal ablation inside the cornea using a femto-second laser system

New: frequency tripled solid state lasers
- Microplasma in the focal spot (1μm)
- All material is fragmented in the focal point
- Duration 3 ns, thus no heat effect

Laser Microsurgery

Microinjection

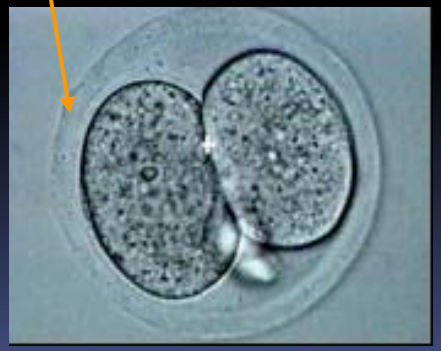

Laser fusion

The force of focused light – Optical Tweezers

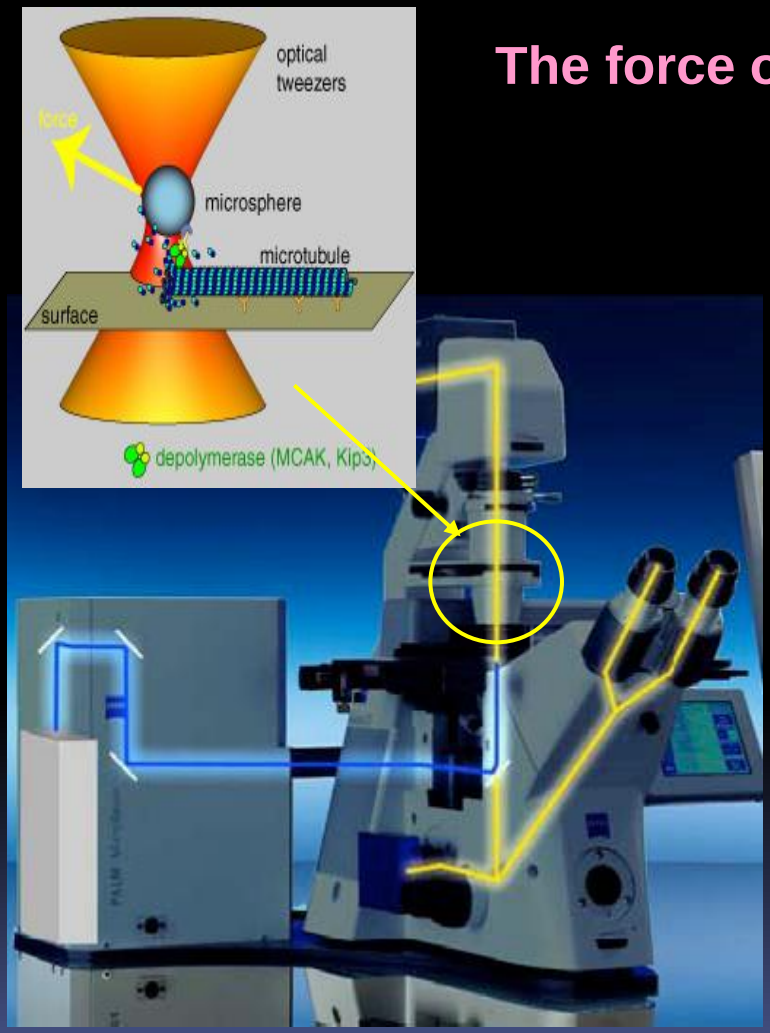

Lasers coupled into microscopes
→ precise micromanipulation tools

- Catch, move viruses, bacteria or cells
- Force measurements: binding forces between molecules, organelles
- Cell fusion
- Laser microdissection of cells

Single kinesin molecules studied with a molecular force clamp

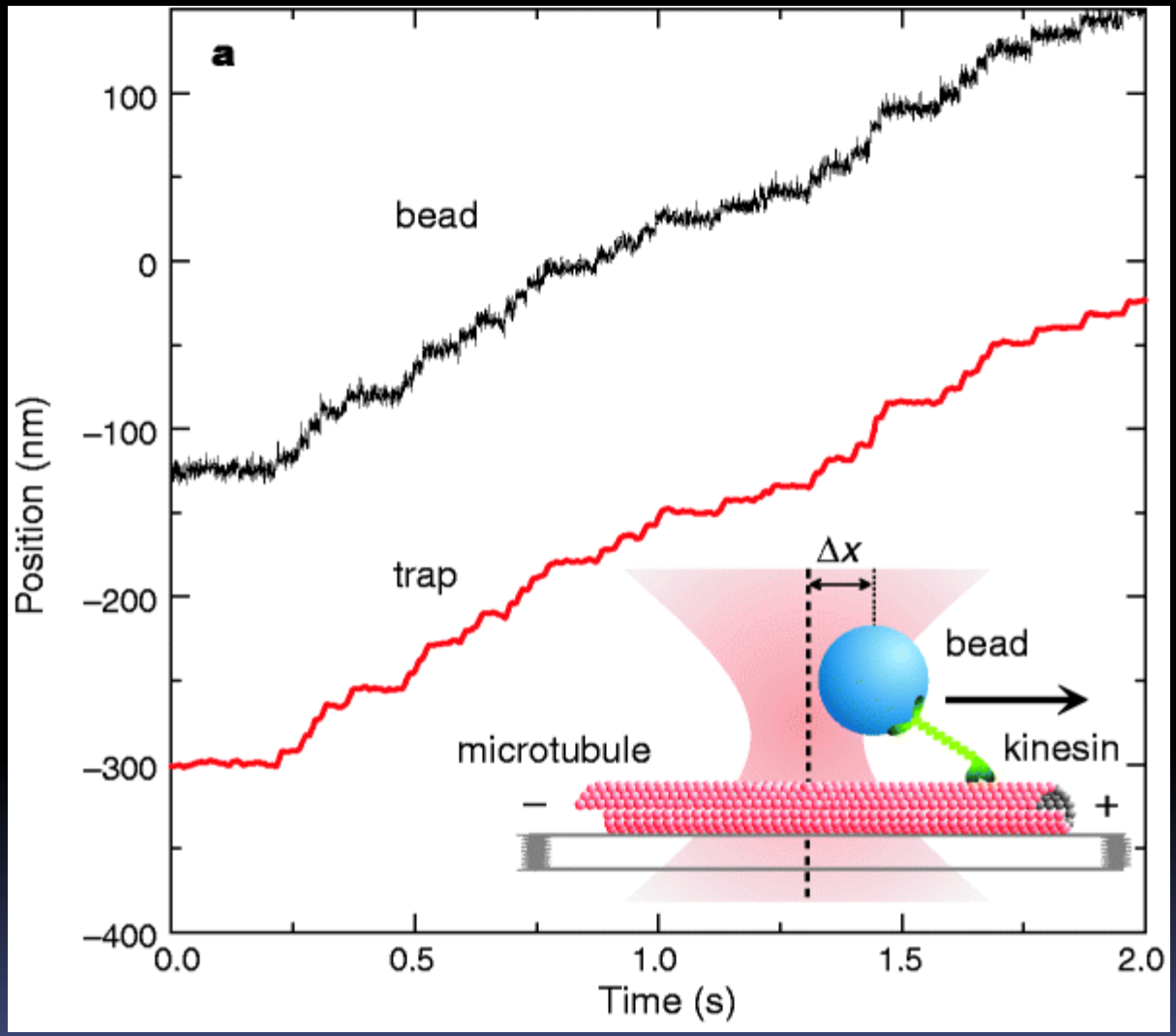

Koen Visscher, et al. *Nature* **400**, 1999

Bioimaging:

Functional and spectroscopic microscopies

Photonics → novel functional and spectroscopic microscopies

Fluorescence 3D imaging combined with FRET

Fluorescence Lifetime Imaging Microscopy (FLIM)

Multiphoton Microscopy (MPM)

Optical Coherence Tomography (OCT)

Combined coherent anti-Stokes Raman spectroscopy (CARS) and two-photon confocal microscope

Scanning near-field microscopy combined with Raman micro-imaging

Near field microscopy

Linear optical (and functional) imaging

Phase contrast microscopy

Differential interference (Nomarski) contrast microscopy

Fluorescence or Förster resonance energy transfer (**FRET) microscopy:** an adaptation of the resonance energy transfer phenomenon to fluorescence microscopy. Used to obtain quantitative temporal and spatial information about the binding and interaction of proteins, lipids, enzymes, and nucleic acids in living cells.

Fluorescence lifetime imaging microscopy (**FLIM**) enables simultaneous recording of both the fluorescence lifetime and the spatial location of fluorophores throughout every location in the image.

Combining FLIM with FRET by monitoring the change in lifetime of the fluorescent donor before and after being involved in resonance energy transfer is considered to be one of the best approaches

Fluorescence imaging combined with FRET, FLIM

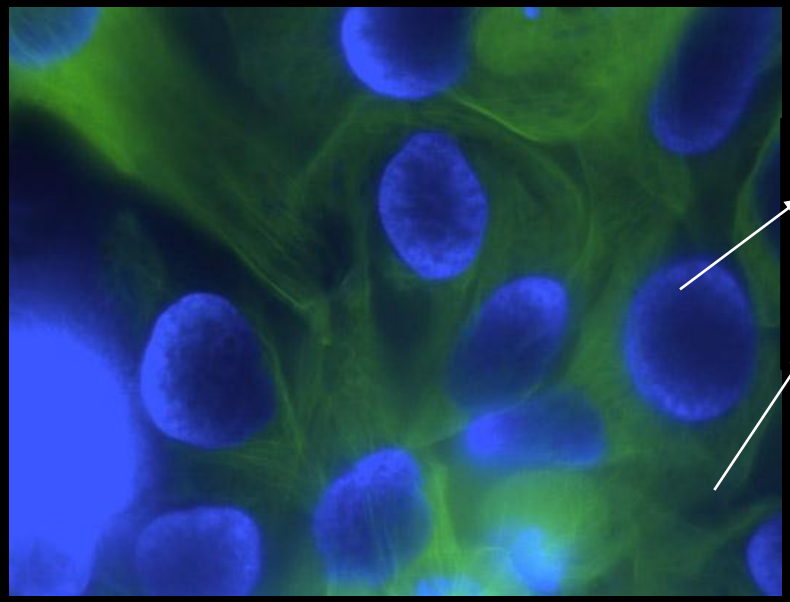

Adenocarcinoma breast cancer cells (MCF7)

nuclei stained with Hoescht 33342
actin filaments stained with Alexa Fluor 488

Cancer cell line of liver

- stained with phospholipids labeled with NBD
- the lifetime is depending on the hydrophobicity

→ lifetime allows to gain information about the molecular structure of cellular compartments

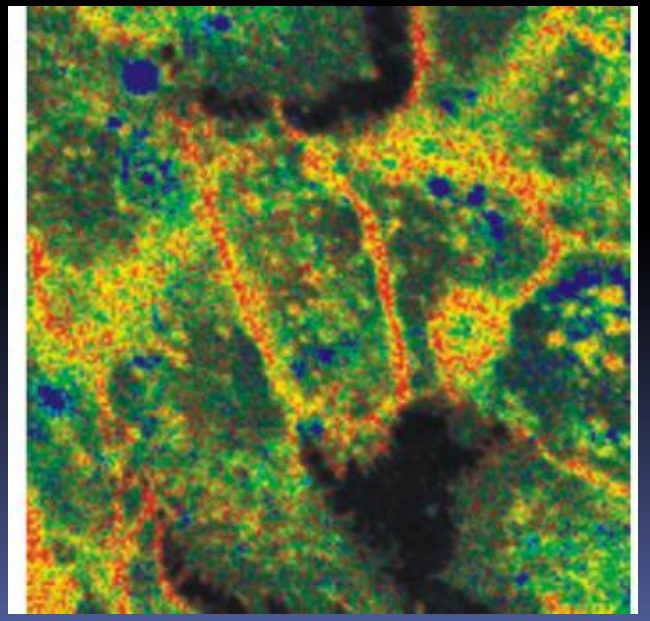

A. Tannert, T. Korte, Humboldt Univ. Berlin, Germany

Translational mobility (lateral diffusion coefficients) of fluorescently labeled macromolecules and small fluorophores can be determined by **fluorescence recovery after photobleaching** (**FRAP**) techniques.

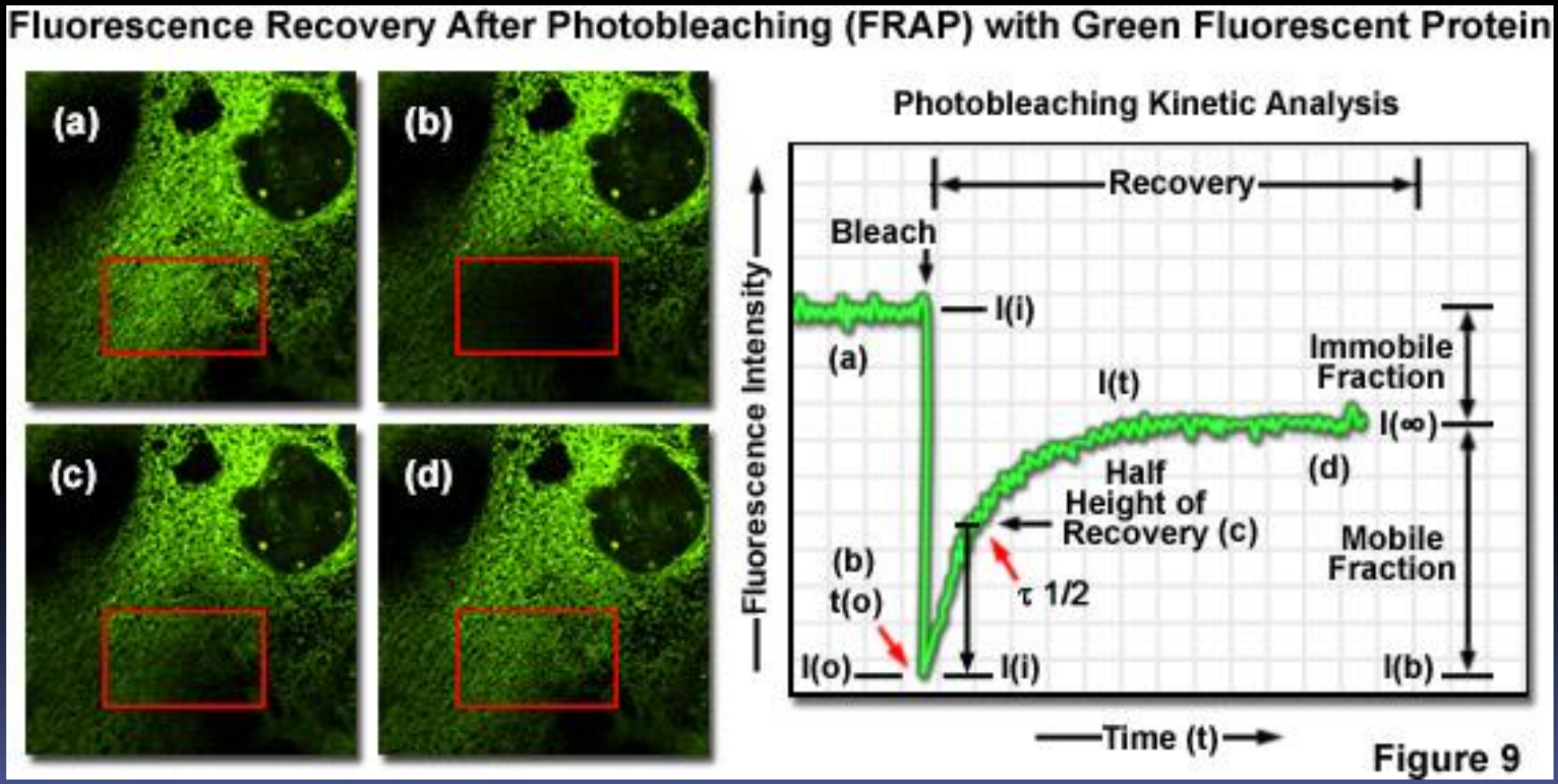

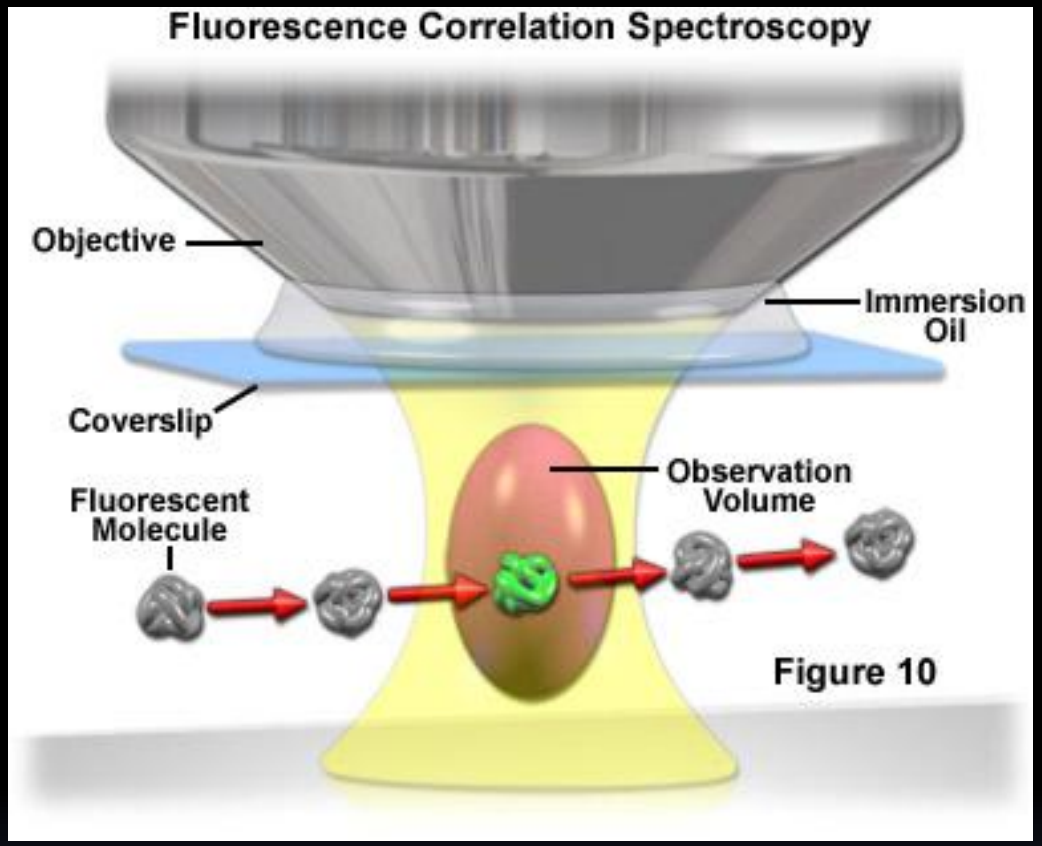

A technique designed to determine molecular dynamics in volumes containing only one or a few molecules, yielding information about chemical reaction rates, diffusion coefficients, molecular weights, flow rates, and aggregation

http://zeiss-campus.magnet.fsu.edu/print/livecellimaging/

Non Linear Optical Phenomena

χ(2)
- **SHG: S**econd **H**armonic **G**eneration
- **SFG: S**um **F**requency **G**eneration
- **EO**: **E**lectro**o**ptic (Pockels) effect

χ(3)
- **CARS: C**oherent **A**nti-Stokes **R**aman **S**cattering
- **TPF: T**wo **P**hoton **F**luorescence
- **THG**: **T**hird **H**armonic **G**eneration

→ NLO Microscopies

- **Confocal**
- **SNOM (S**canning **N**ear Field **O**ptical **M**icros.)
- **Tip** enhanced (plasmon, local field)
- **STED** depletion of stimulated emission
- **MPM** (multiphoton microscopy)
- **CARS** microscopy

Multiphoton Microscopy (MPM)

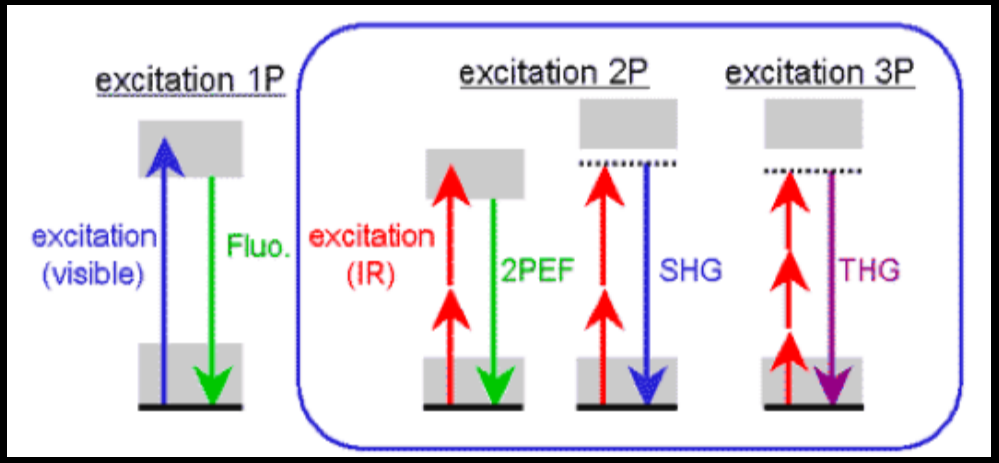

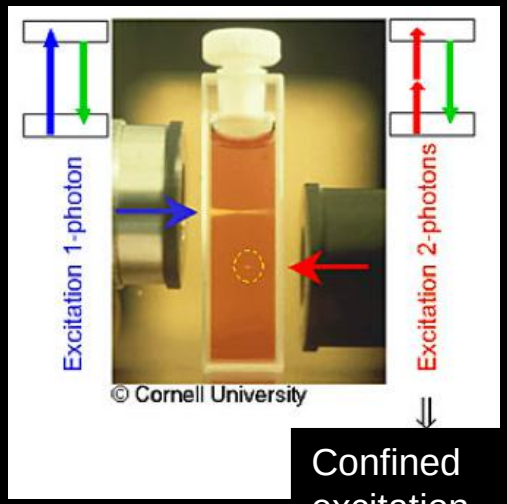

Confined excitation

- The excitation using near-infrared wavelengths allows excellent depth penetration → 400 μm
- Good light confinement in the focal point of the laser
- Laser excitation → non-linear phenomena (2PEF, SHG, THG)
- SH, TH coherent → information on the structure and optical properties of a specimen

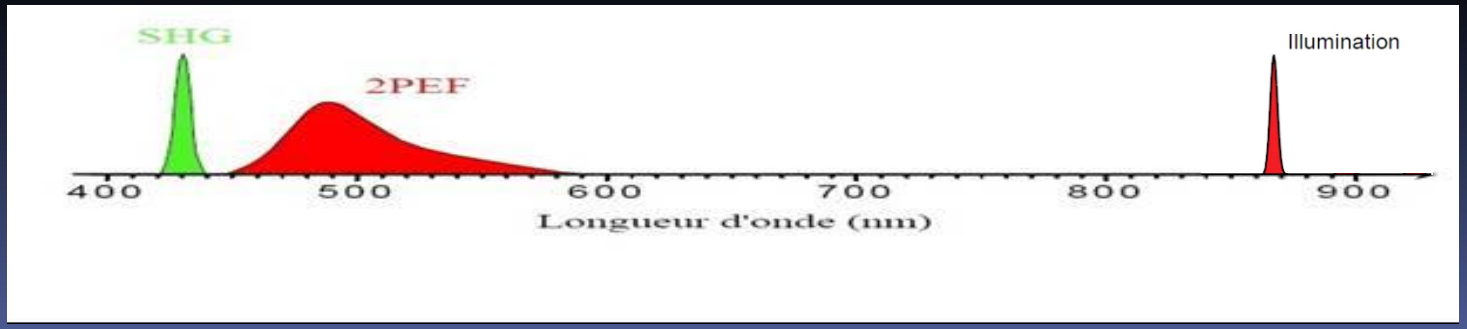

Second harmonic generation (SHG) and two photon fluorescence

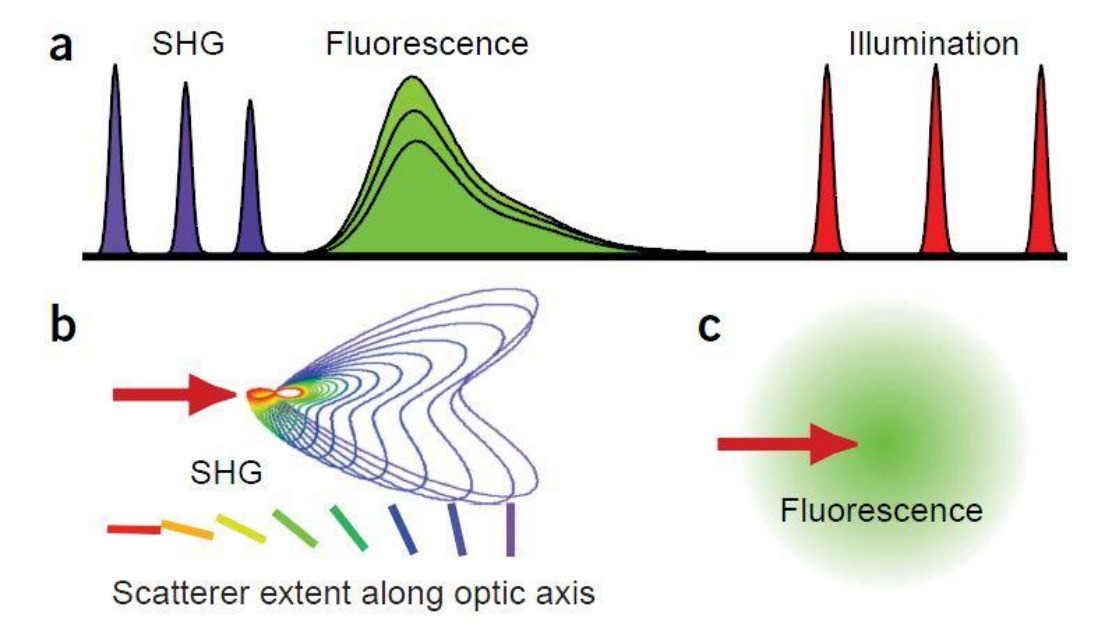

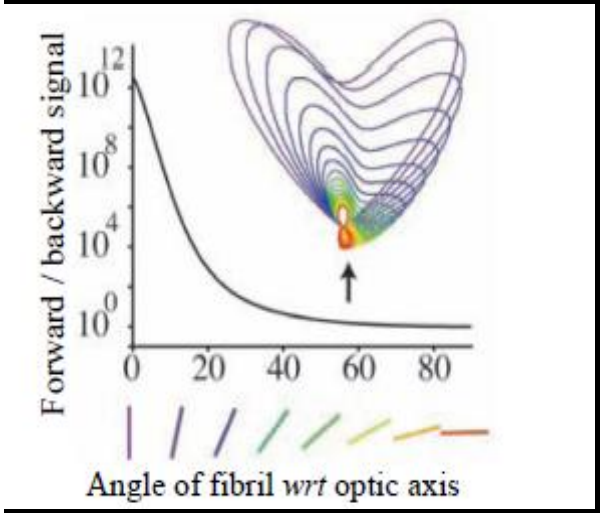

a: SHG emission at half of the excitation wavelength and 2 photon excited fluorescence (2PF)
b, c: SHG is directional depending of dipole orientation whereas 2PF is isotropically emitted

SHG in non-centrosymmetric molecules

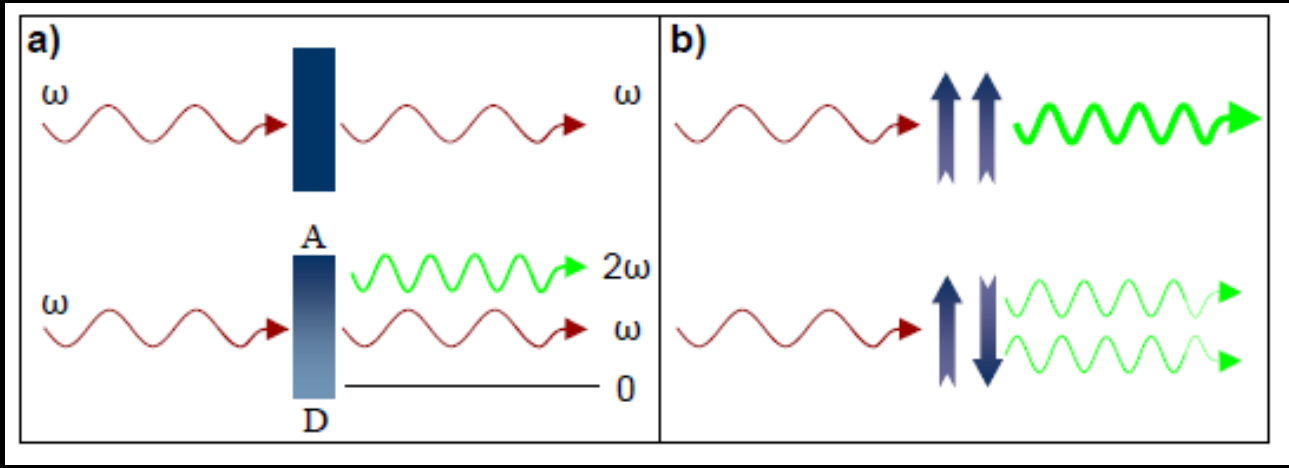

a) *Top*: Excitation of a symmetrical molecule produces a diffuse radiation at the same frequency, called Rayleigh diffusion.
Bottom: A non-centrosymmetric molecule creates additionally a radiation with a double frequency (harmonic diffusion).

b) *Top*: Harmonic diffusion of two molecules located at a distance smaller than wavelength; constructive interference signals for parallel molecules.
Bottom: destructive interference of antiparallel molecules leading to a null signal.

Second Harmonic generation in biological systems
with with polarisable electrons

Ex: chromophores, FAD, NADH

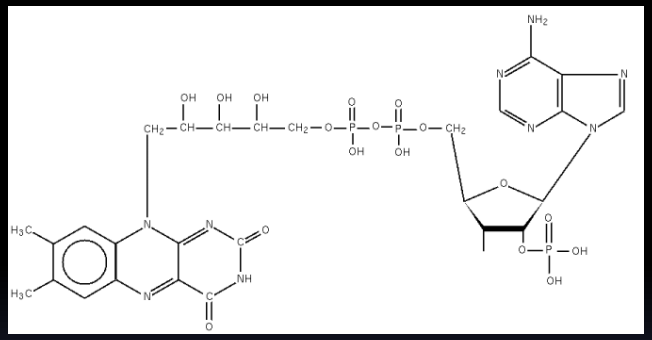

Flavin adenine dinucleotid
(in oxido-reductive enzymes)

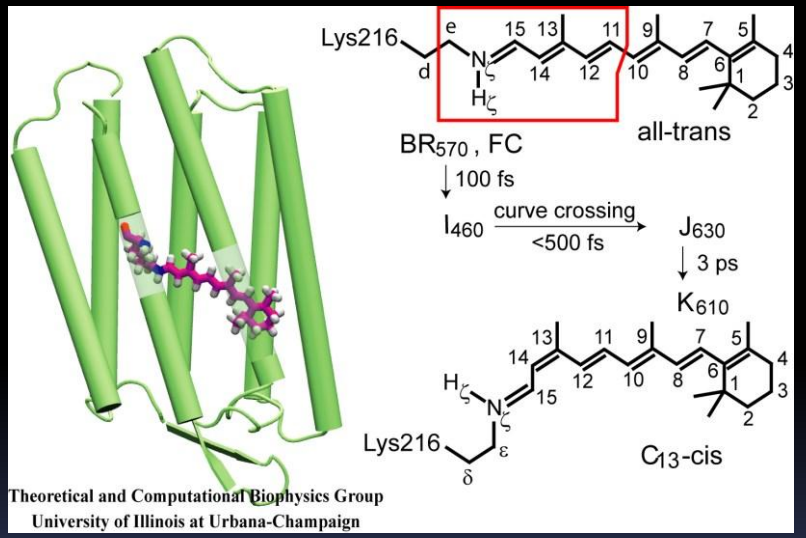

Chromophores
(in chromo/retinal proteins)

Second Harmonic generation in biological systems
with non-centrosymmetry

Ex: collagen, microtubules, sarcomères

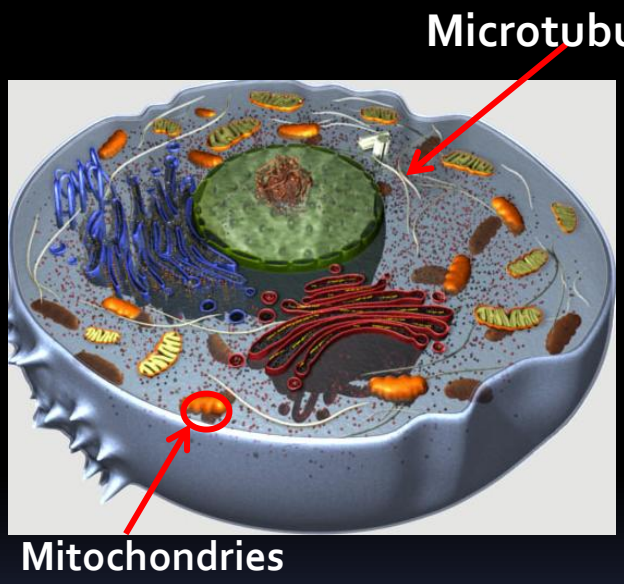

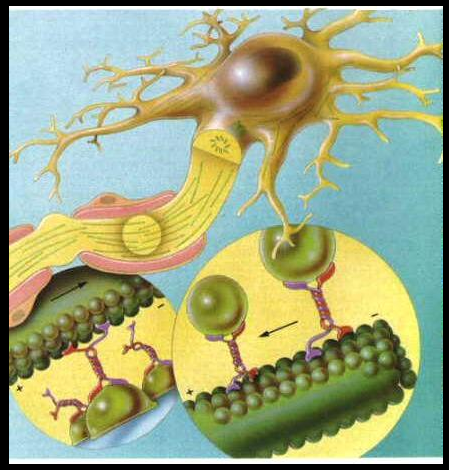

Microtubules
= target of chimio-therapeutic treatment in cancer

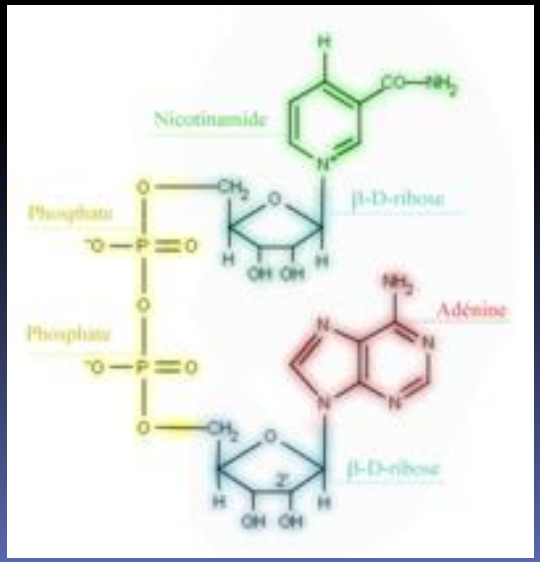

NAD, NADH
in mytochondries

Monitoring SHG intensity f(polariz):
→ orientation of microtubules

$$r = \frac{I_{par} - I_{perp}}{I_{par} + 2I_{perp}}$$

Microtubules in mammalian cancerous MCF7 cells

treatment

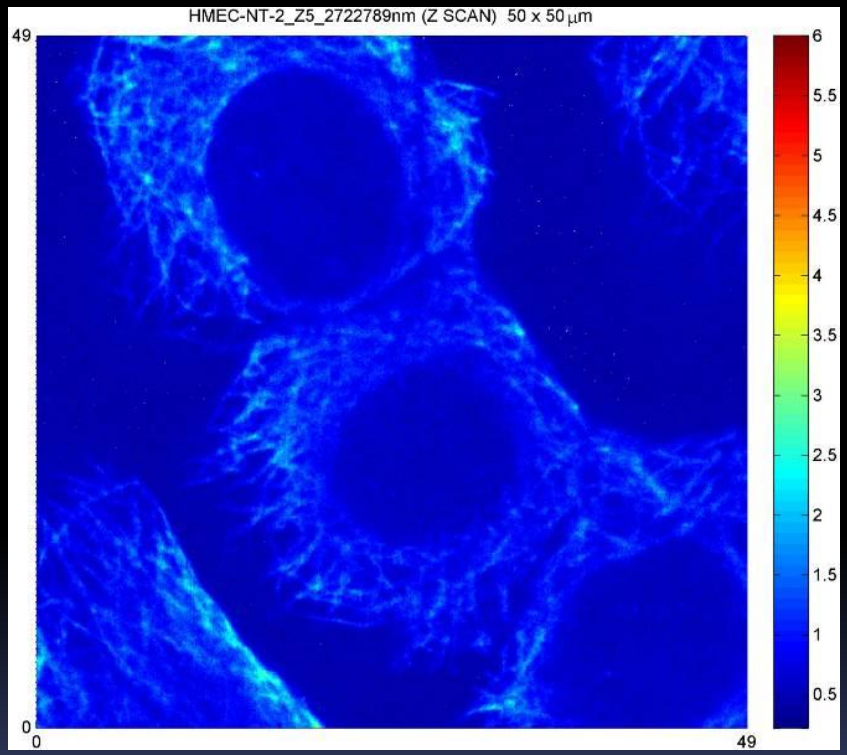

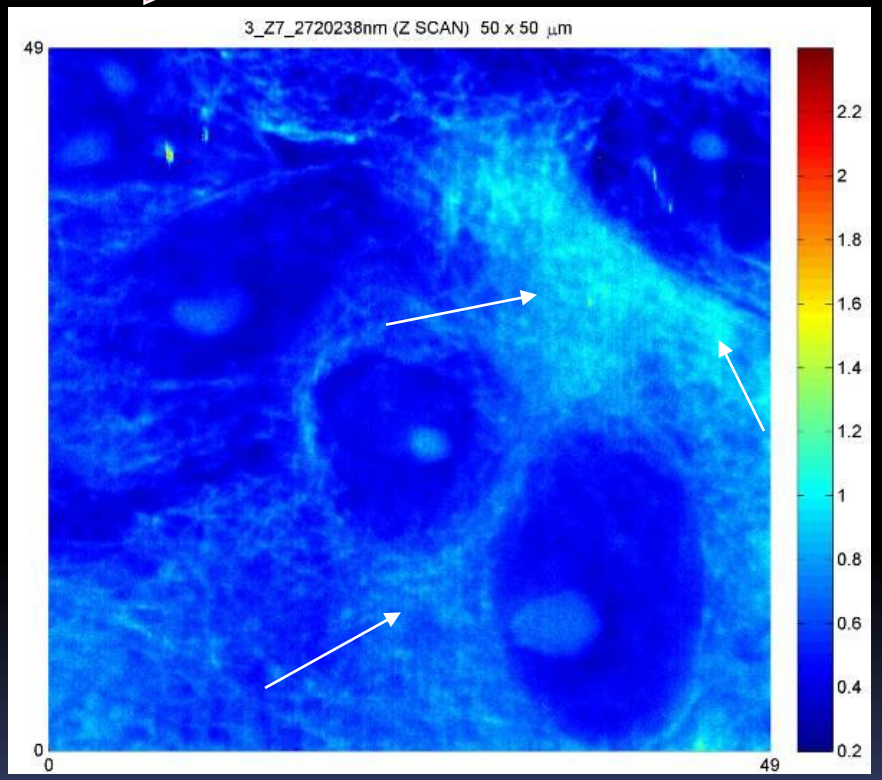

Modification in microtubules organisation
after an oncologic treatment

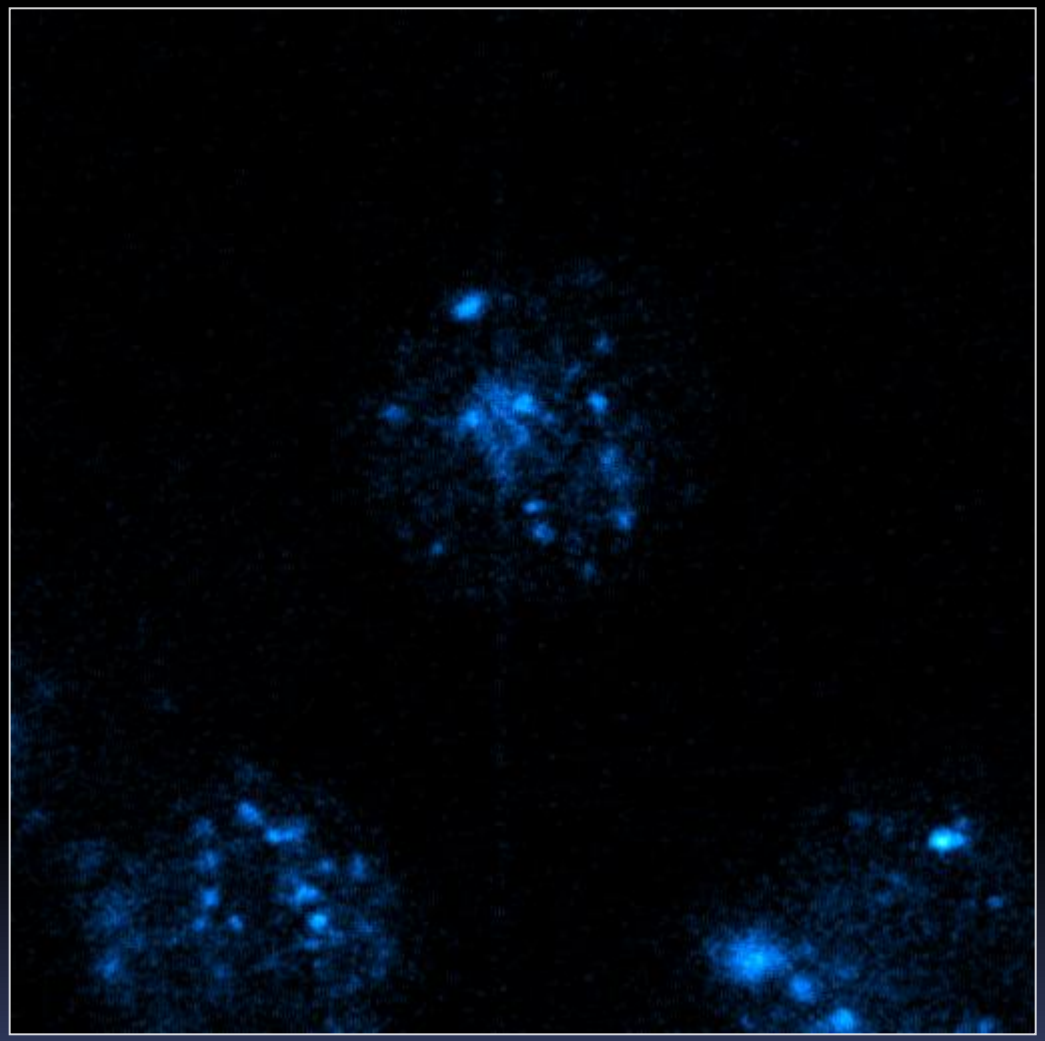

The mitotic spindle (young microtubules) and the mitocondries have a contrast in SHG

Cancerous live cells in division

as seen in MPM- SHG (no labeling needed)

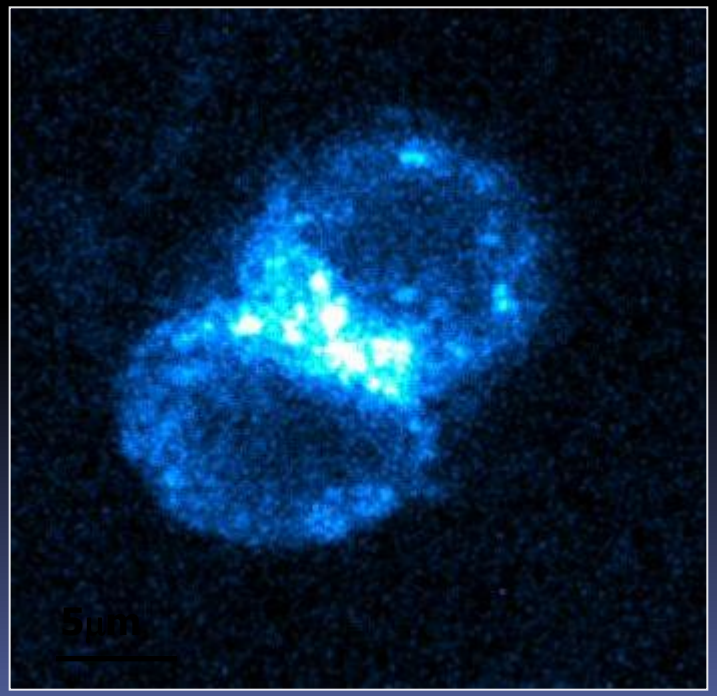

Regenerative growth mode of neurons after injury

Sensory neurons

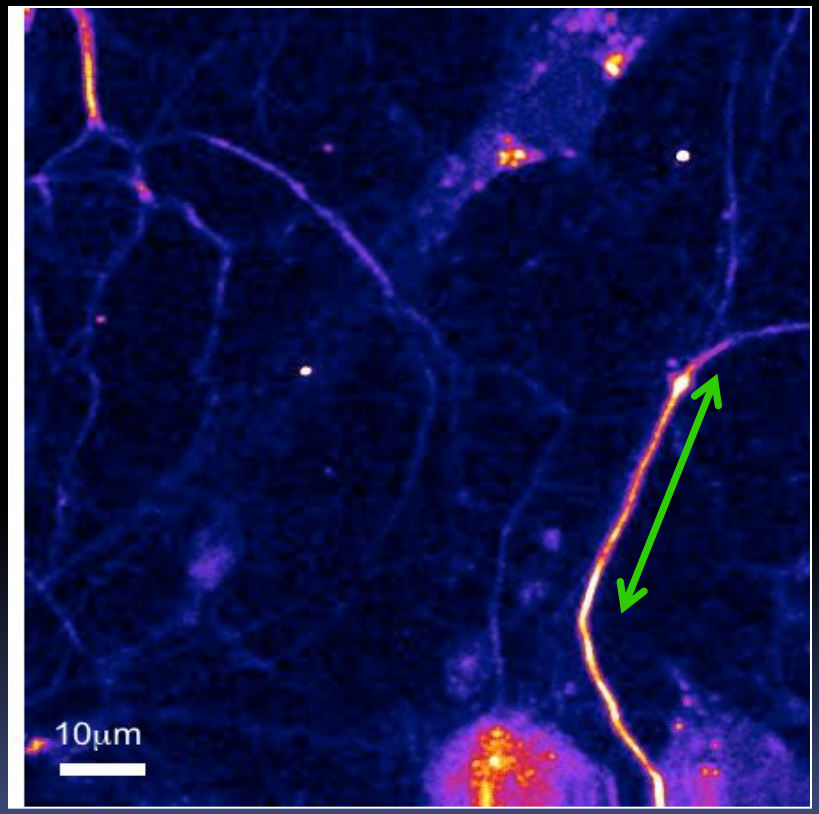

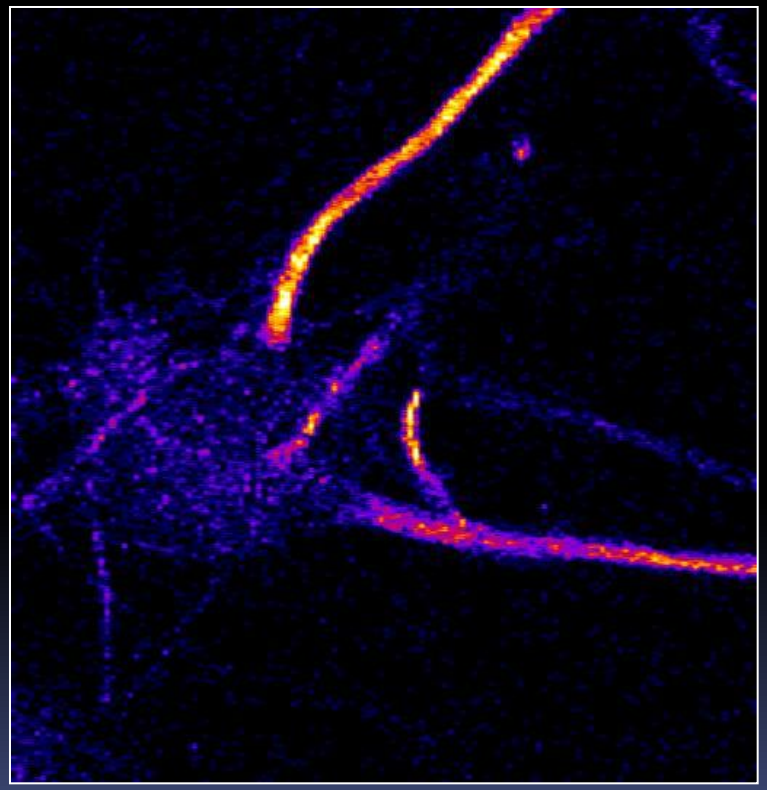

SHG emission in the axones and mitochondries

Monitoring neuronal activity by measuring membrane potential variations of a light-excitable chromophore FM4-64

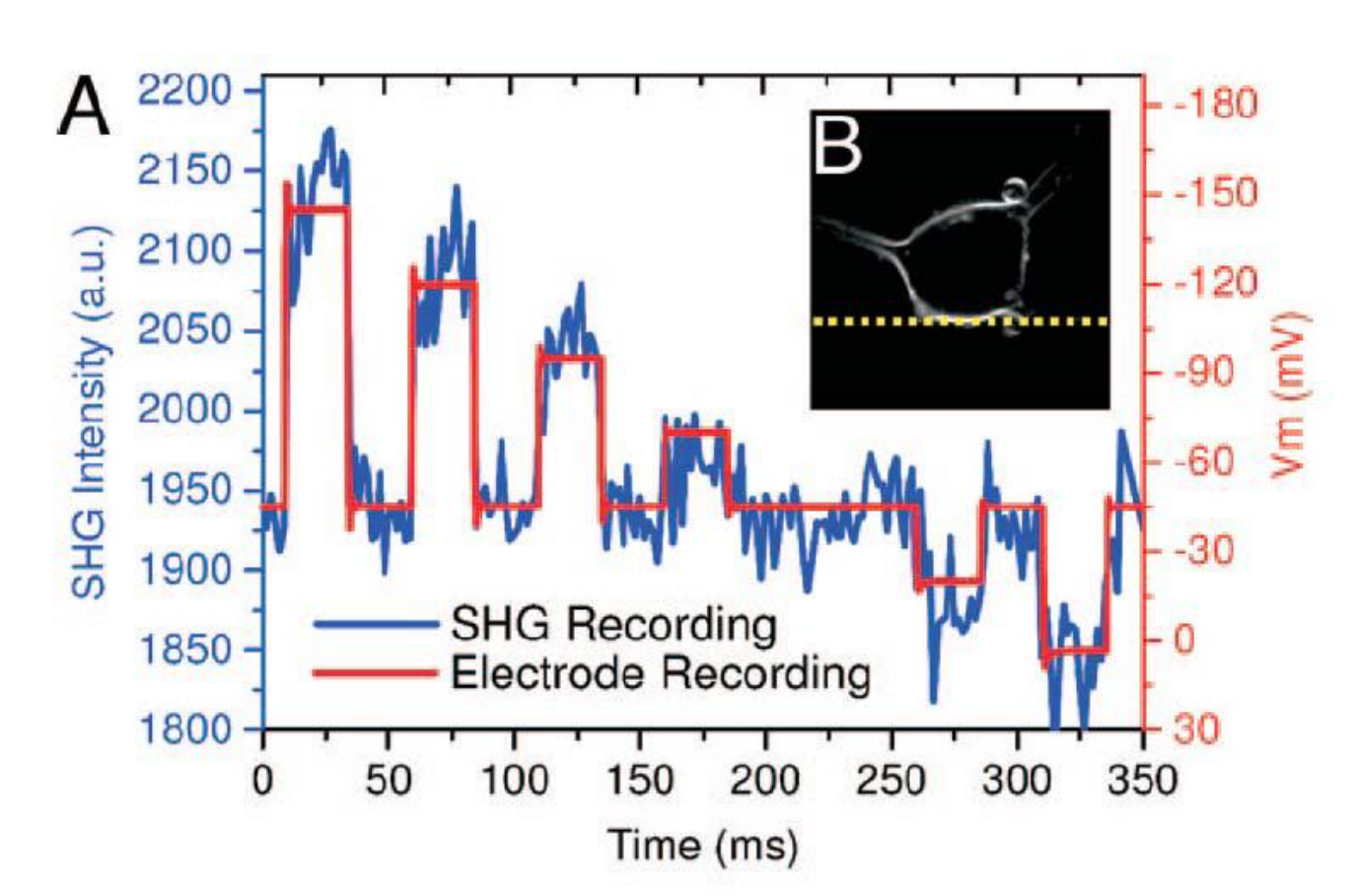

SHG line scan recording V_m during voltage steps in a patch-clamped neuron filled with FM4-64

Sacconi, PNAS 103, 3124 (2006)

Polarization anisotropy of SHG on neurons
→ The molecular orientation is deduced

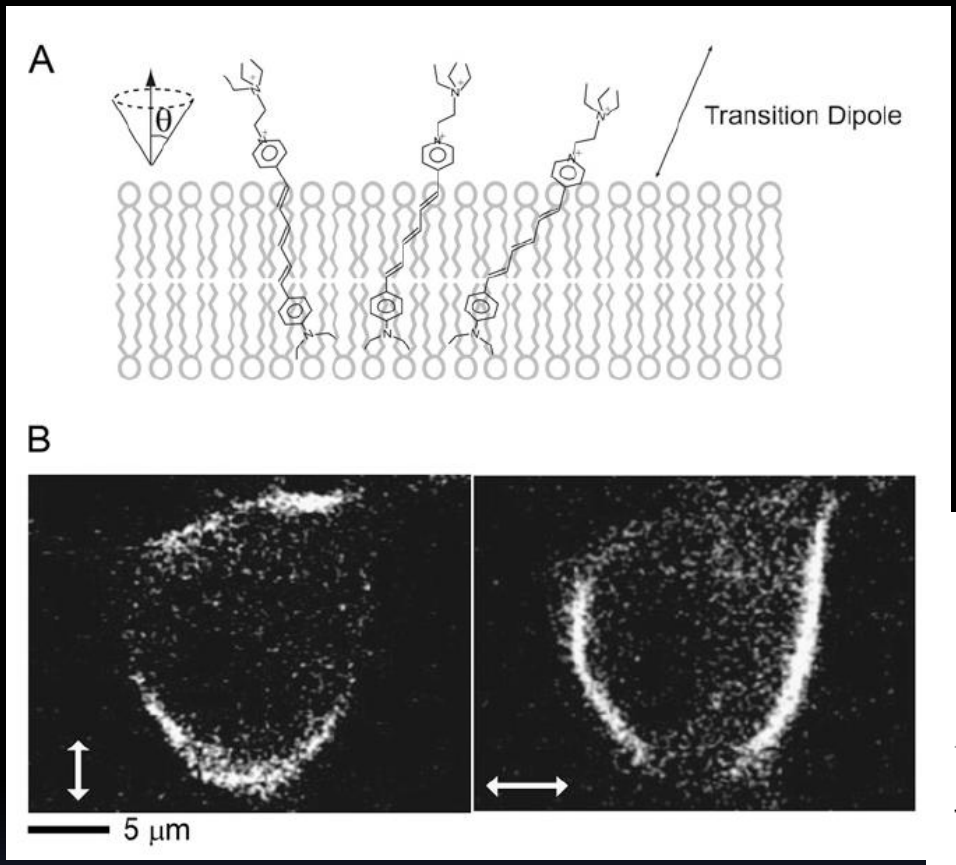

(A) Simplified representation of FM 4-64 geometry in membrane.
Arrow = average orientation of the uniaxial hyperpolarizability,
with θ = tilt-angle to membrane normal

(*B*) Membrane SHG signals polarization dependence;
arrow indicates laser polarization.

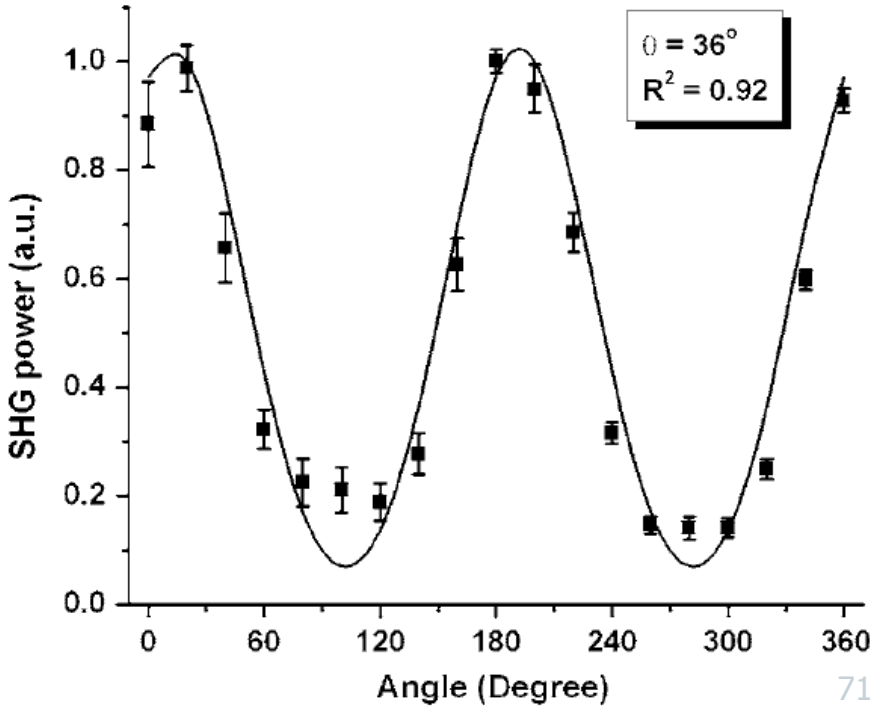

Jiang, Biophys J. 107, L26 (2007)

Dental Tissue

Healthy Dentin: perpendicular to canalicules

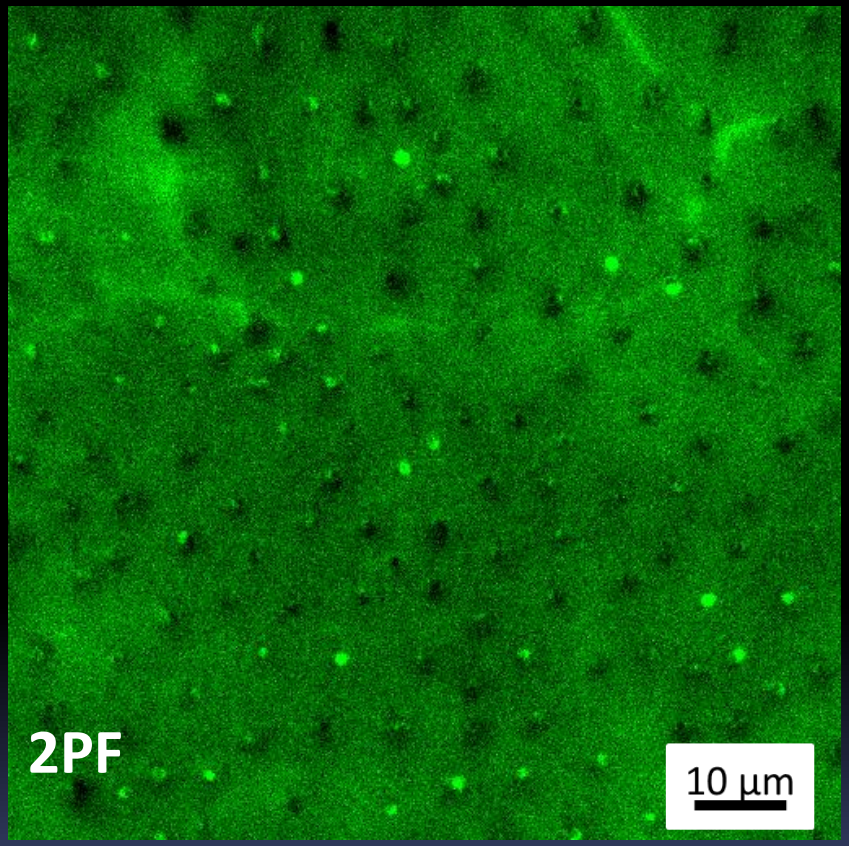

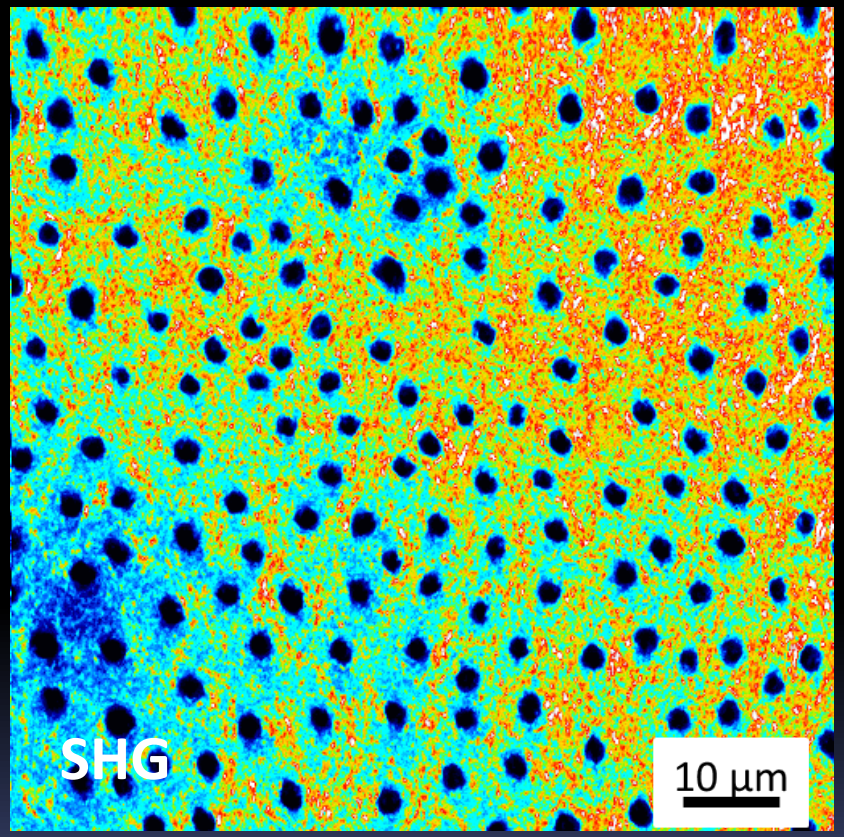

MPM images recorded after a Ti-Sa (120 fs) laser excitation (840nm)

Zoom on a healthy dentin

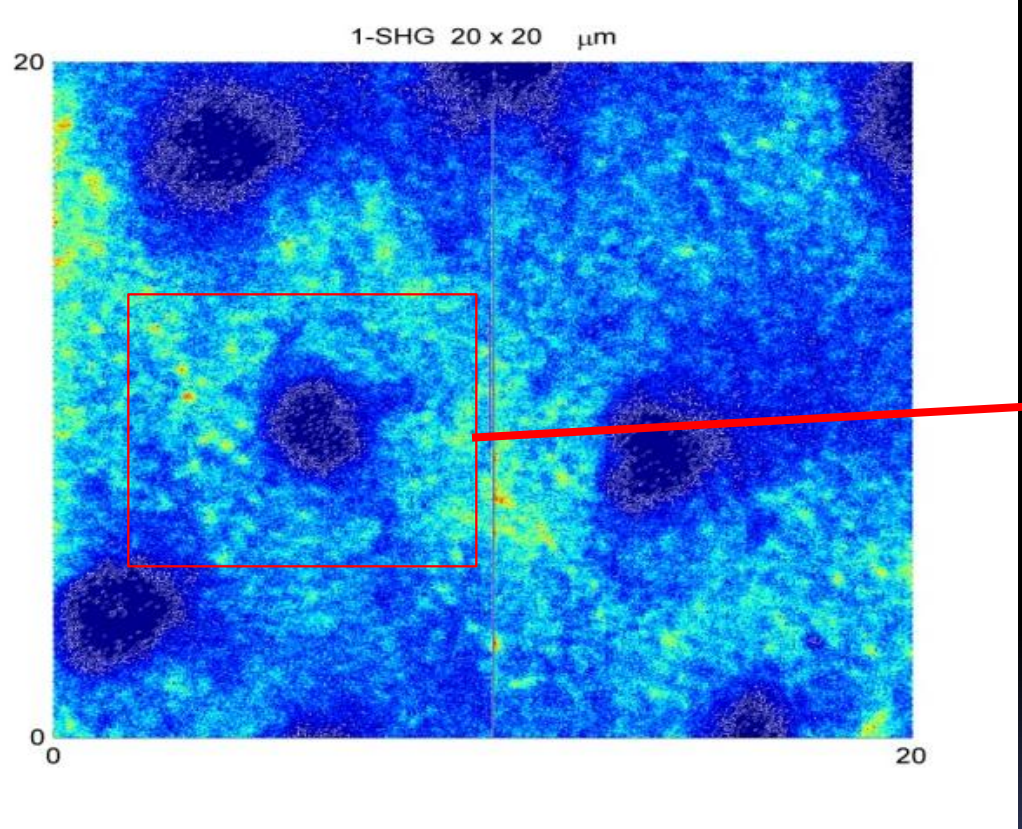

300nm globular structures.

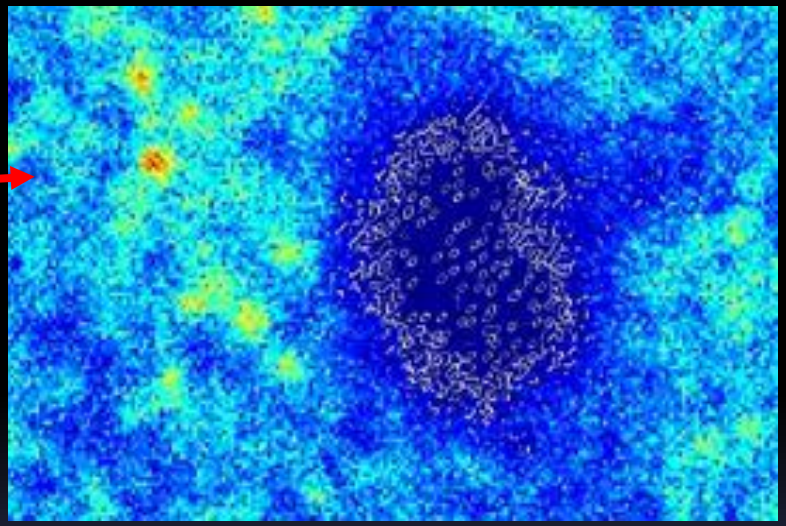

SHG, $h\nu_{laser}$= 797nm, PM: 800V, laser filter: 4+20% ot-filter: 398nm

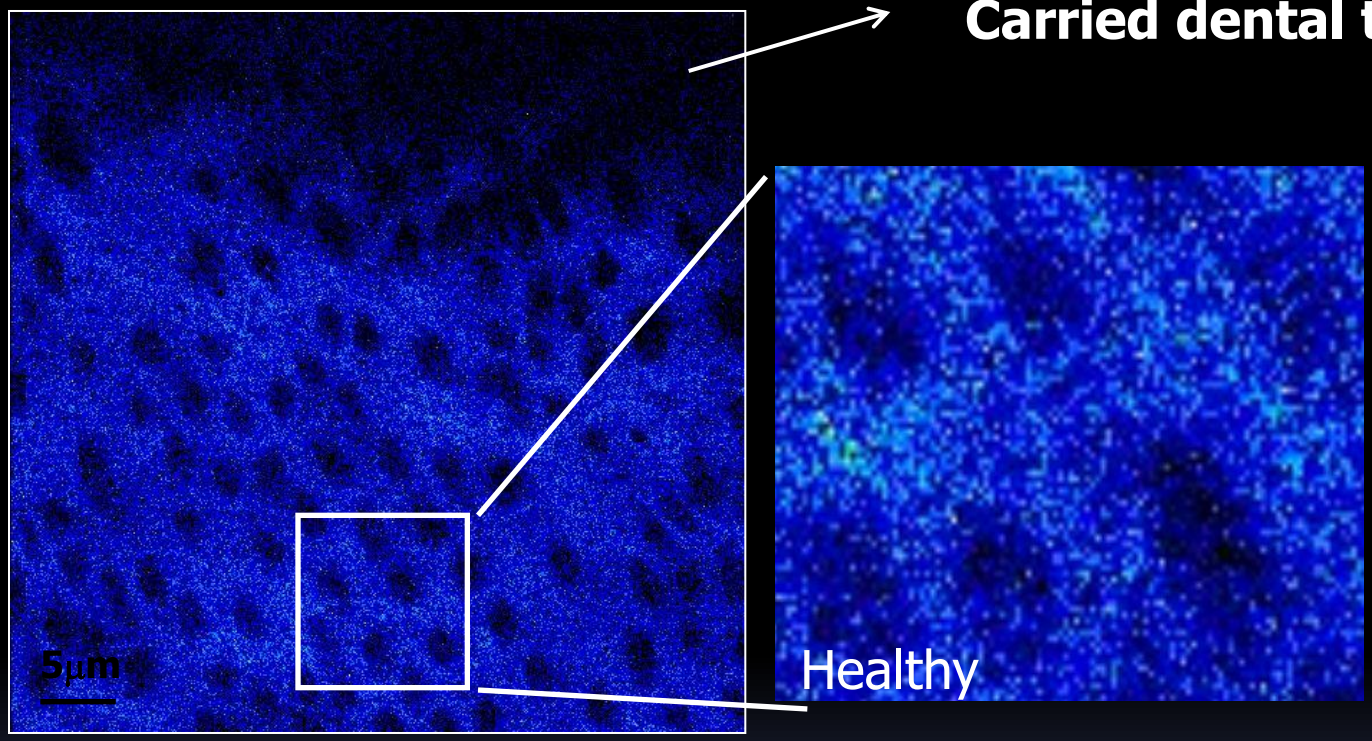

SHG image in MPM → The collagen structure is dissapearing in the sick tissue

Healthy tooth: Dentin enamel junction (DEJ)

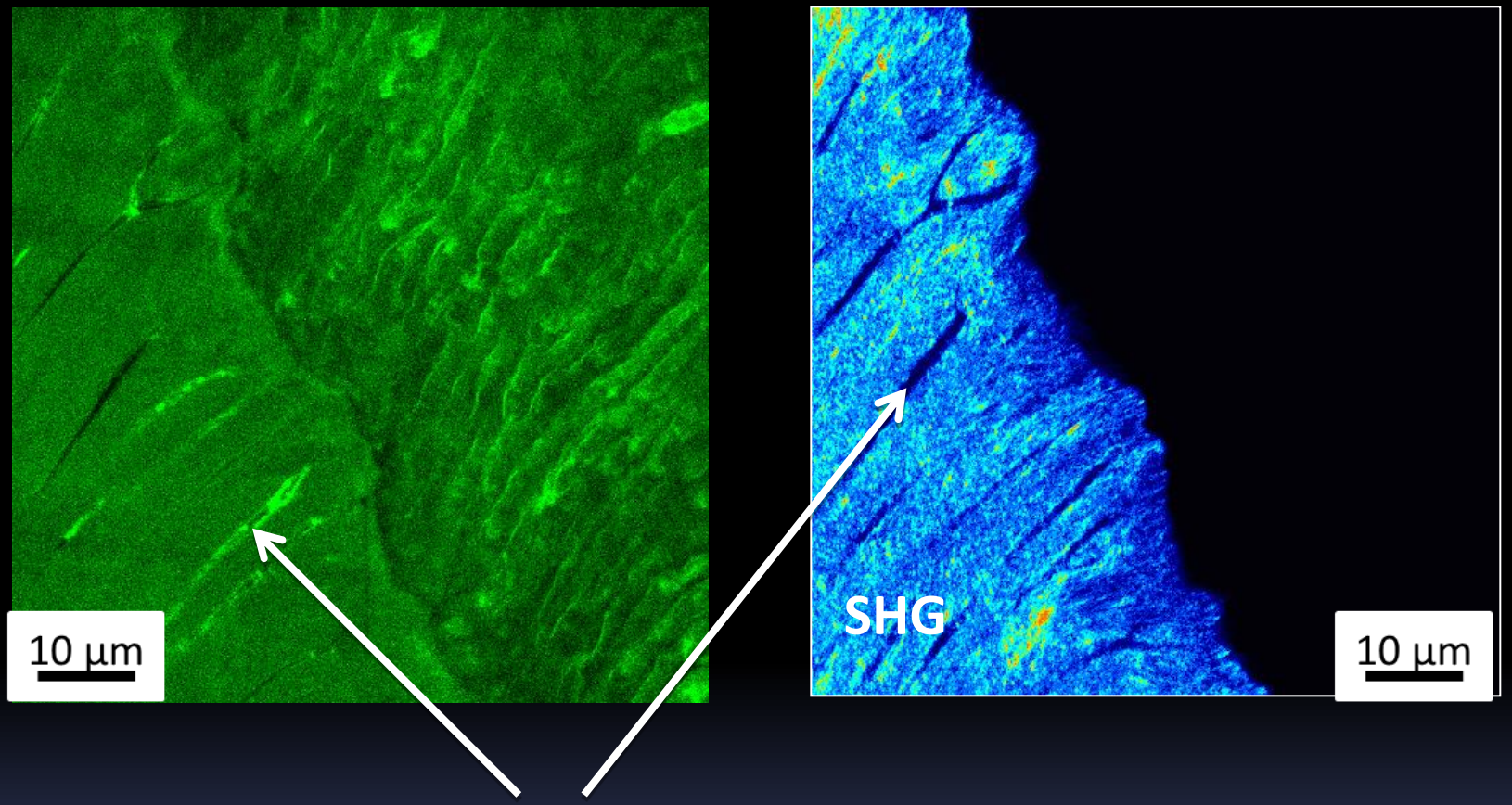

Proteins inside tubules are fluorescent without SHG signal

Enamel is fluorescent but has no SHG ; Dentine has SHG due to collagen fibers

SHG imaging of muscular structures

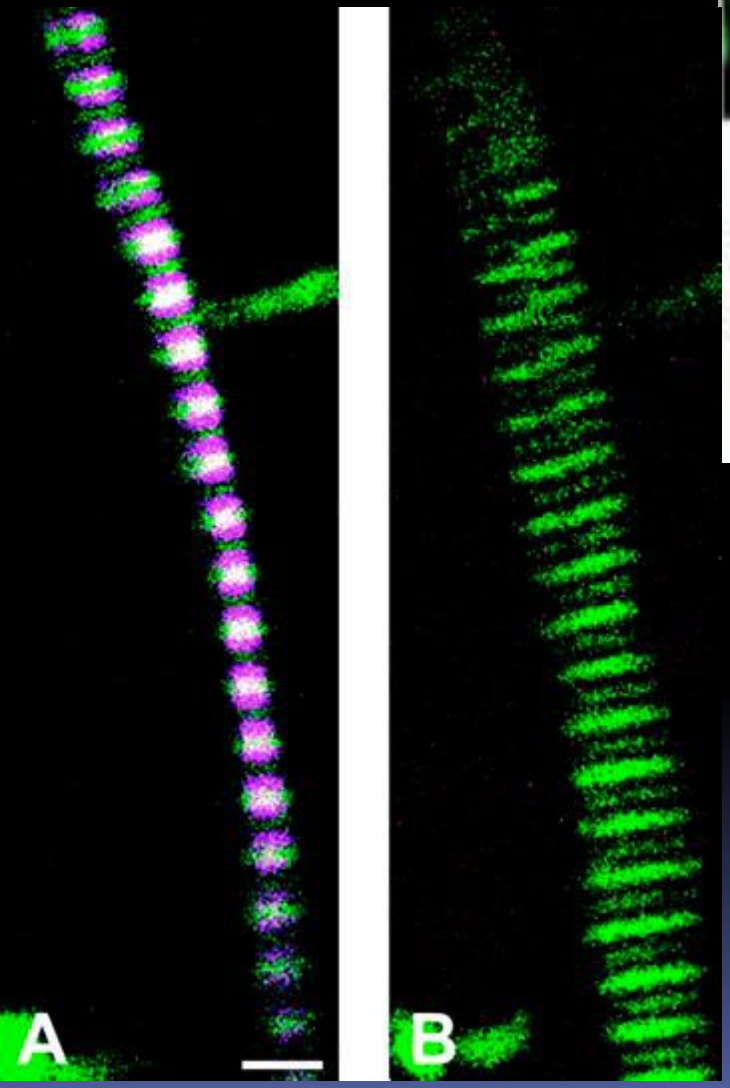

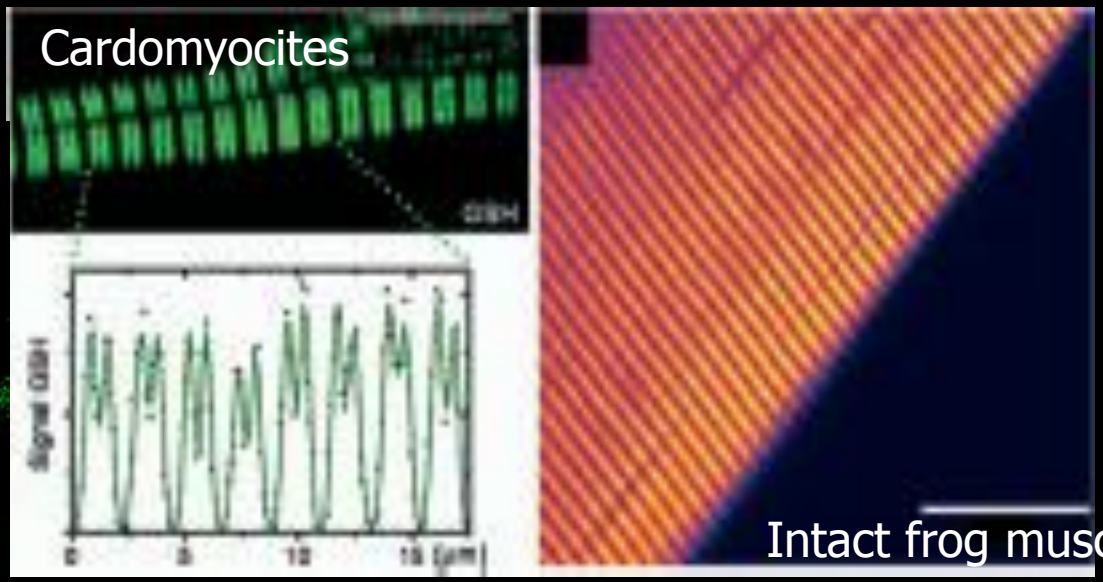

SHG and fluo image of myosin filaments
(A) SHG (purple) and fluorescence (green) from an isolated, unfixed mouse myofibril stained with AlexaFluor 488-
(B) The same myofibril after myosin extraction.

→ **SHG requires myosin**

Campagnola Biophys. J. 2002

Polarization anisotropy of sarcomeric SHG

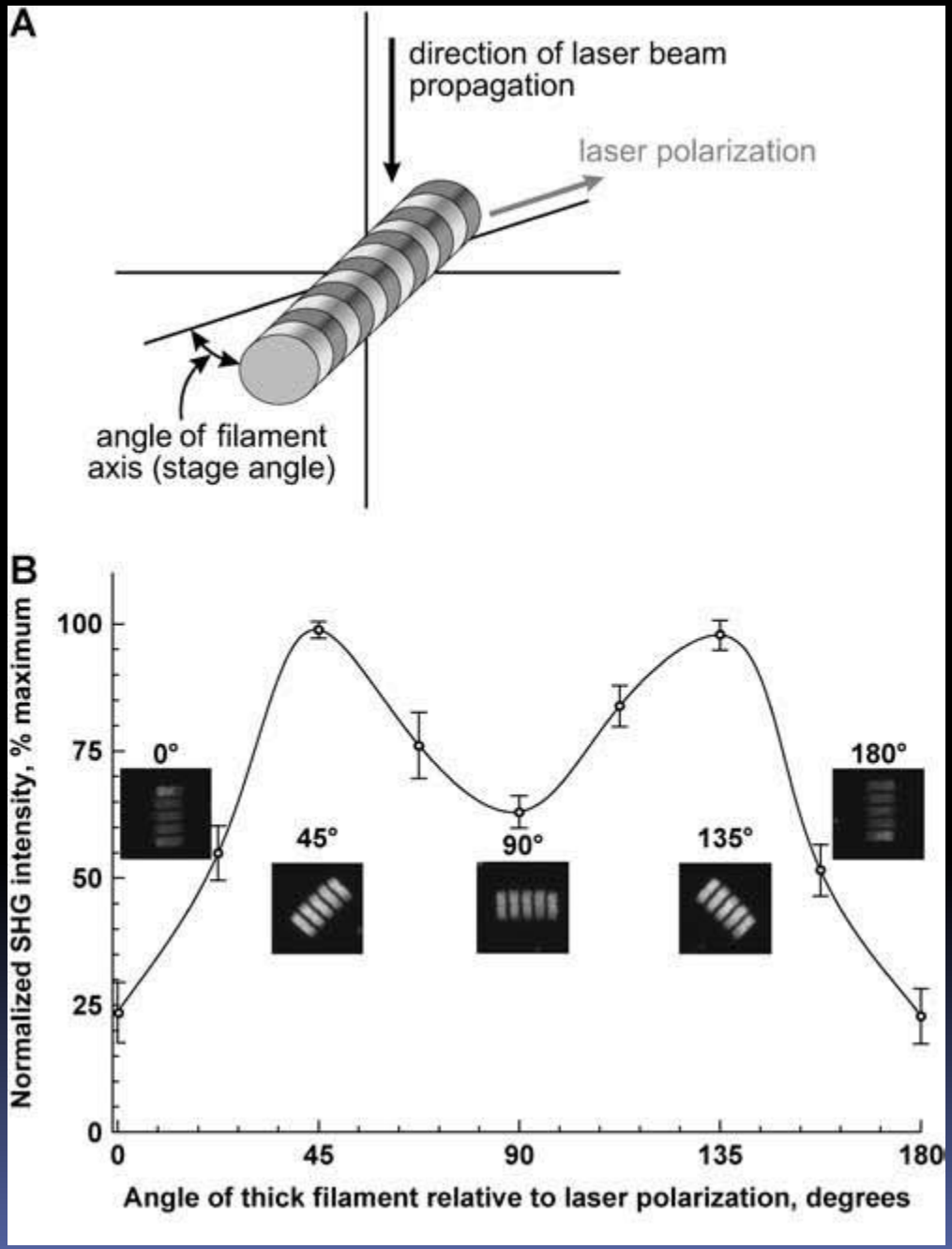

Profile of SHG intensity versus the relative angle of scallop myofibrils to laser polarization axis.

Inserts show changes of SHG intensity with rotation relative to a fixed laser polarization.

Campagnola Biophys. J. 2002

Emission dipole based selective imaging

Laser polarization __ polarizer

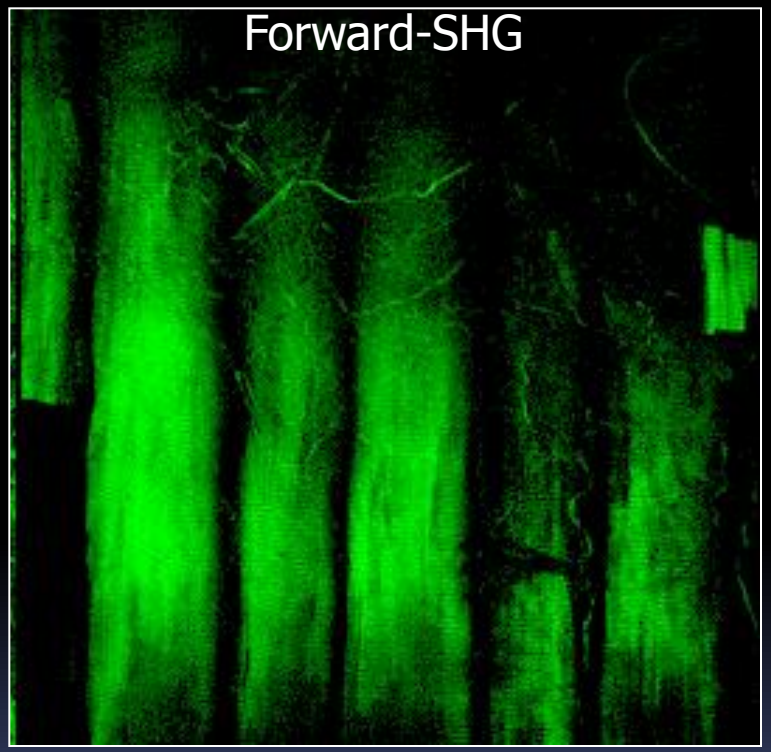

Muscle fibers: FSHG dominated

No polarizer

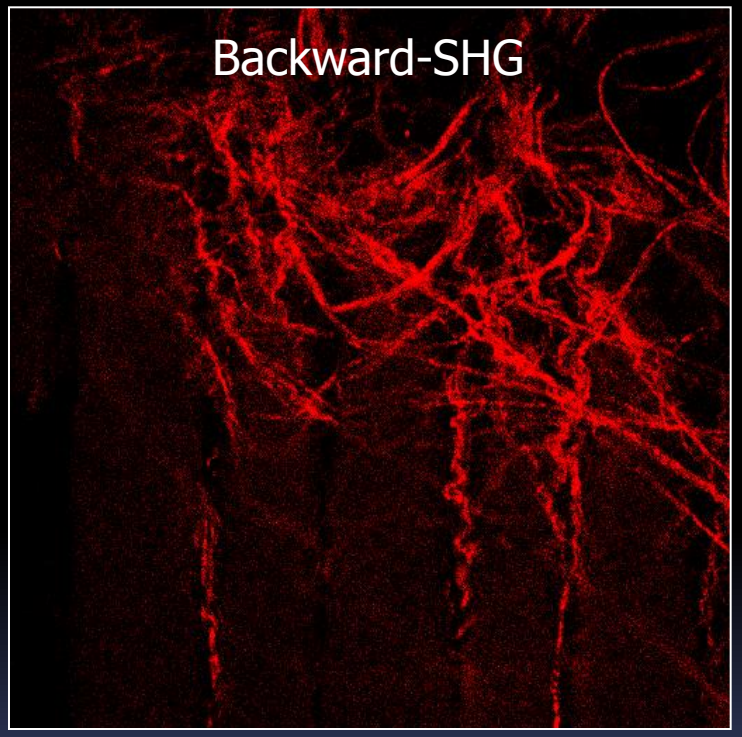

Collagen: both FSHG and BSHG

Chu, *J Biomed Opt* 14, 010504, 2009

Thickness of a collagen fibril

determined by FSHG/BSHG ratio→ ~10 nm precision

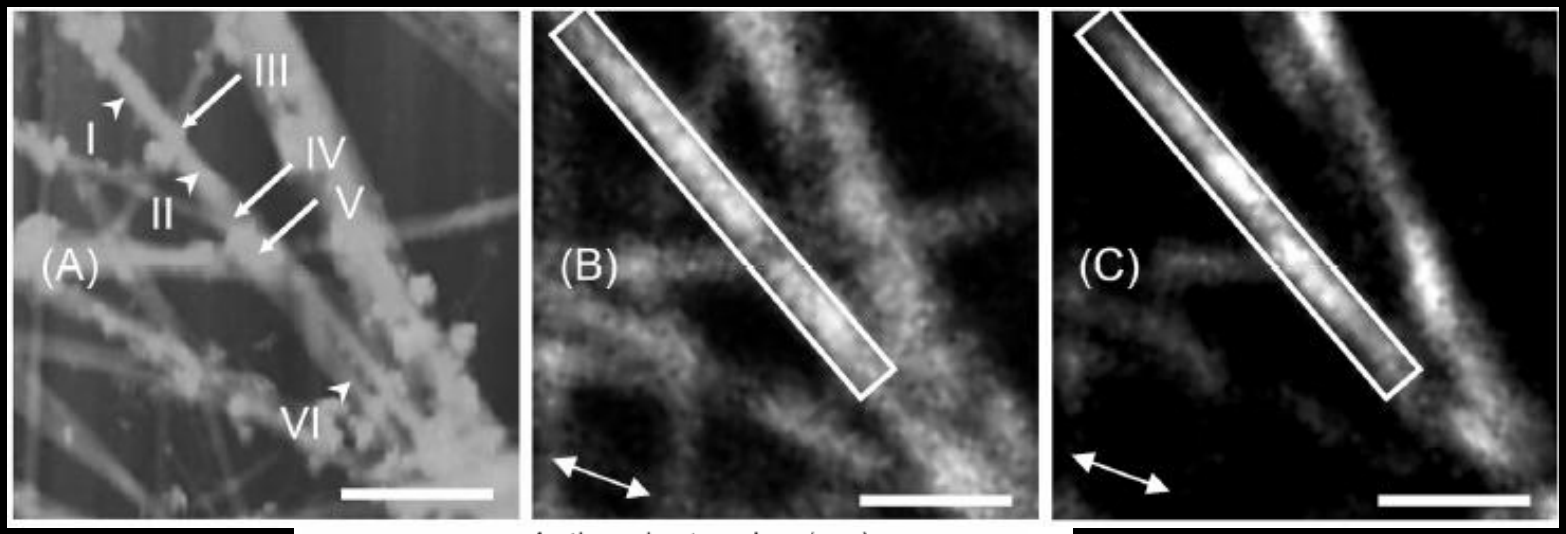

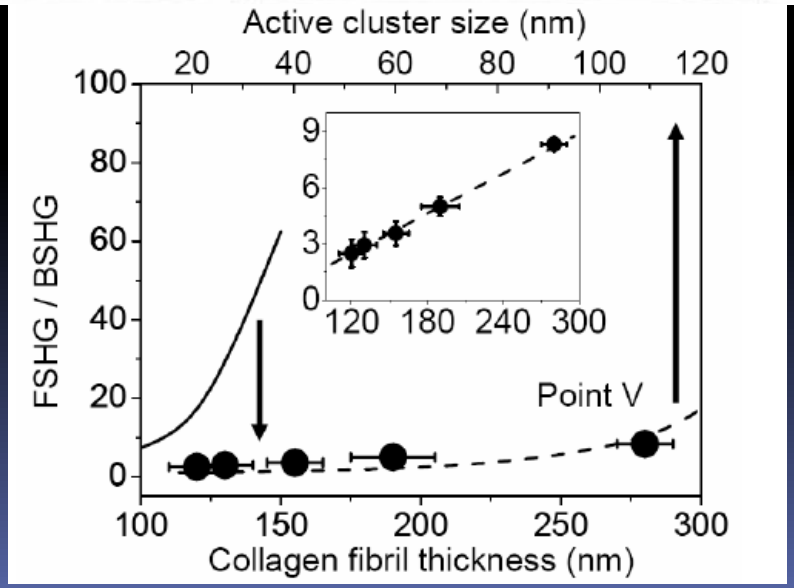

Chu, *Opt. Express*, 15, 12005 (2007)

Optical coherence tomography

OCT is analogous to ultrasound, but instead of using sound waves, it uses low-coherence (broadband) light.

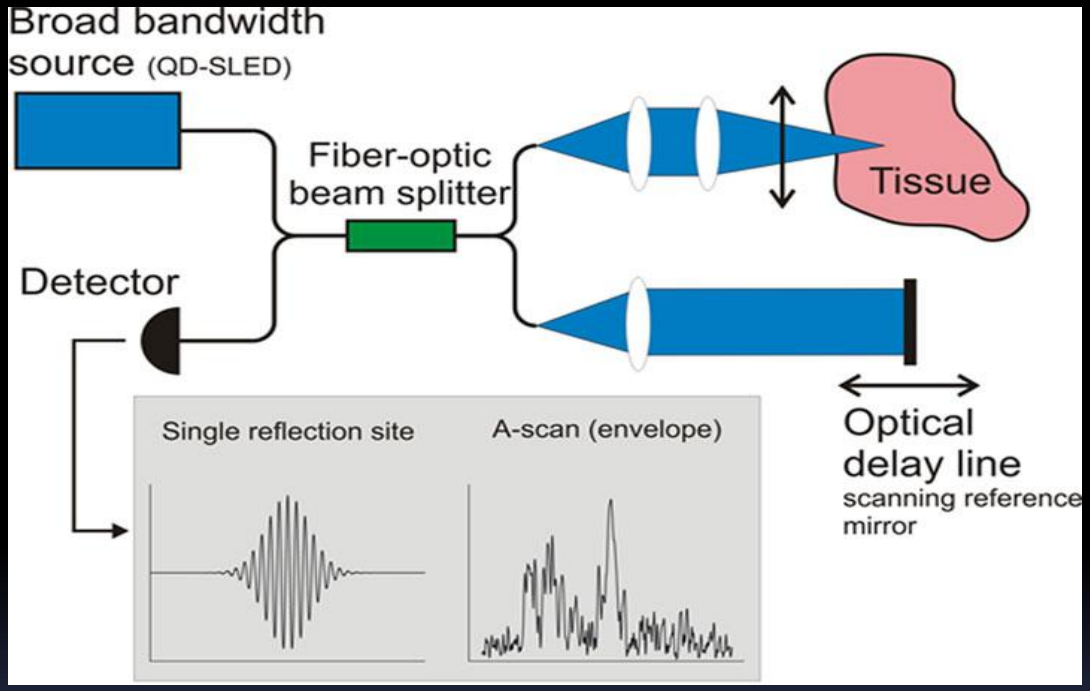

R. Hogg, Univ. Sheffield, UK

- A broadband source illuminates a fiber-optic **Michelson interferometer**
- **An interference pattern is detected** when the sample and reference path lengths match within the coherence length of the source
- **Images of tissue (2D, 3D,cross-sectional**) may be obtained non-invasively and in situ with appropriate scanning

Biological window for tissue imaging

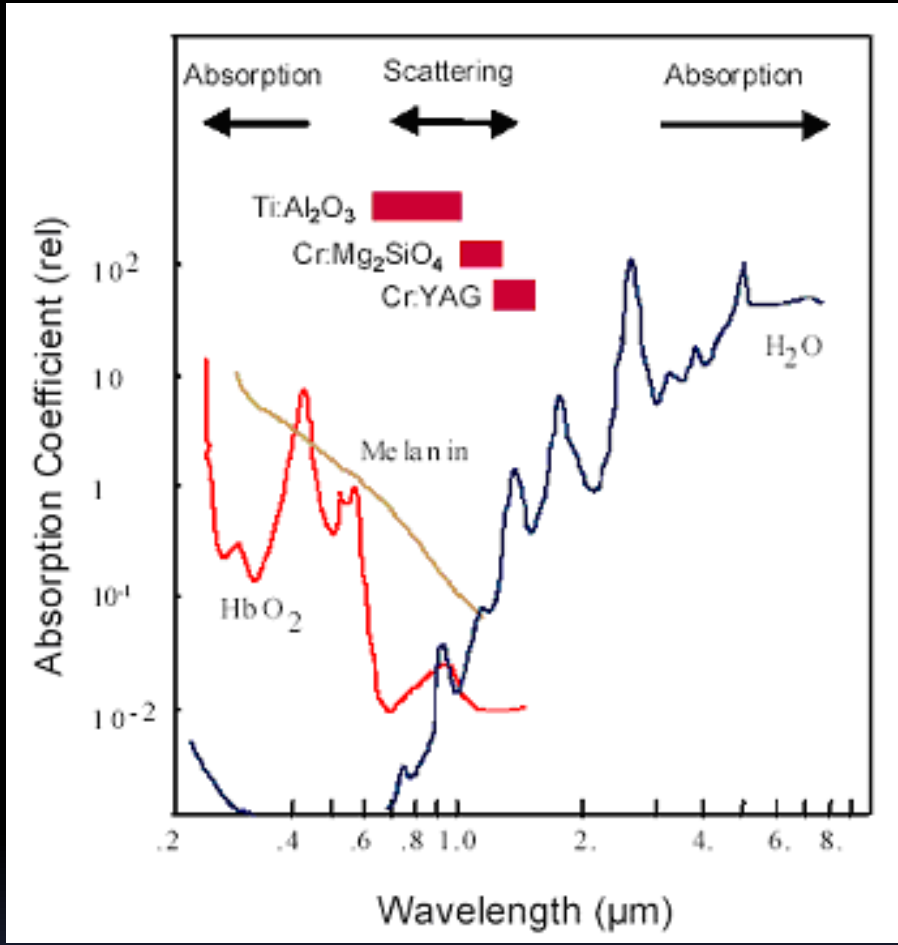

In the "biological window" ranging from 800 to 1300 nm attenuation of light is due largely to scattering, rather than absorption.
OCT utilizes a low-coherence light source within this range of wavelengths to image deep into tissue.

Profio & Doiron, Photochem. Photobiol 46:591, 1987

Optical coherence tomography: developing zebrafish

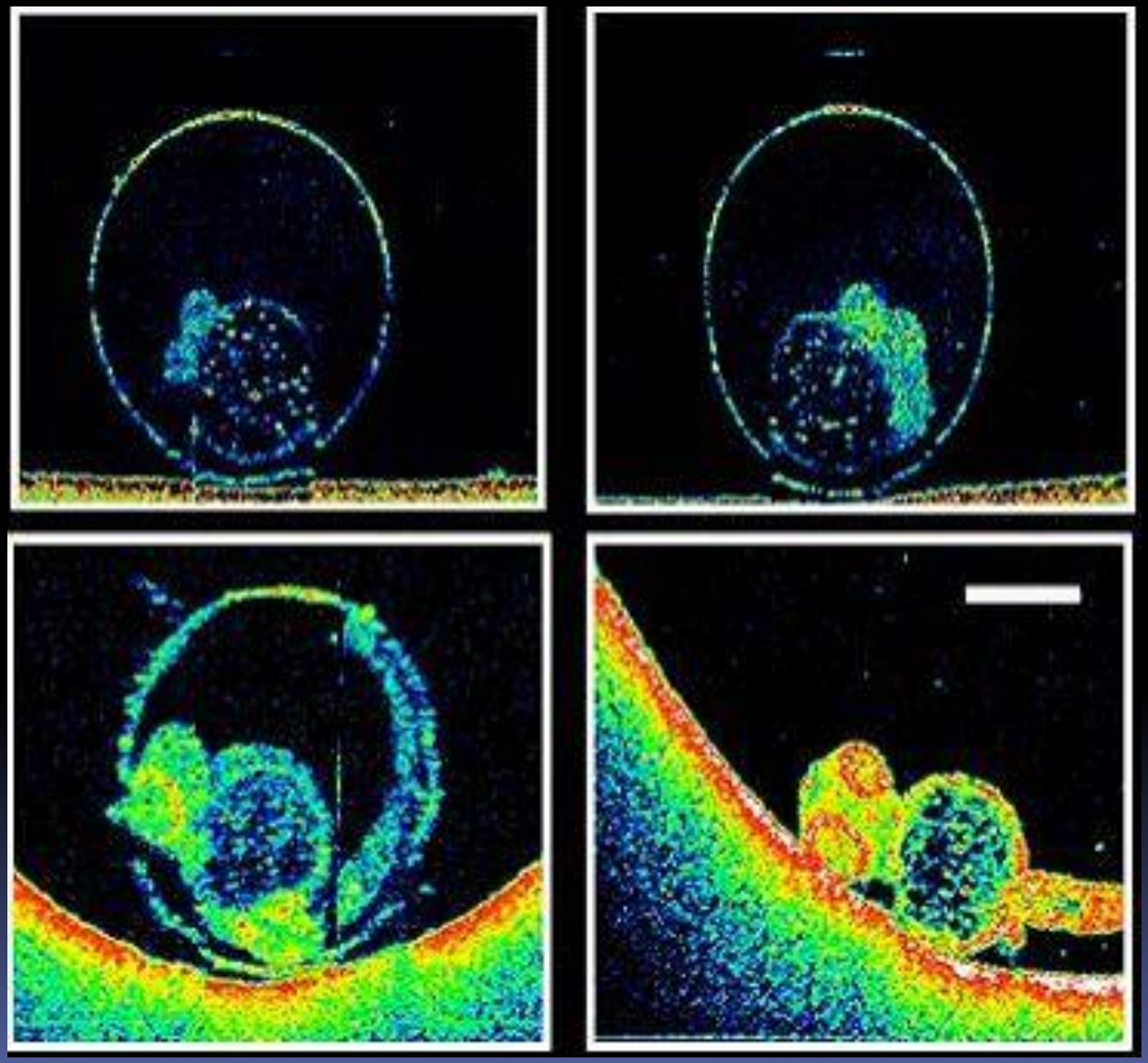

Integrating multiphoton microscopy (MPM) with optical coherence tomography (OCT)

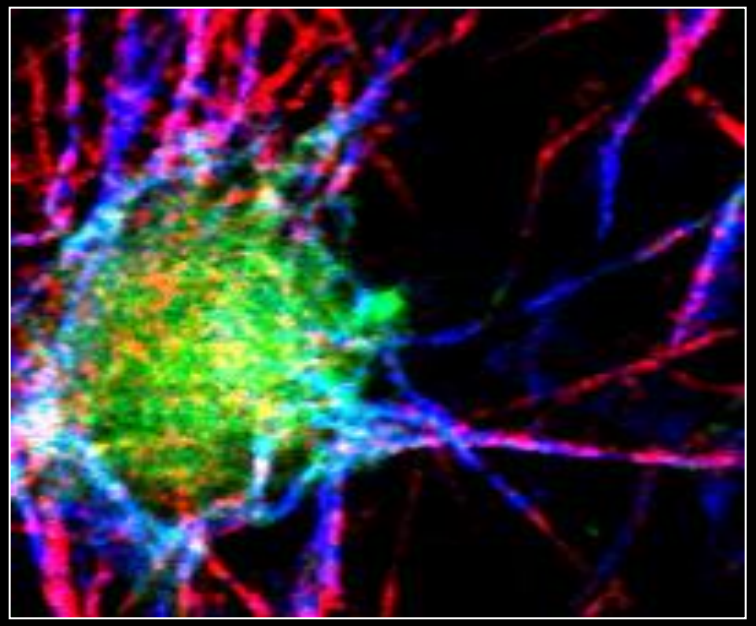

- MPM is sensitive to cells and extracellular matrix
- OCT to structural interfaces and tissue layers.

→ acquire structural and functional imaging of tissues simultaneously

Micro-endoscopes are applied to study lung and ovarian cancers

→In vivo optical imaging to detect cancer in its early stage

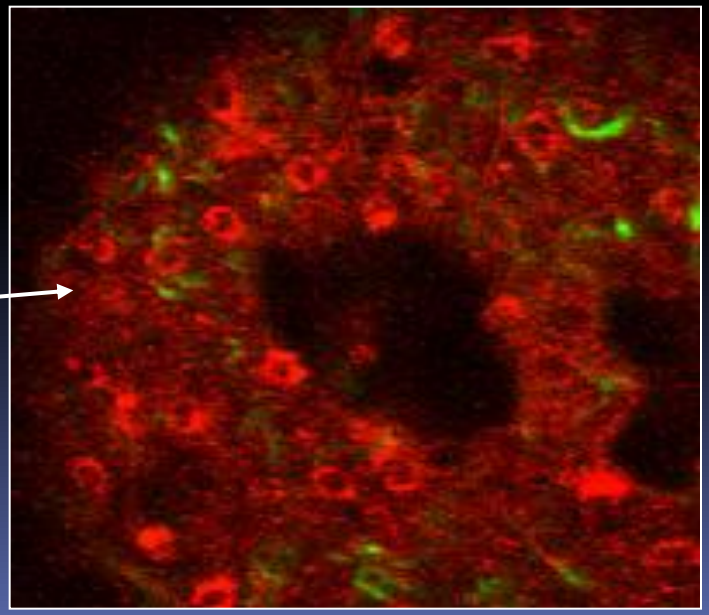

Mina, University of British Columbia

Near-field scanning optical microscopy (**NSOM**) for ultra-high optical resolution: a sub-micron optical probe is positioned a very short distance from the sample and light is transmitted through a small aperture at the tip of this probe.

Superresolution techniques:
-stimulated emission depletion microscopy (**STED**) uses a donut-shaped depletion beam surrounding a smaller excitation beam to achieve an axial resolution < 50 nm
-photoactivated localization microscopy (**PALM**)
-structured illumination microscopy (**SIM**)

Coherent anti-stokes Raman scattering microscopy based on the vibrational properties of the target molecule; does not require the species to be electronically excited by ultraviolet or visible light. Fast (ps) laser pulses in the NIR region from two sources are focused onto the specimen with a microscope objective and scanned in the lateral and axial planes.

Scanning near-field microscopy combined with Raman micro-imaging

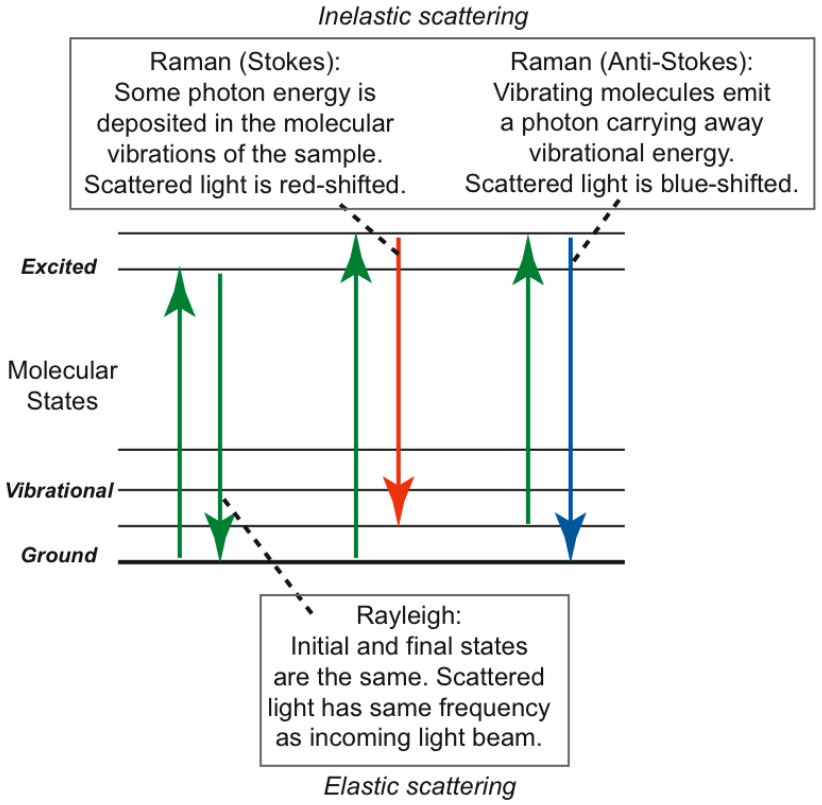

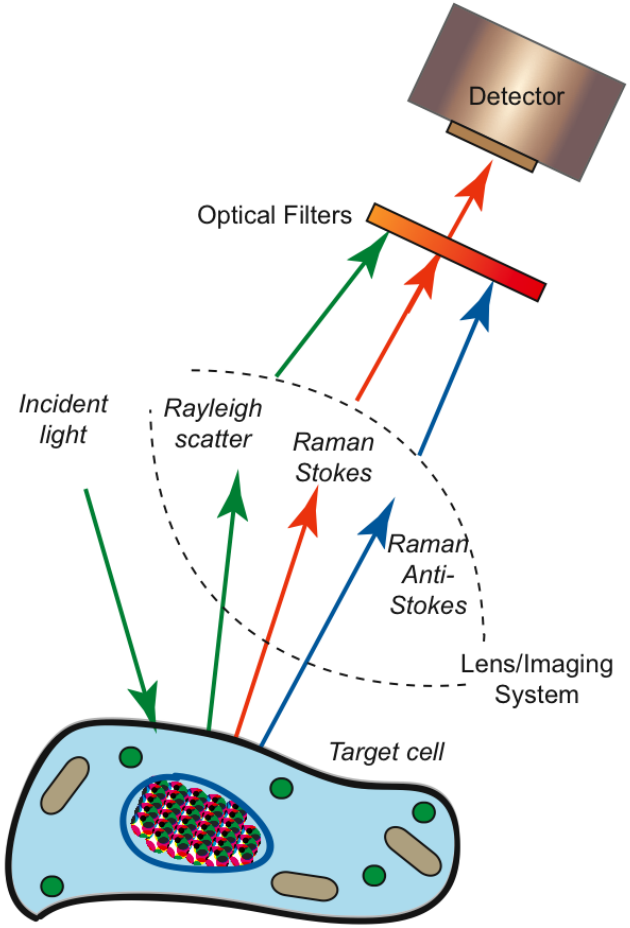

In Raman scattering, target cell organelles produce different degrees of red-shift, forming the basis for molecular spectroscopy.

Internalization of chemotherapeutic drugs into cancerous cells monitored by Raman confocal microscopy

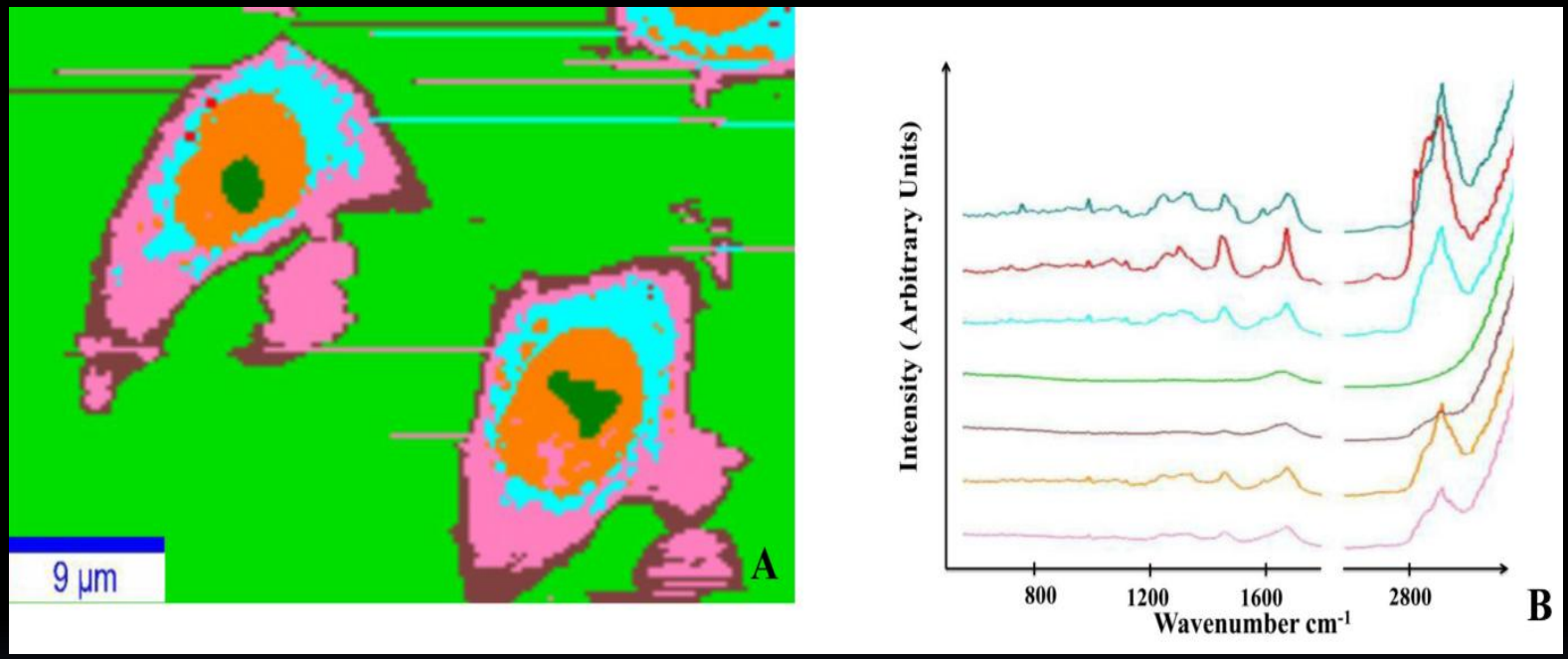

(A) Seven cluster Raman map of MCF7 cells.
(B) Average spectra corresponding to clusters in panel A. (same colors as in A): the average spectra of nucleus (orange) nucleolus (dark green), cytoplasm (pink), membrane (brown), endoplasmic reticulum (light blue), PBS buffer (light green) and paclitaxel (red).

Raman images of MCF7 cells incubated in paclitaxel.

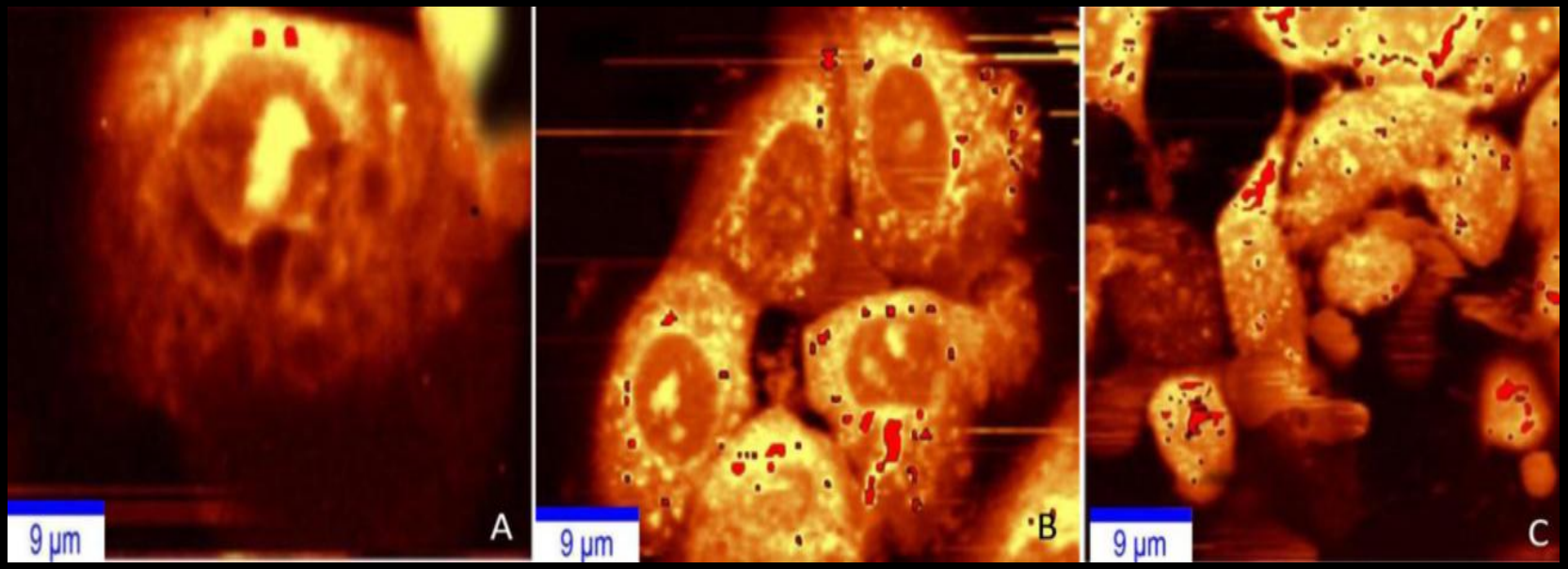

Integrated Raman intensities in the 2800-3000 cm $^{-1}$ region of the cell, marking paclitaxel as red spot. (A) 3 hours; (B) 6hours; (C) 9hours incubation of cells in culture medium containing paclitaxel.

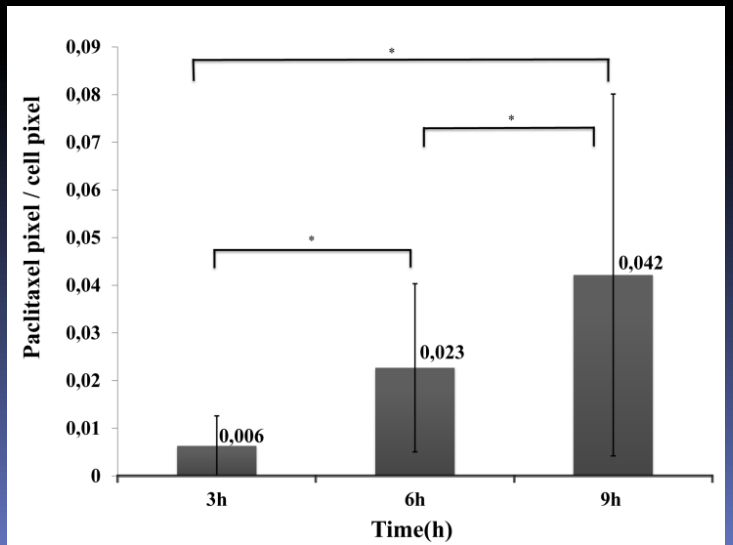

Light for Biosensing

Diagnosis: towards novel biosensing

Simple molecule detection using Fluorescence Correlation Spectroscopy (FCS)

FCS is based on the fluctuation of light emitted by dye molecules crossing a small laser spot and detected with confocal optics

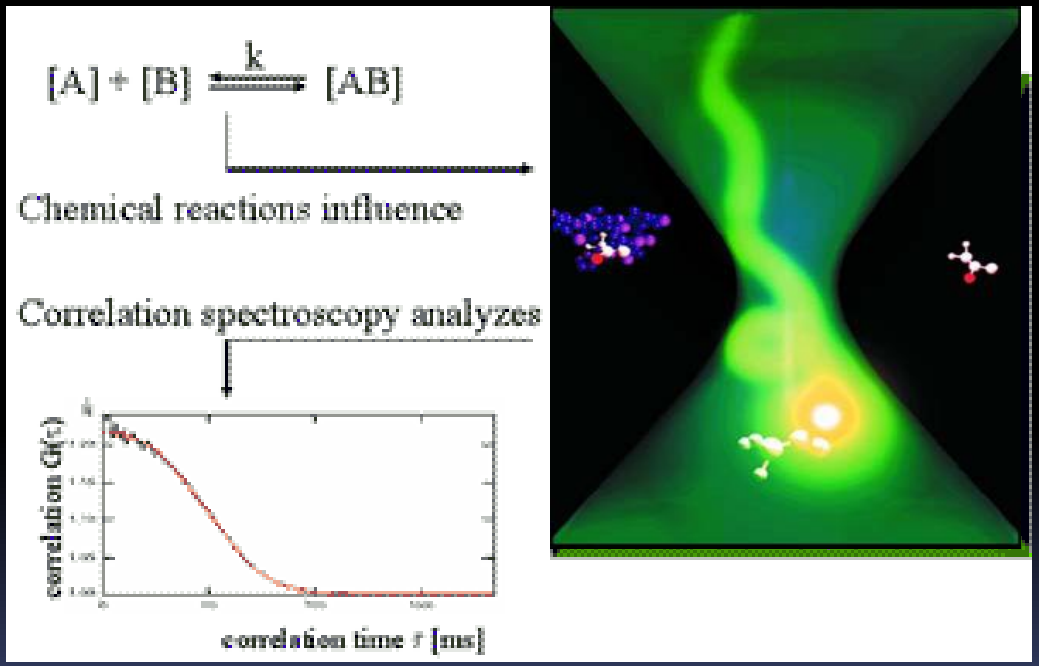

Stowers Institute, USA

Detecting two different sizes of molecules by their different diffusion constants

Affinity based label-free optical biosensors

to detect selective binding between target molecules and capture agents:
ligand-receptor, antibody-antigen, nucleotides pairing, etc.

Biacore:
optical biosensor that uses surface plasmon resonance for detection

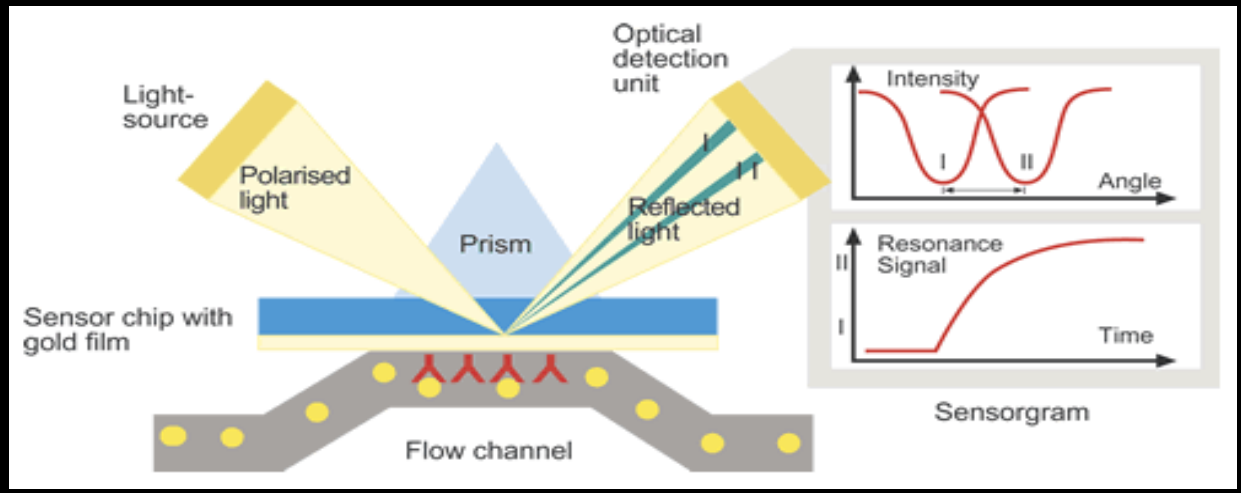

O. Chaloin, IBMC, Strasbourg

-large sensing area
-sensing limited to several nm
-substrate dependent binding of molecules driven by unspecific interactions → giving rise to serious limitations in the detection accuracy

? Miniaturization + large sensing area + specificity needed at the same time

Photonic crystals

Biosensors

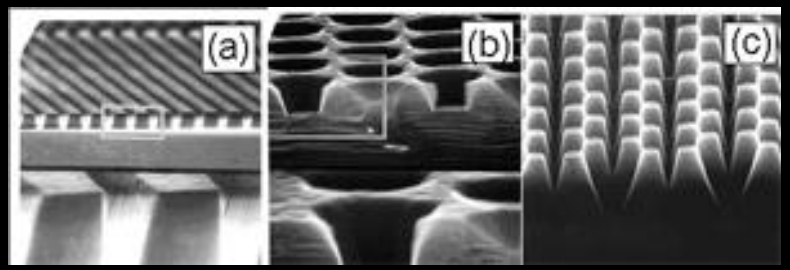

(Y. Chen, LPN)

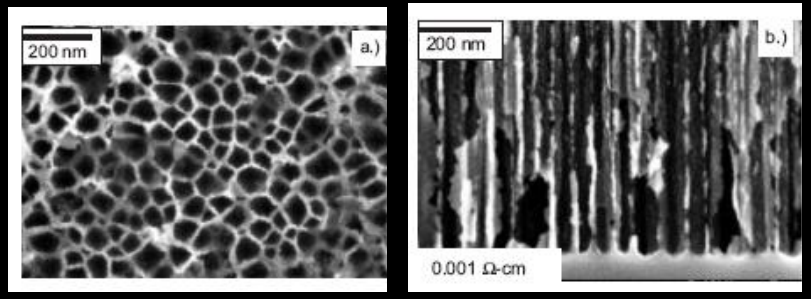

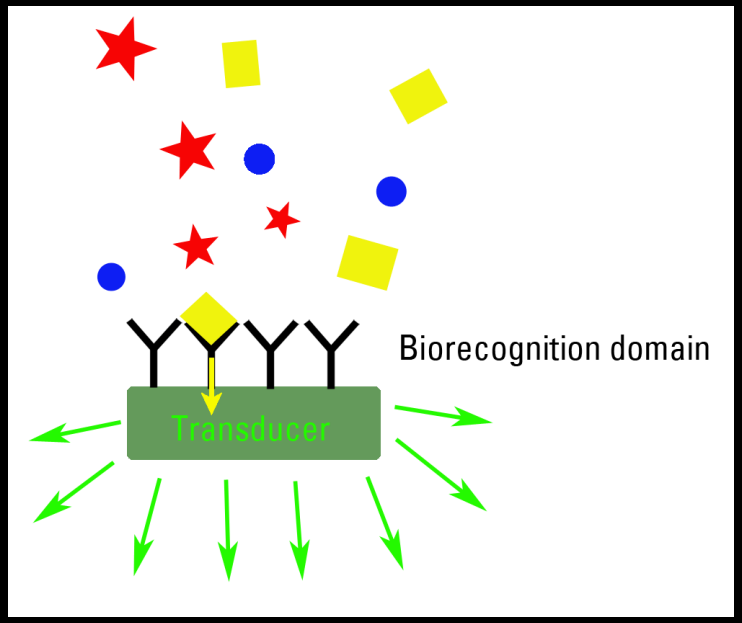

- ✓ Miniaturization
- ✓ Large sensing area

- ➢ detection based on the presence of the topological defects (biomolecules) within the photonic crystals
- ➢ specific recognition of the substrates by biological molecules

Key aspects in the development of biosensors

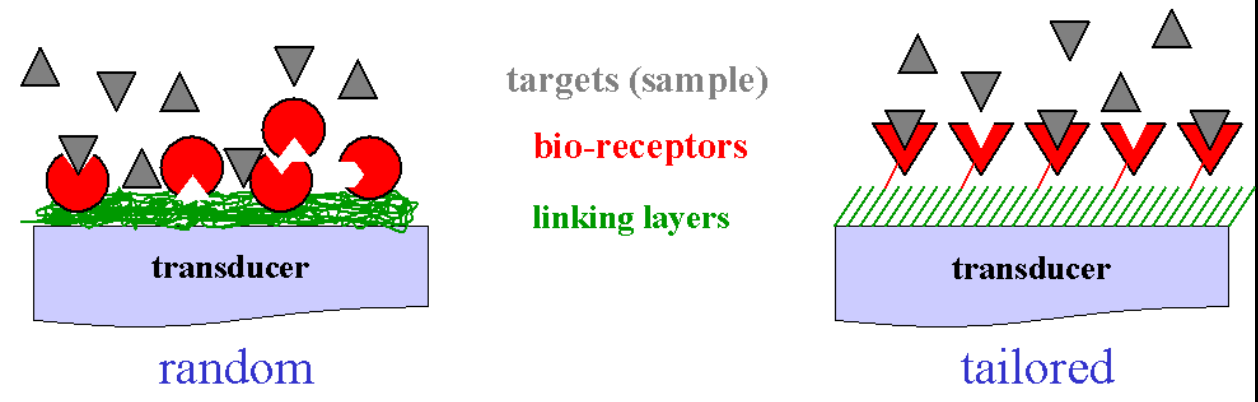

- the interaction between inorganic (the transducer) and organic material (the biological receptors)

- the increasing miniaturization of biosensor transducers (and thus of their active areas)
+ the demand for high sensitivity
require a
tailored coupling of bio-molecules to the transducer surface

- certain semiconductors (GaAs, InAs) are toxic →
for biocompatibility previous surface functionalization is needed

Photonic Crystals: Refractive Index Sensors

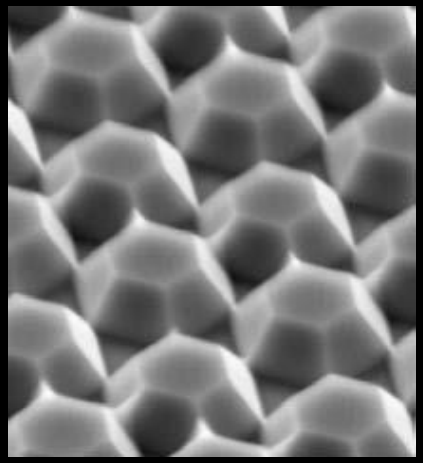

(I,Watson, Glasgow)

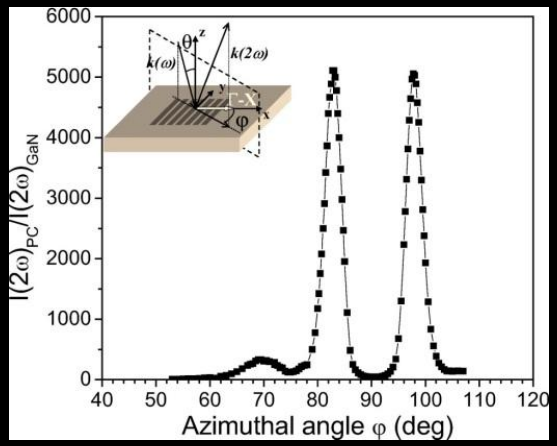

-confinement of light in very reduced zones
- exaltation of the nonlinear answer

-to reduce probed volumes and the quantity of fluorophores to reach a high sensitivity

PhC: - nanostructured substrate
- contrast in refractive indices

-specific detection based on refractive index modifications
-structures for light guiding

? ➢**Selective localization of molecules to keep r.i. contrast**
→ ordered array of a specific molecule

Examples of photonic structures

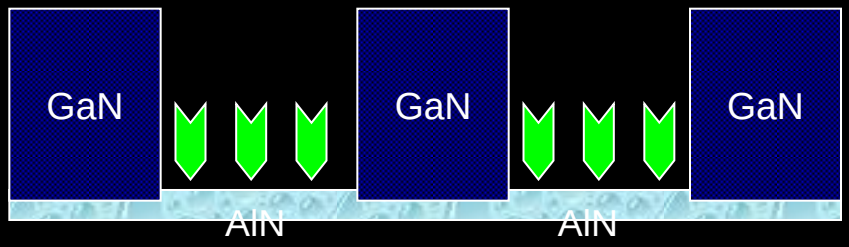

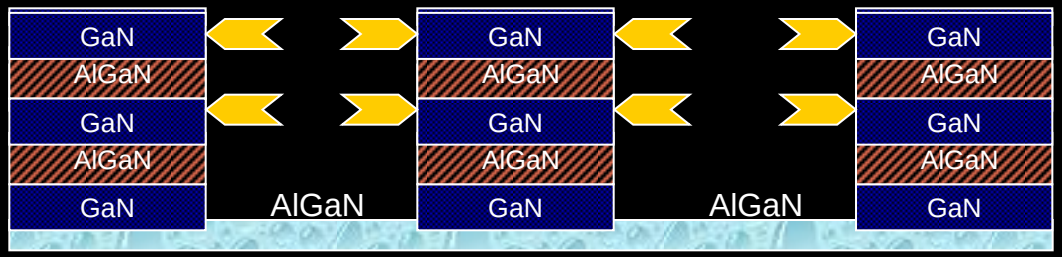

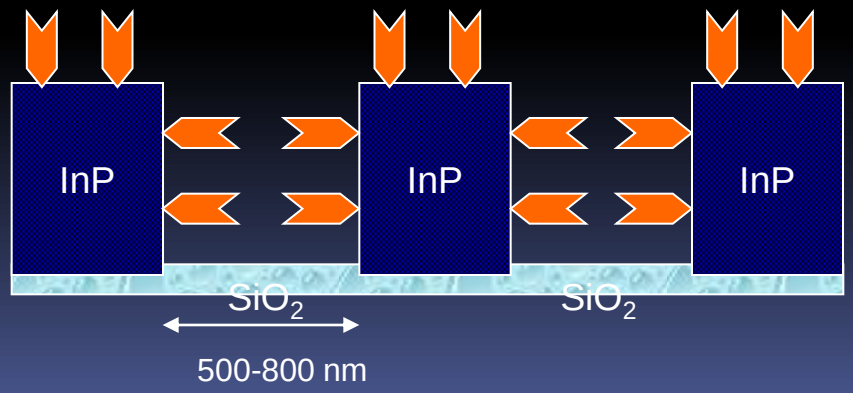

their functionalization with peptides which recognize the SC specifically

Optical detection based on refractive index changes monitored by :

-PhC resonances
-Evanescent field propagation within the waveguide structures

Selective functionalization of semiconductor substrates

Phage

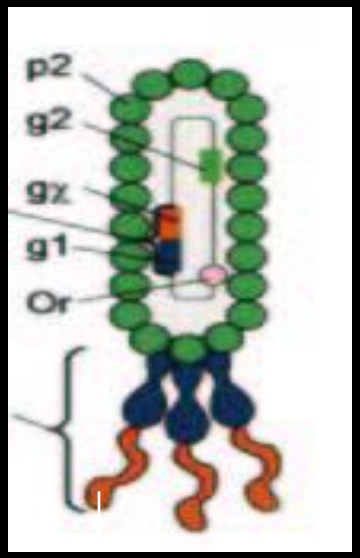

Adhesion peptides (12 amino-acids)

Phage display technique

Affinity-based selection biotechnological method

10^{10} combination peptides
→ Several peptides with surface recognition properties

GaAs (100) : Ser Val Ser Val Gly Met Lys Pro Ser Pro Arg Pro

InAs (100) : Ser Ser Met Glu Pro Asp Pro Phe Leu Ala Leu Tyr

GaN (0001) : Ser Val Ser Val Gly Met Lys Pro Ser Pro Arg Pro

ZnSe(100) : Leu Leu Ala Asp Thr Thr His His Arg Pro Trp Thr

+ GaAs(111)A, GaSb(100), CdSe(100), ZnTe(100), InP, Si

E. Estephan et al. Biotechnology & Bioengineering 2009

Selective functionalization via peptides

SiO_2 mask: lift-off method

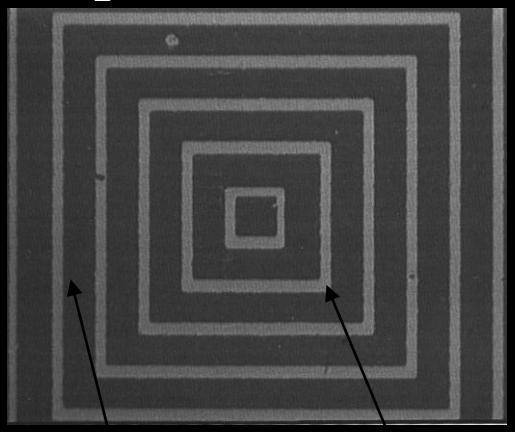

SiO_2(120µm) GaN (30 µm)

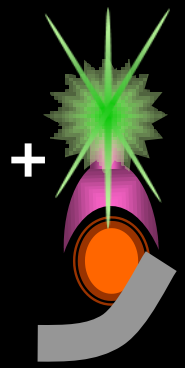

Fluorescence Microscopy

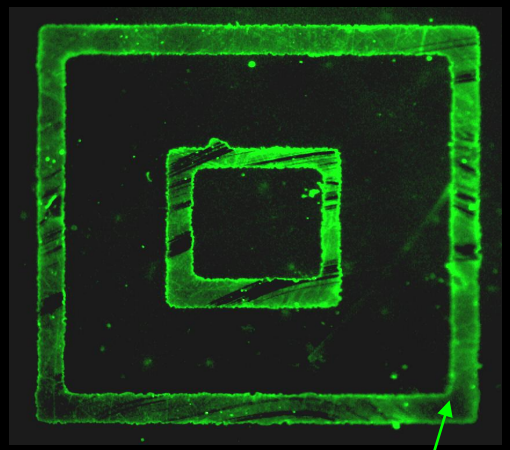

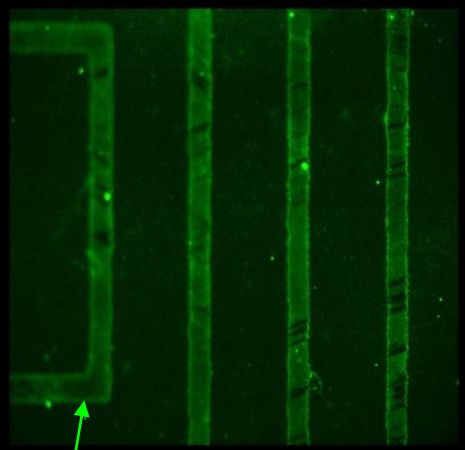

GaN

peptide
+BSA
+
Biotine ---+
Streptavidine
marqued by Cy3

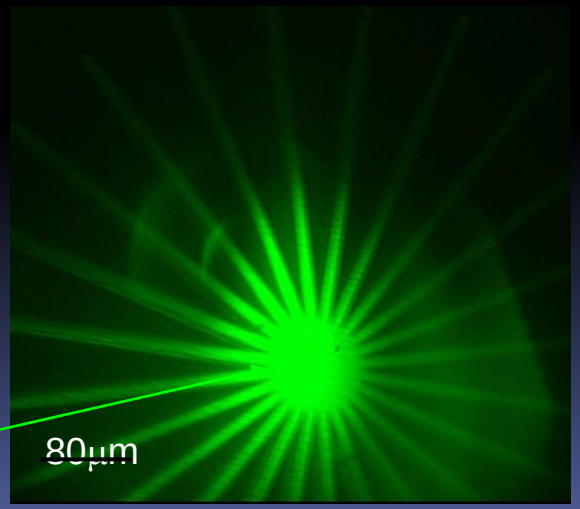

InP

S. Lourdudoss, KTH

E. Estephan et al. (2009). J. Coll. Int. Sci. *E. Estephan et al. (2008) J. Phys. Chem.B*

GaAs Metal Semiconductor Field Effect Transistor

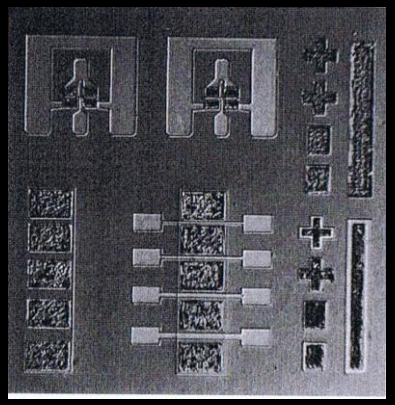

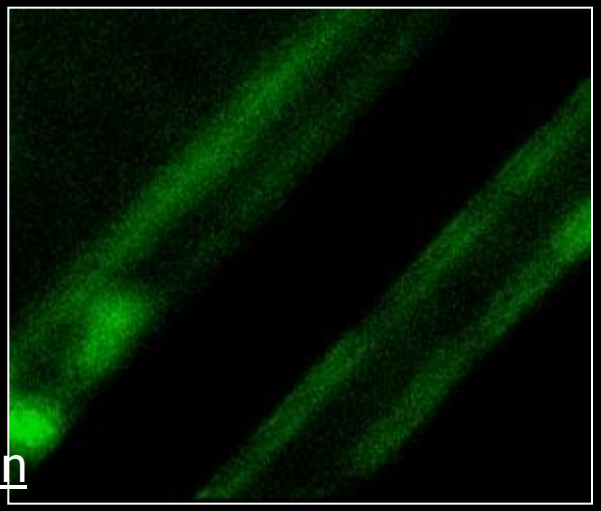

+ peptide – Biotin + FITC -streptavidin

Localisation of the peptide on the GaAs region between the Drain and Gate and between the Gate and Source → controlled placement and specific localization of biomolecules can be achieved without covering the drain and the source.

Quantifying the interactions between the peptide and the surface

(AFM- Force spectroscopy)

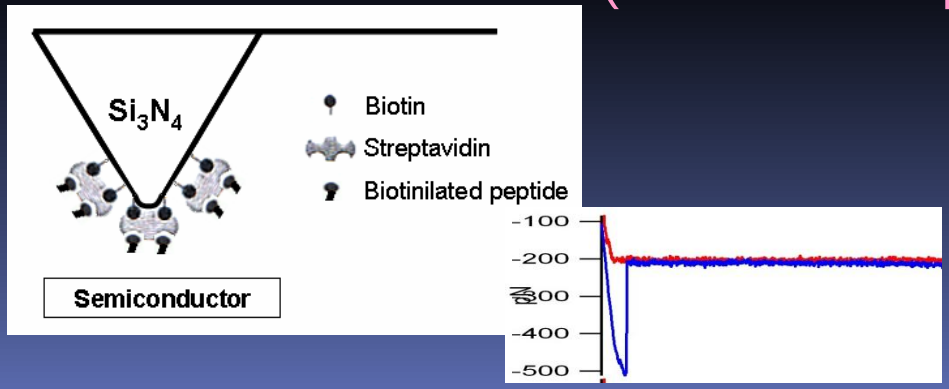

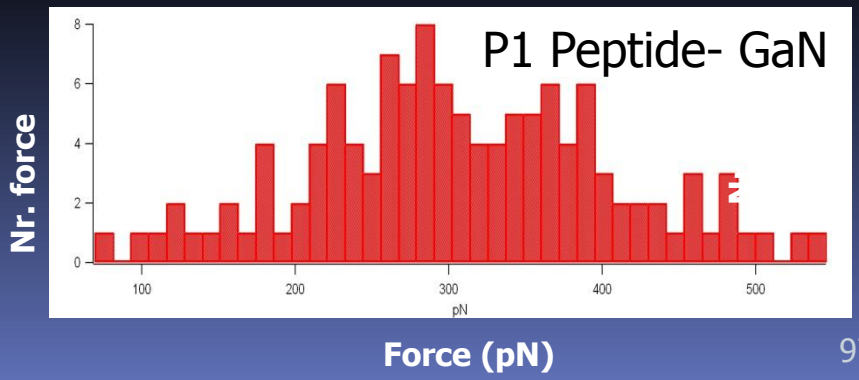

Photonic biosensors

1. Porous silicon microcavities

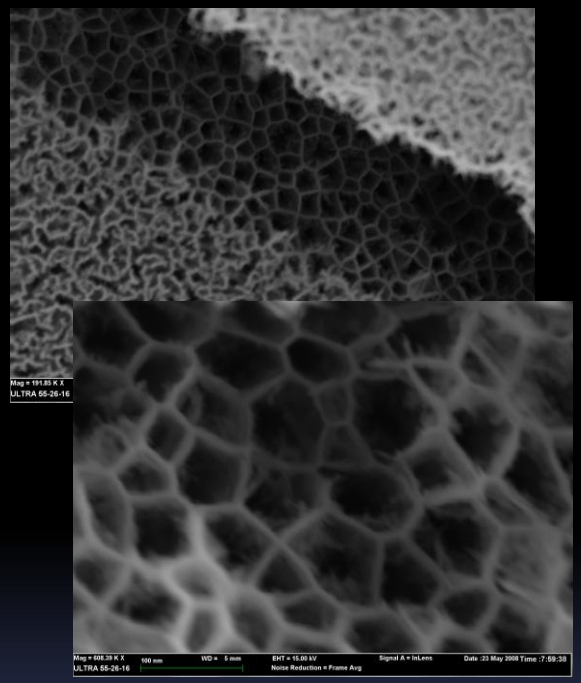

2. GaAs/AlGaAs PhC

0.6 μm GaAs patterned core

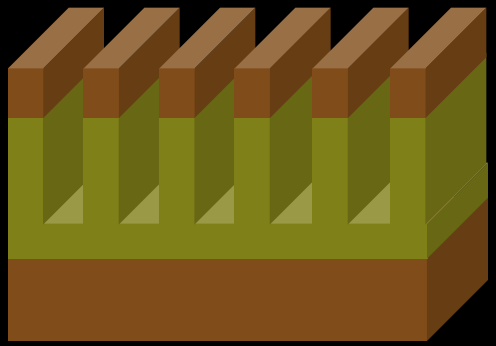

1.1 μm AlGaAs patterned cladding

GaAs substrate

-Miniaturization + large sensing area

- Biological binding converted into optical response (refractive index change)

PSi fabrication: wet etching in an electrochemical anodization system

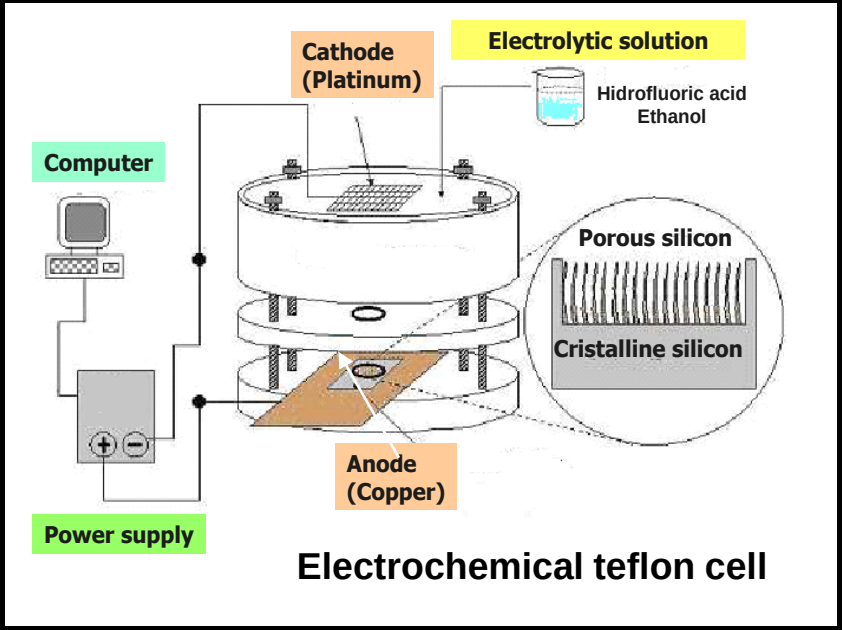

Electrochemical teflon cell

Porosity and pore size can be easily tuned by adjusting the electrochemical conditions

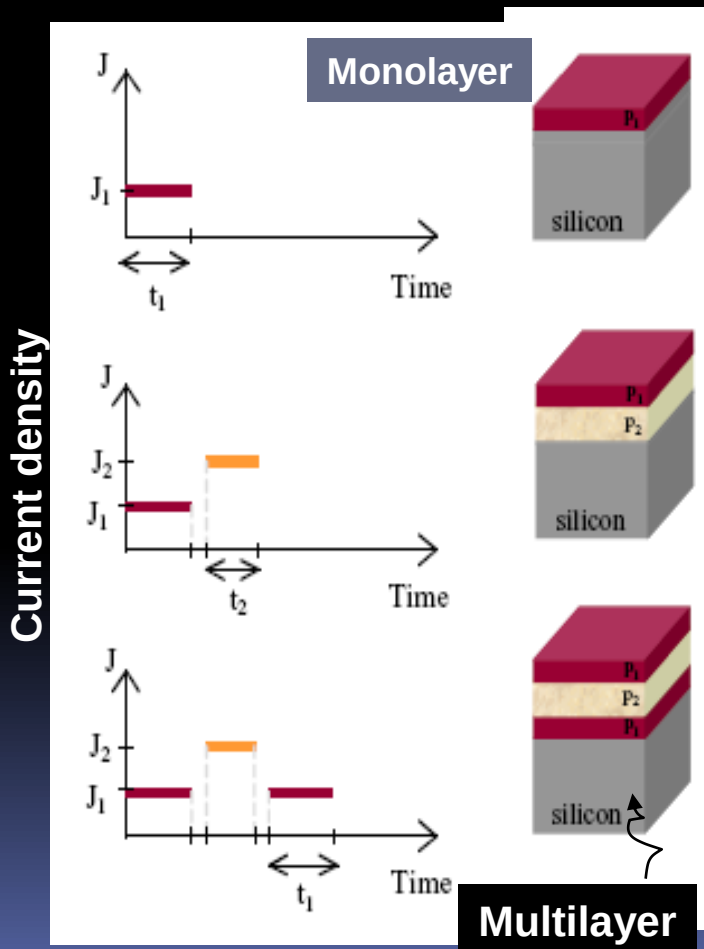

PSi mirrors and microcavities as photonic substrates

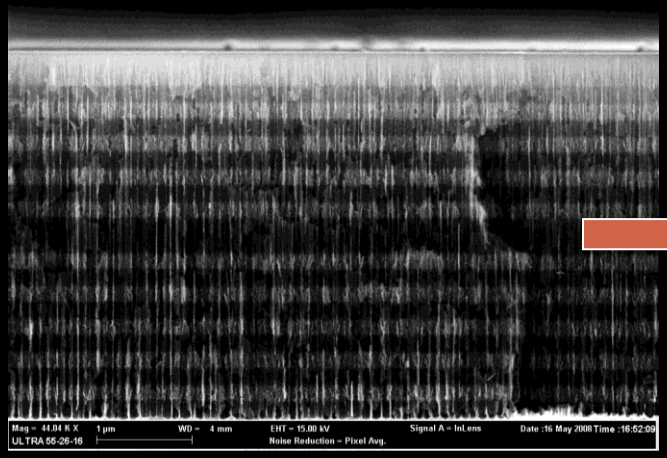

λ/4 mirror

λ/2 Fabry-Perot Optical cavity

λ/4 mirror

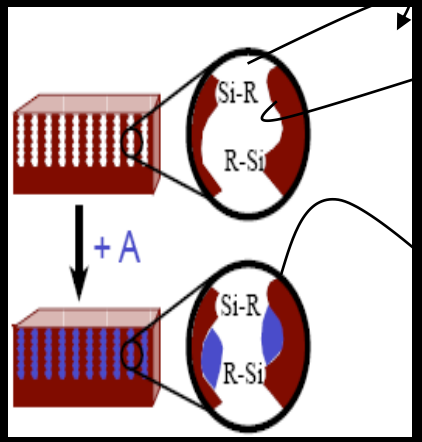

Hidride bond

Oxide bond

Biological or chemical species

Microcavity

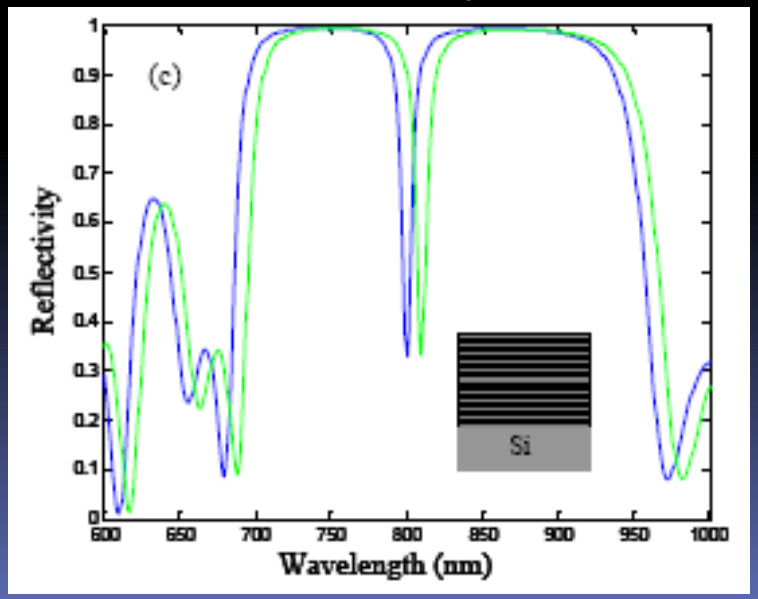

Bragg Mirror

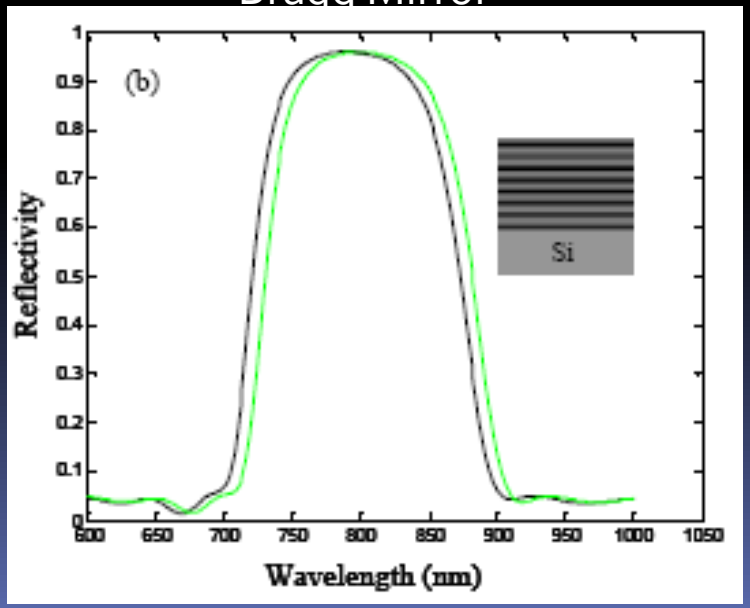

Fluorescence Enhancement in PSi

Functionalised PSi Bragg Mirrors + confinement of fluorescein

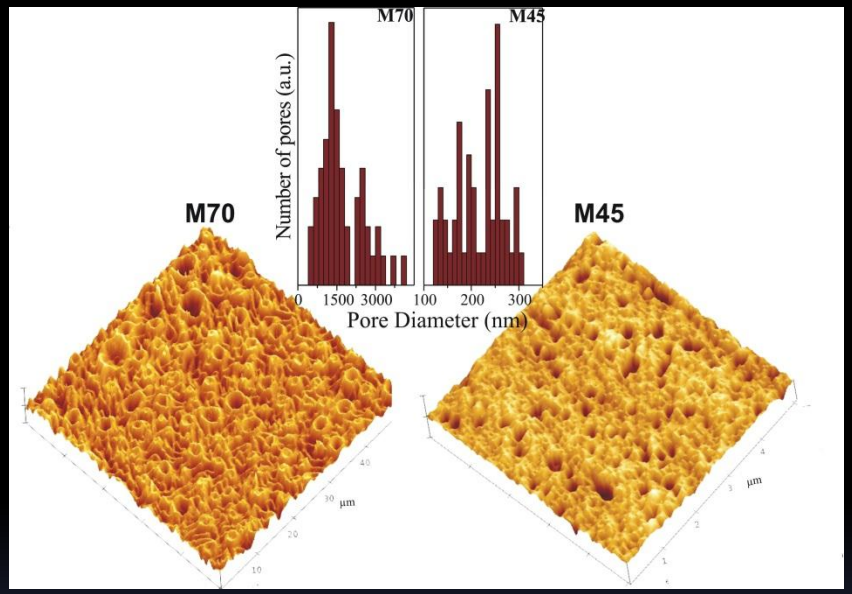

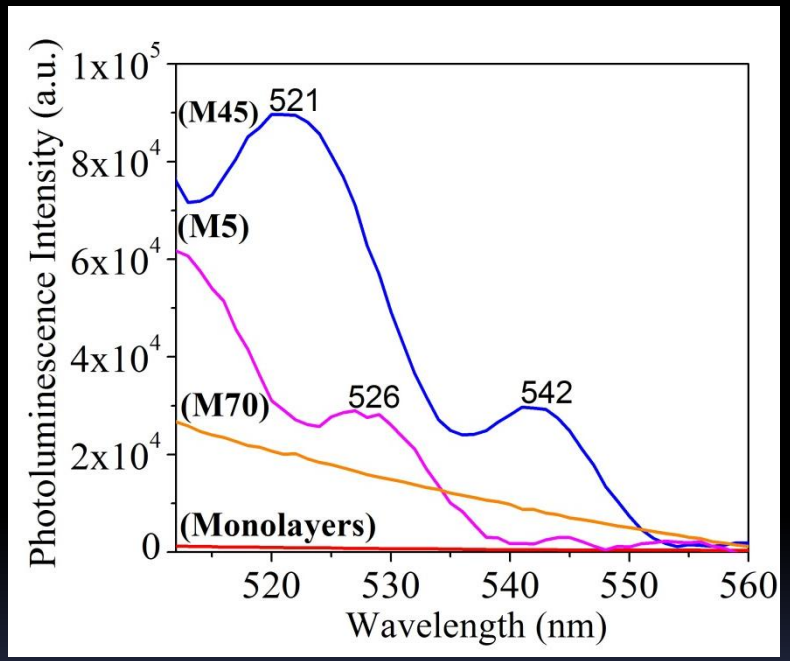

Fluorescent emission of the fluorescein molecules adsorbed on the M45 mirror
cooperative effect of the pores dimensions + resonance conditions

G. Palestino et al. APL, 91, 12 (2007) + Biophotonics Int/ by. Hogan, 2007

Biosensor: Glucose Oxydase (GOX) + porous silicon microcavity

GOX adsorbed on PSi after functionalisation

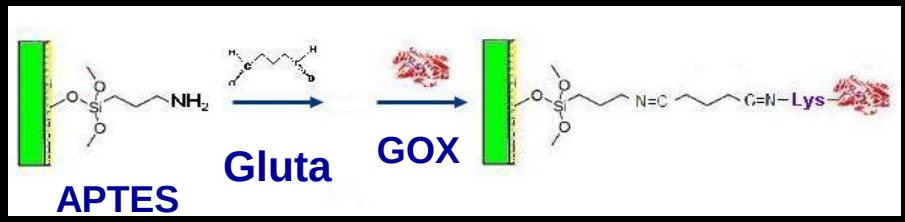

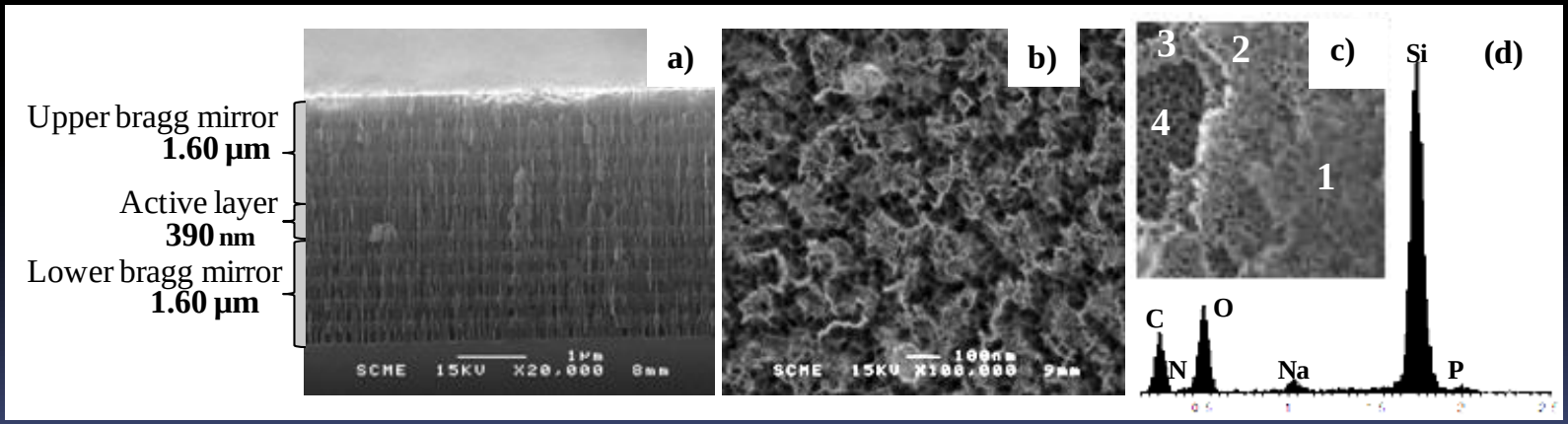

Organic molecules inflitrate the whole structure

G. Palestino et al. (2007) *Proc. SPIE Vol. 6592, 65920E1-9*

Molecular sensing monitored by specular reflectance

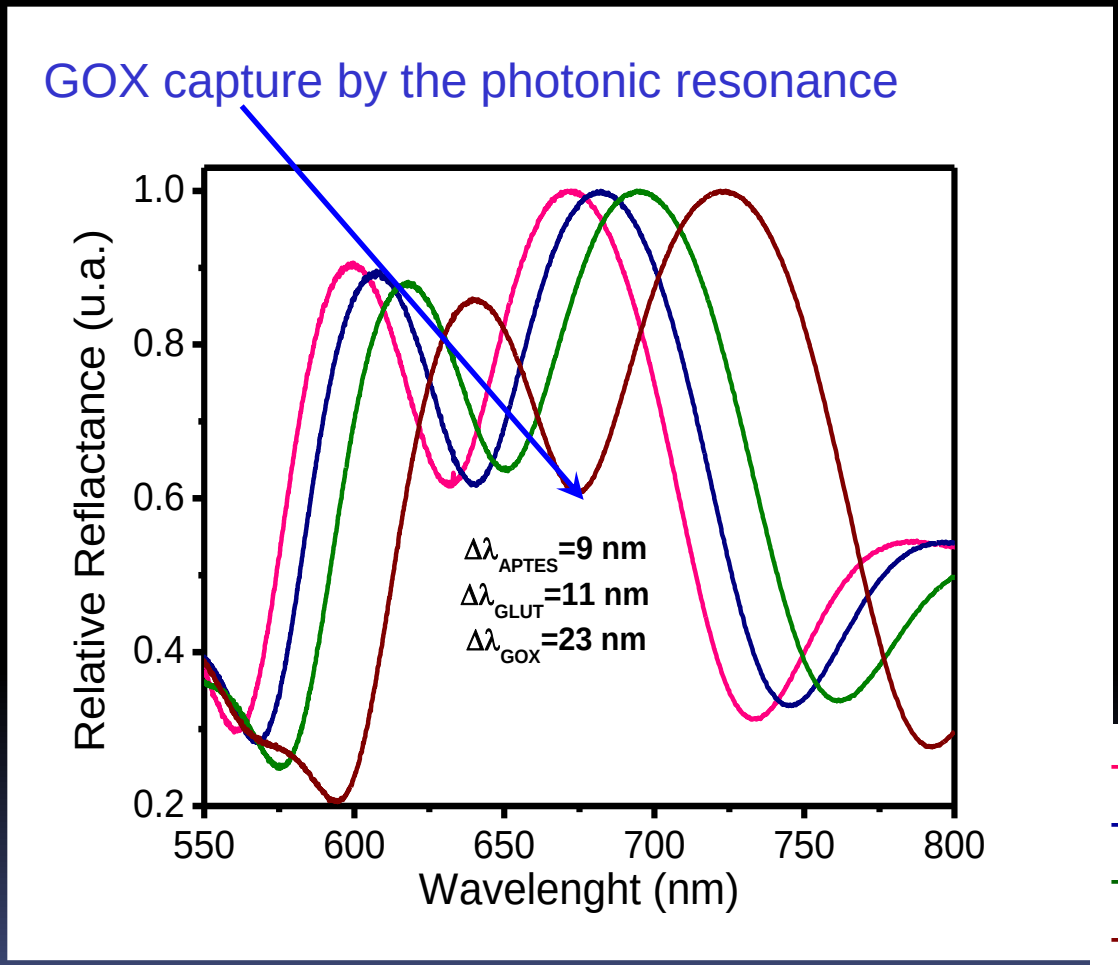

PSi Microcavity

ext pore : 400-4000nm

-- pSi after themal oxidation
-- pSi + APTES (silanization)
-- pSi + APTES + Glu
-- pSi + APTES + Glu + GOX

A functional GOX-Psi sensor has been obtained

Dose response curve

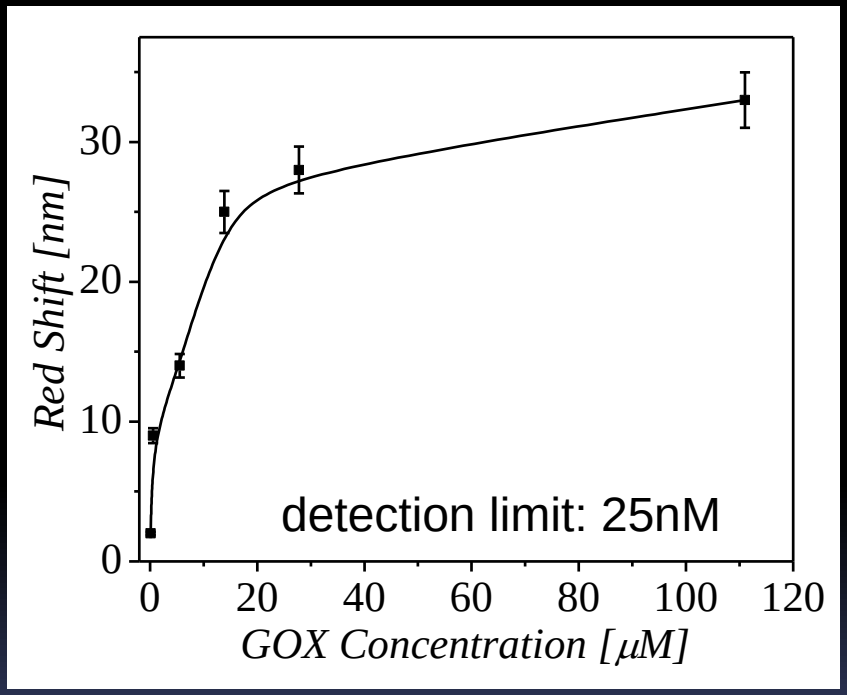

Enzymatic acitivity of the adsorbed GOX

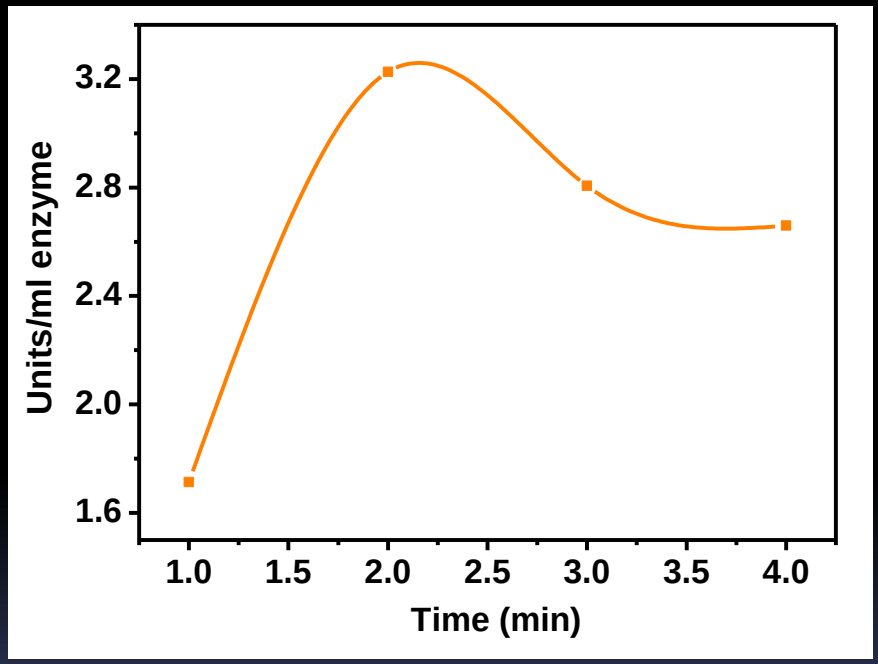

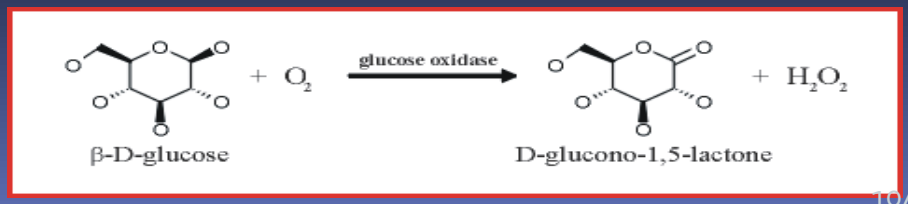

PSi mirror and microcavity structures enhance GOX fluorescence response

Green natural fluorescence of Glucose Oxidase:

λ_{exc} = 450nm – FAD (low emission intensity in solution)

Monolayer | **Mirror** | **Microcavity**

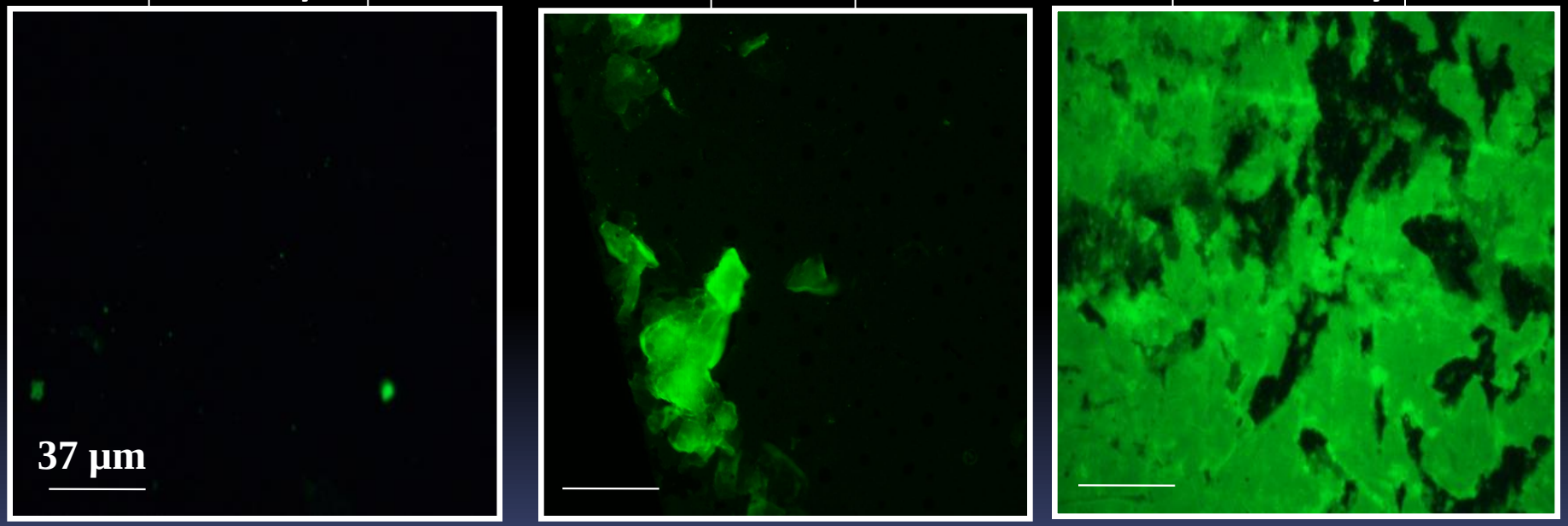

	Monolayer	Mirror	Microcavity
Integrated density	**51.96**	**116.58**	**2042.5**

G. Palestino et al. (2008) *Langmuir*

Correlation between photoluminescence of GOX and the cavity mode

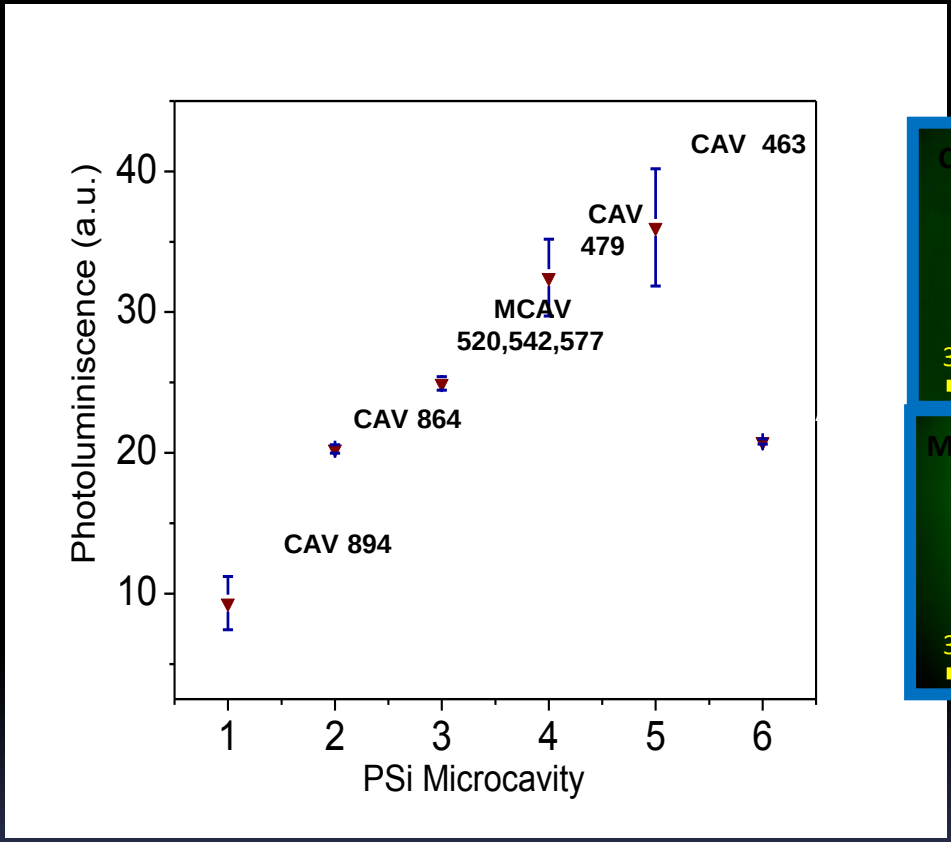

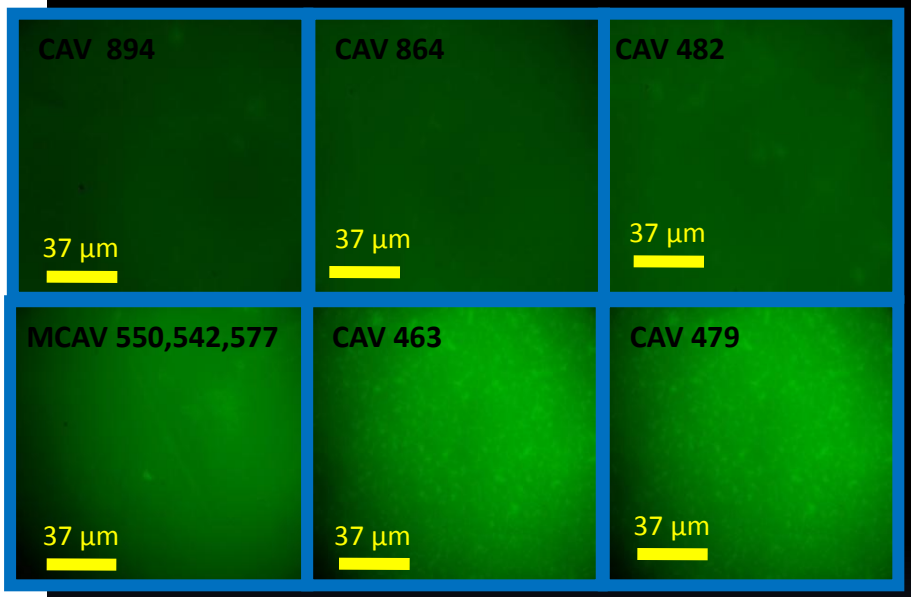

GOX ex: 452-465 nm
em: 520-530nm

CAV no – microcavity mode
MCAV – microcavity with multiple resonance modes

PSi

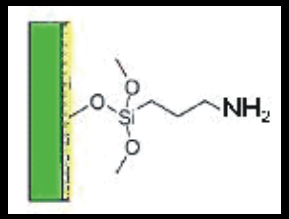

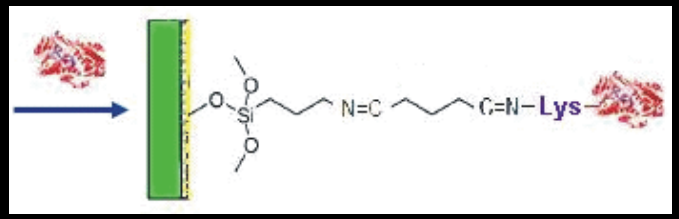

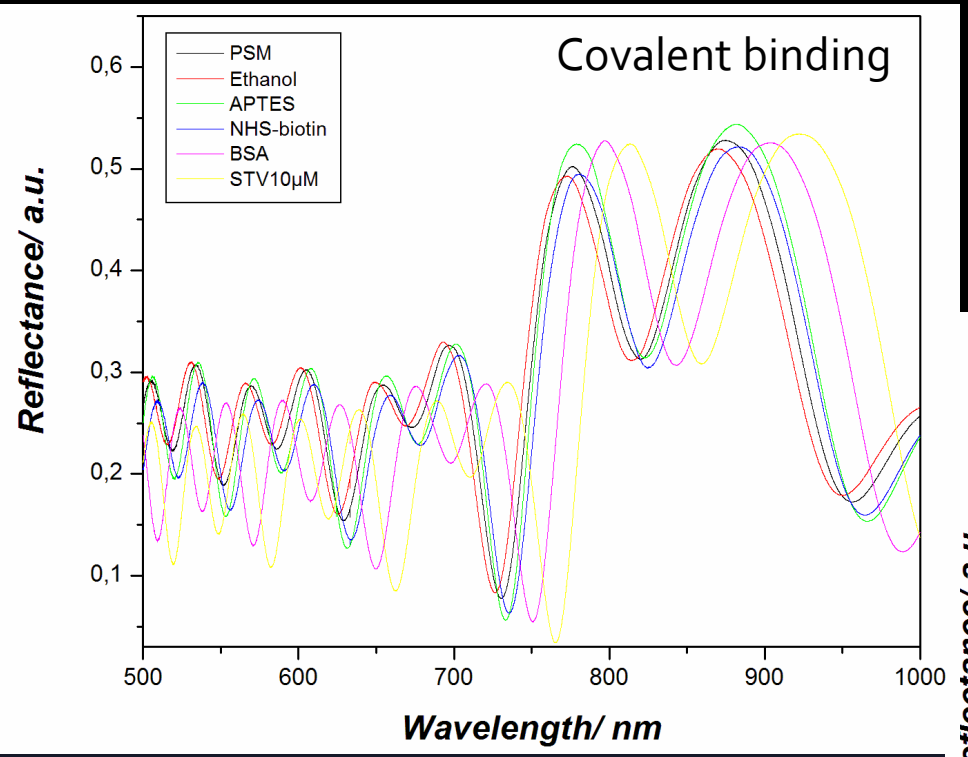

Capture of Streptavidin via Biotin- PSi MC

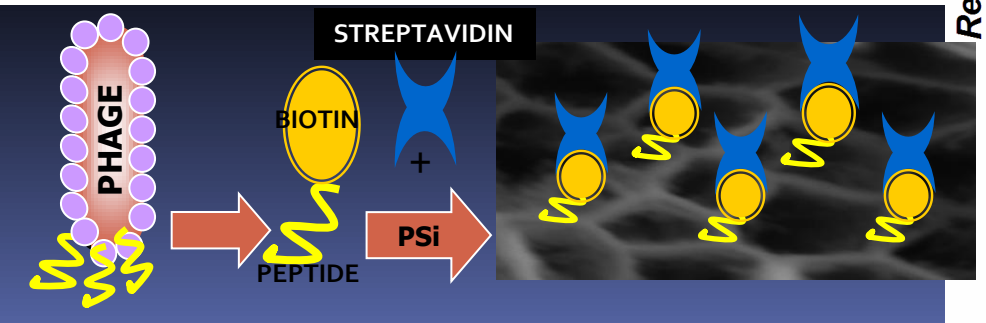

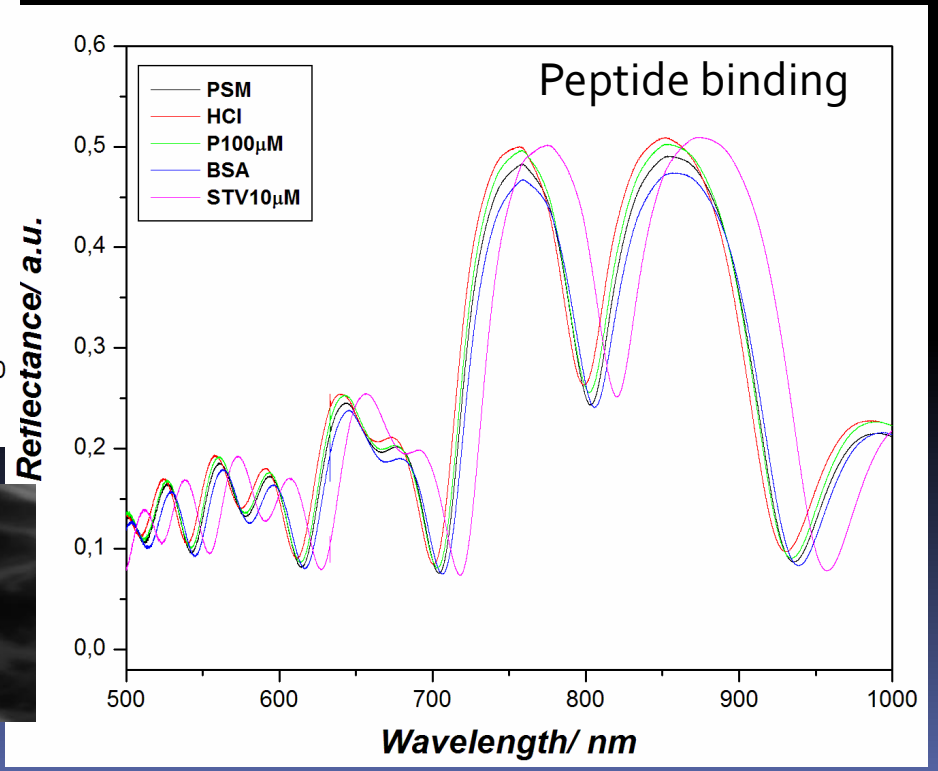

Materials Views
www.MaterialsViews.com

ADVANCED FUNCTIONAL MATERIALS
www.afm-journal.de

Peptides for the Biofunctionalization of Silicon for Use in Optical Sensing with Porous Silicon Microcavities

*Elias Estephan, Marie-Belle Saab, Vivechana Agarwal, Frédéric J. G. Cuisinier, Christian Larroque, and Csilla Gergely**

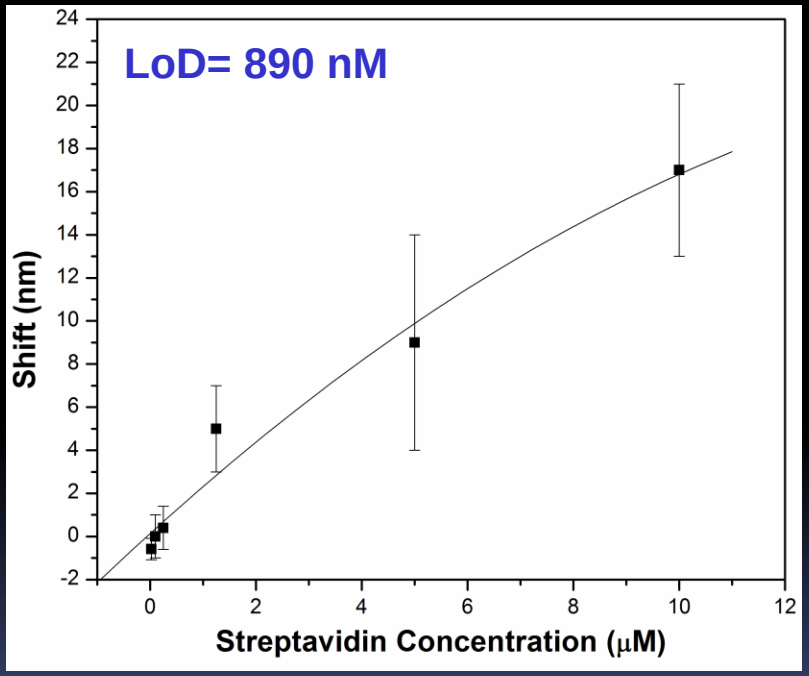

The limit of detection via PSi microcavities is greatly enhanced by the peptide binding

→ **Functionalization VIP !!!**

Dose response curve: covalent / peptide

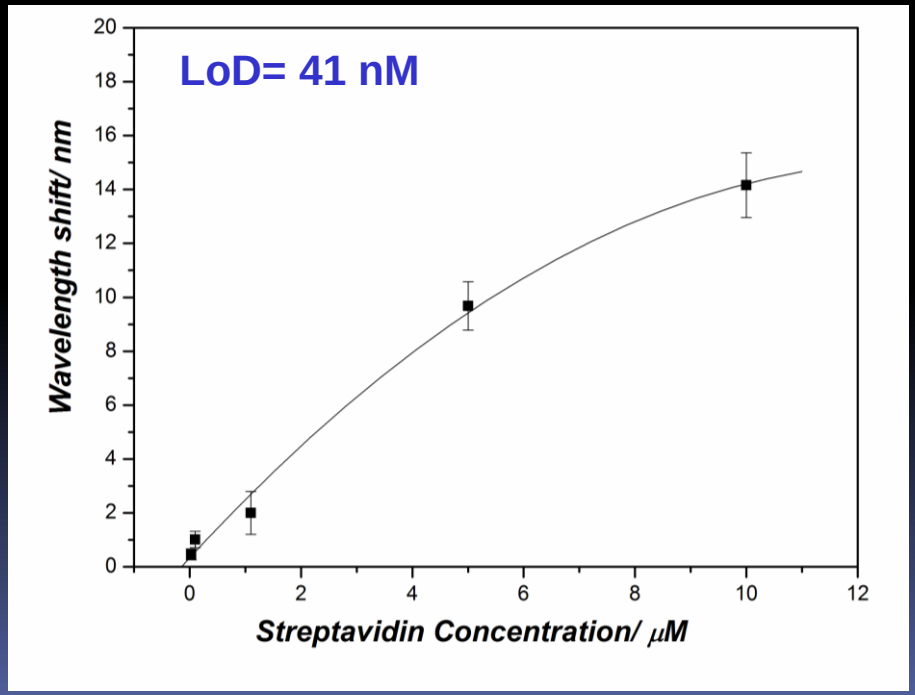

E. Estephan et al. Adv. Funct Mat. 2011

PSi photonic crystal:

capable of controlling light within the structure analogous to the way that semiconductors transmit electricity through computer chips

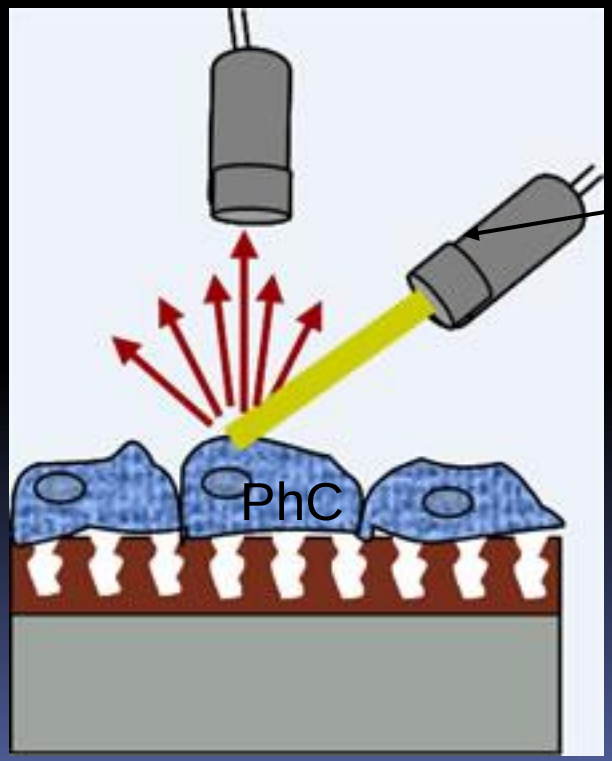

measuring the scattering of light with a sensitive spectrometer

detect small changes in the shapes of liver cells as they reacted to toxic doses of cadmium

M. Sailor, USC San Diego

GaAs/ AlGaAs photonic crystal

0.6 μm GaAs patterned core

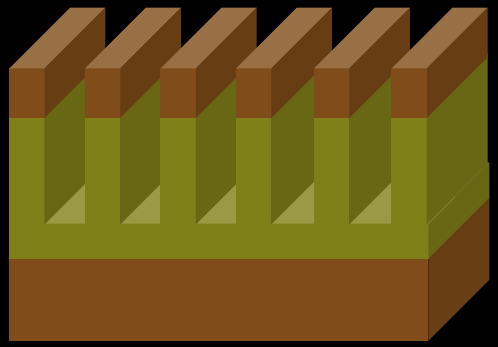

1.1 μm AlGaAs patterned cladding

GaAs substrate

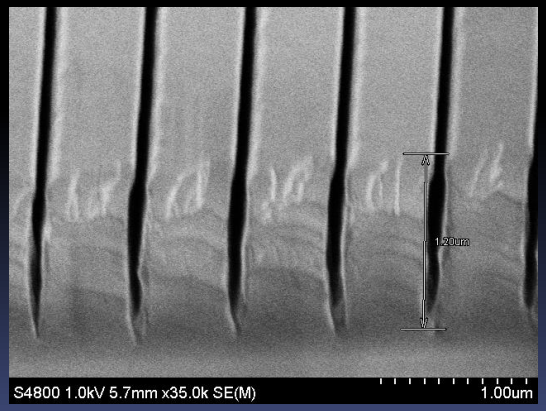

SEM image shows 1.7 μm etch depth

Sharp photonic resonances in simulated spectra

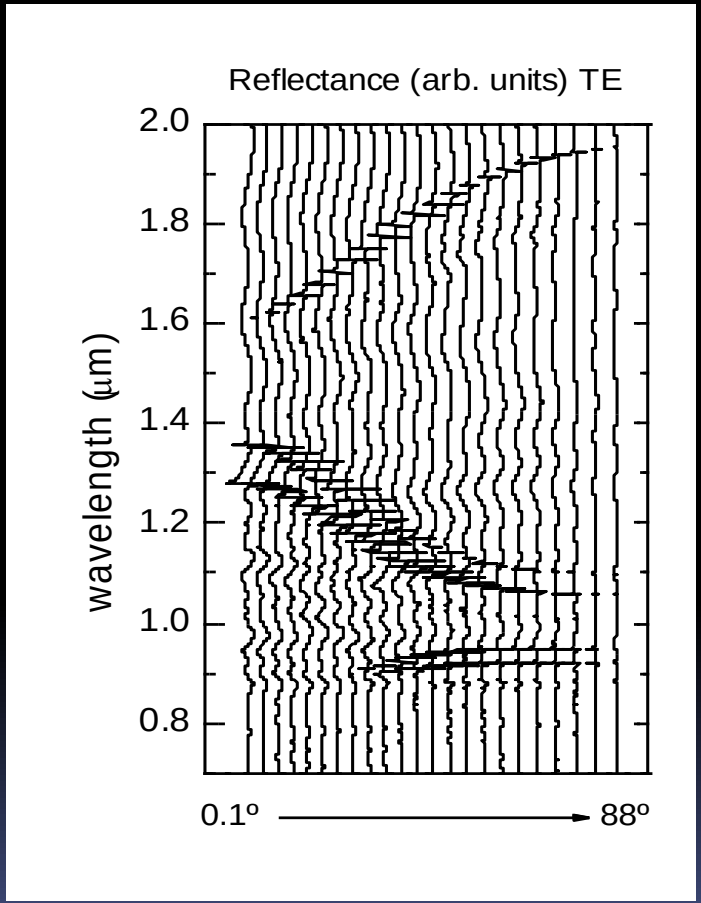

Electron beam lithography by the technological "nanostructuring platform" within the Network of Excellence (ePIXnet)

Aim : molecular detection of the recognition event by photonic modes

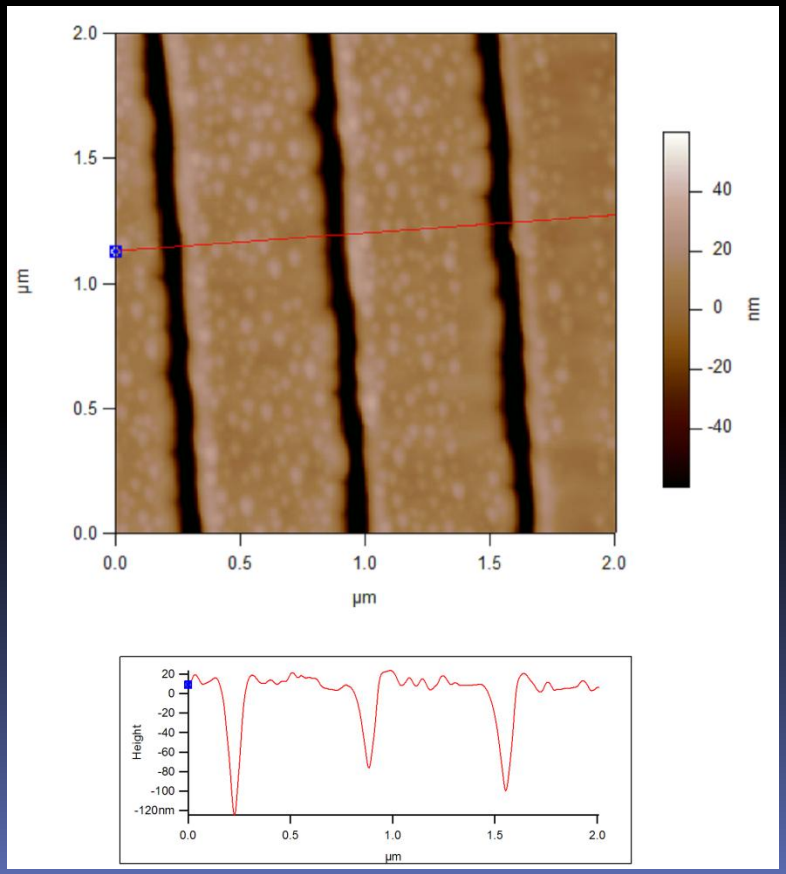

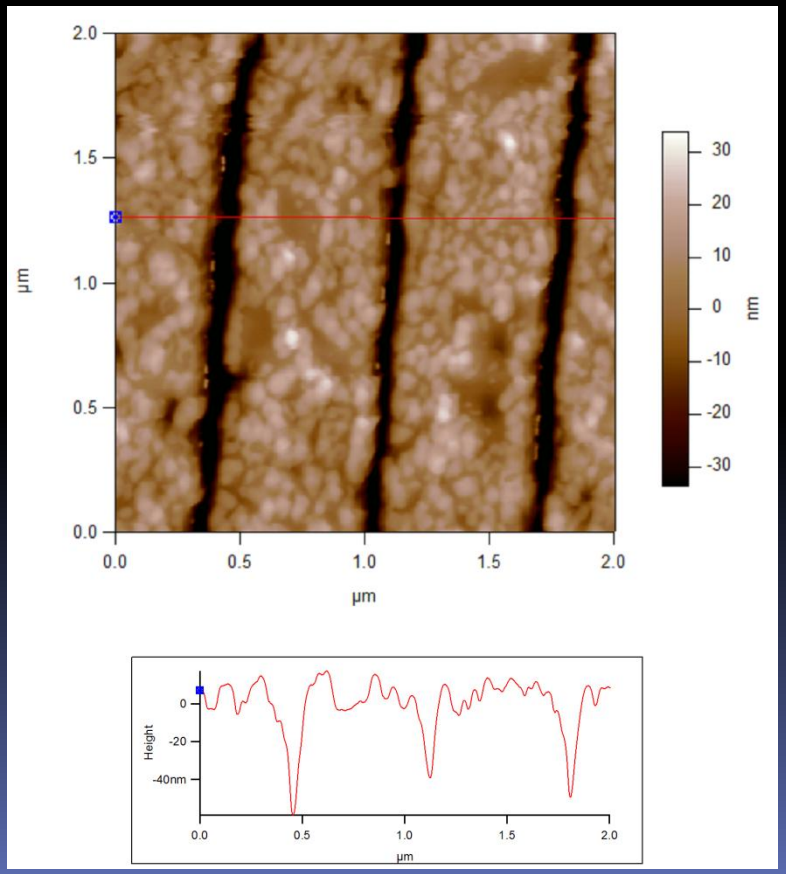

Characterization by optical reflectance

Linear optics characterization shows well defined photonic modes,

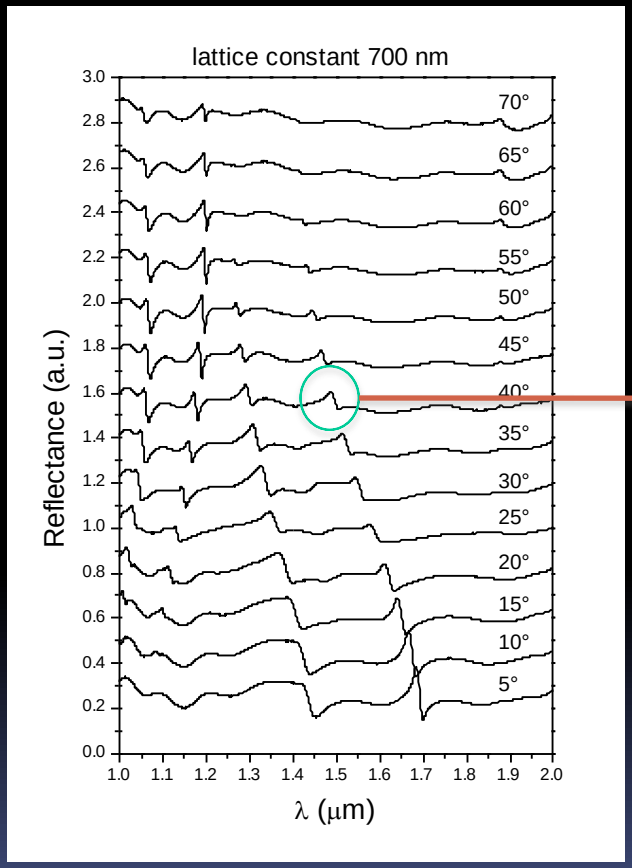

However,
no changes in the linear resonances after deposition of biotin and streptavidin

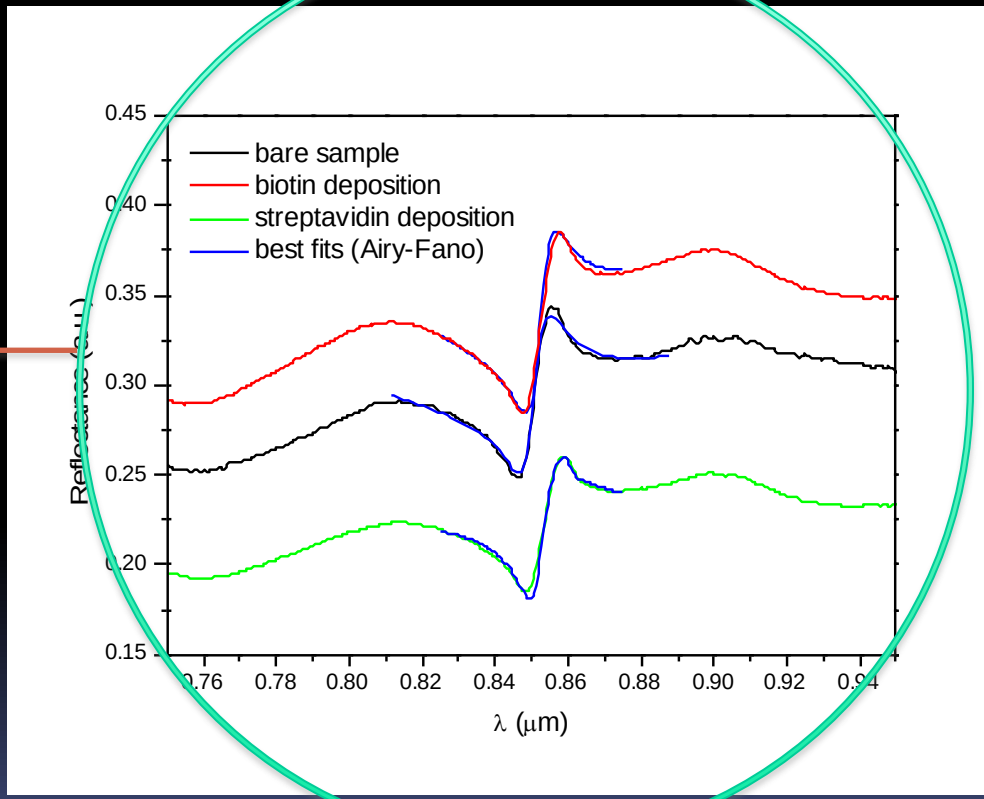

PhC + peptide

Biotin --- + Streptavidin

GaAs/AlGaAs PhC

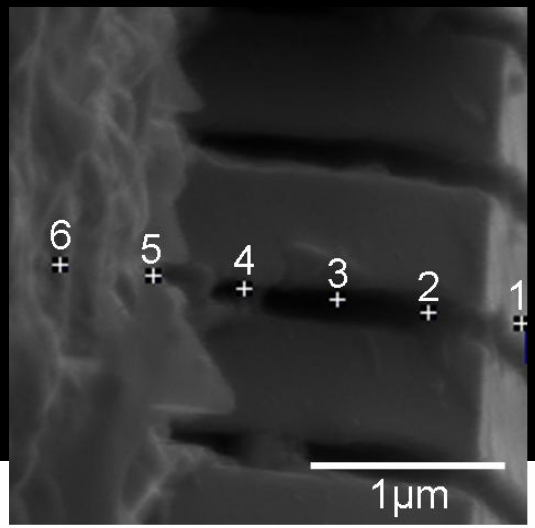

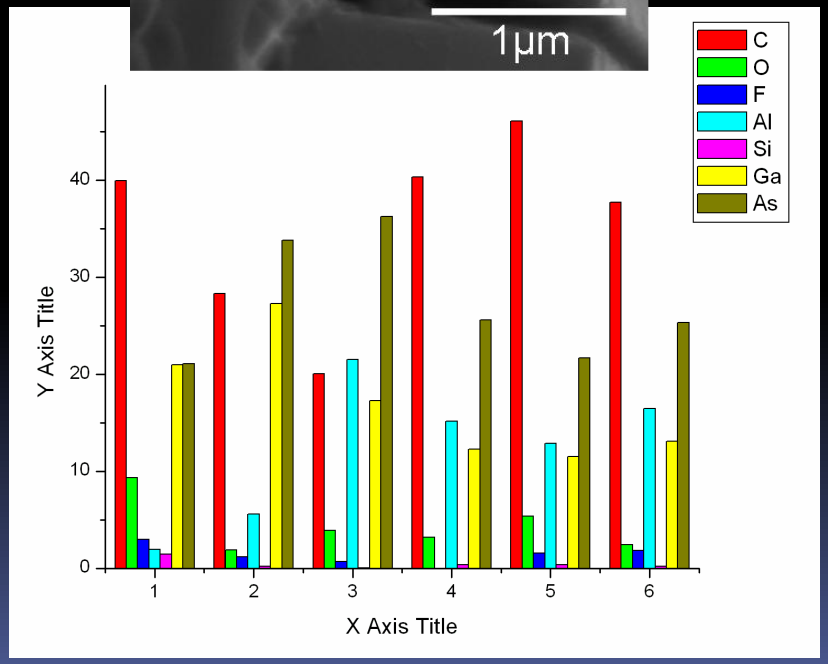

GaAs/AlGaAs PhC + peptide + STV

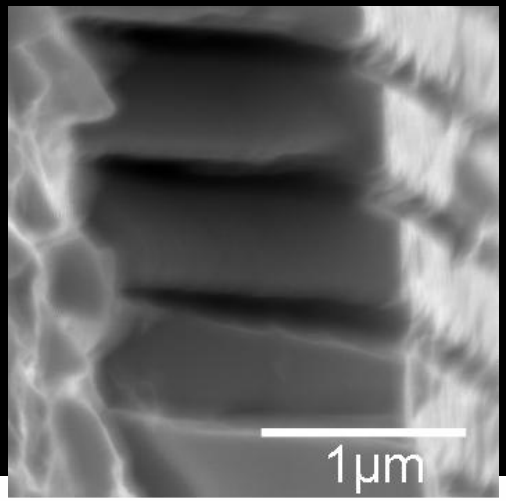

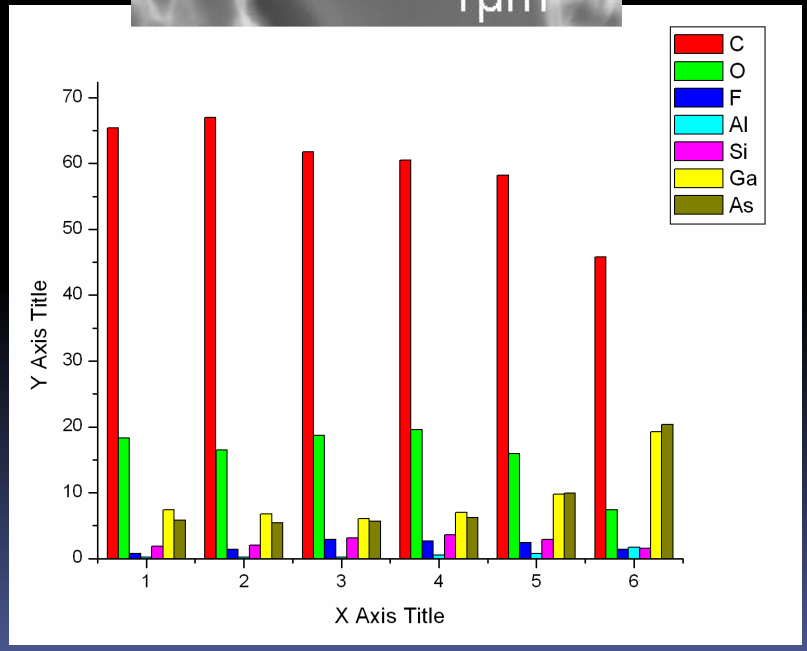

SEM images (section view) and EDX analyses

Second harmonic characterization

Streptavidin shows SH generation
in addition to GaAs (100)

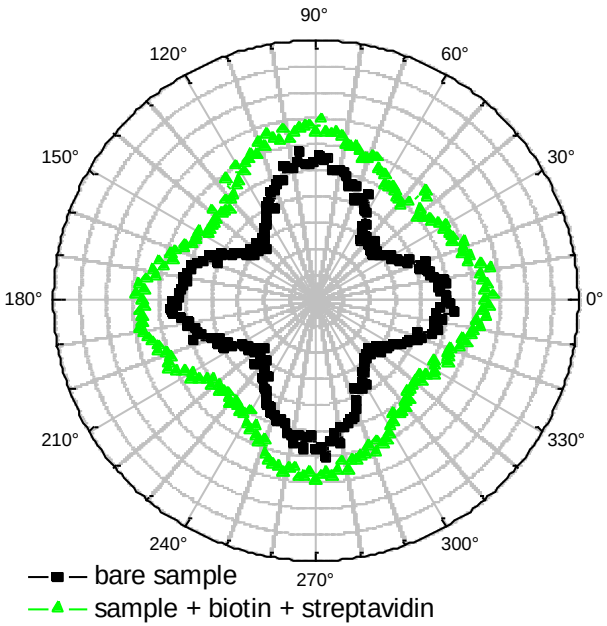

angle tuning allows exploring of photonic bands
via second harmonic generation

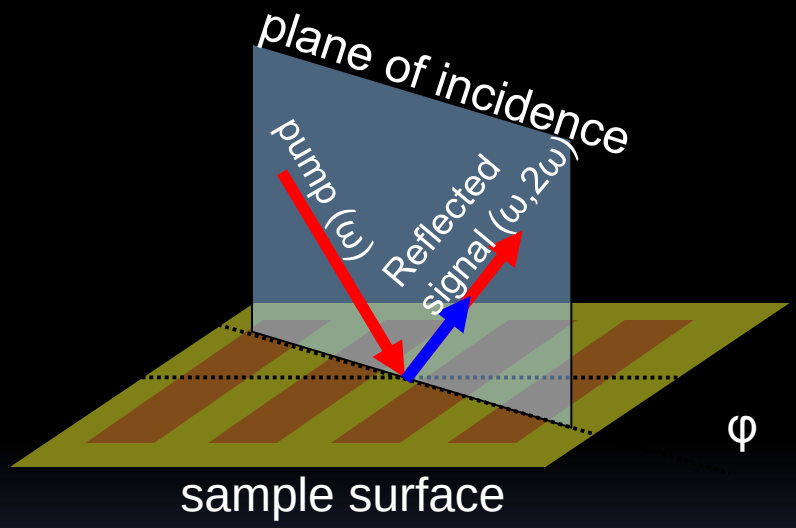

laser source:
OPO, 1.550μm, 120 fs, 20 μW, 80 MHz

→ SHG – Good probe for monitoring molecules capture due to dipoles orientation when adsorption from liquid occurs

E. Estephan et al. 2010 Langmuir

SHG results by angle tuning

harmonic signal detected in reflection

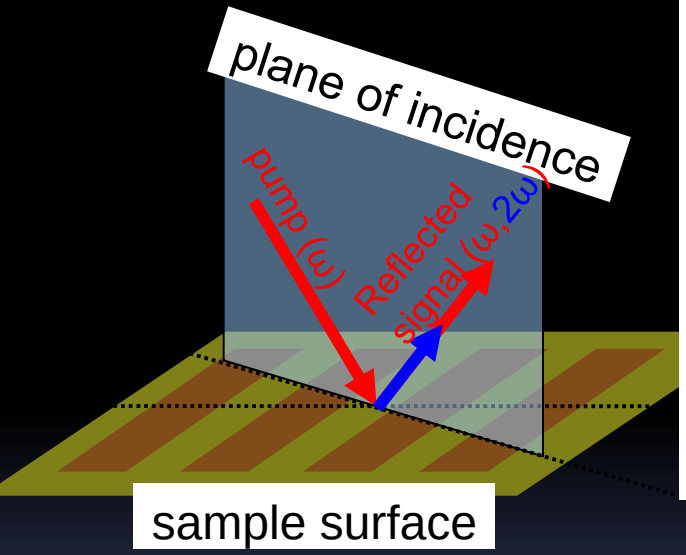

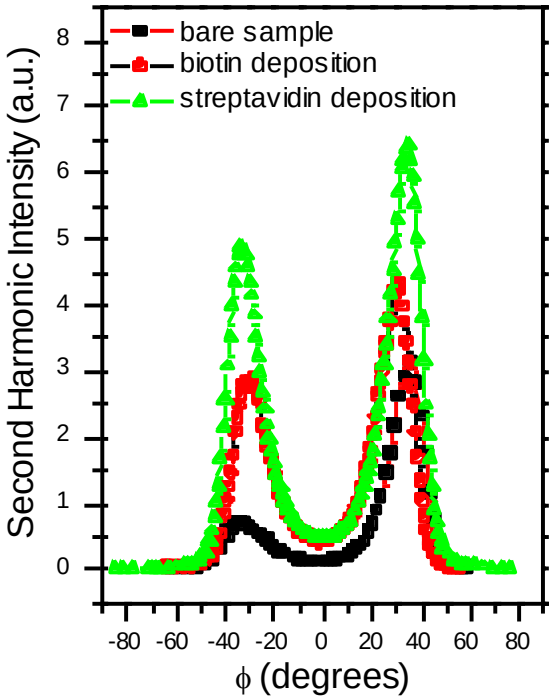

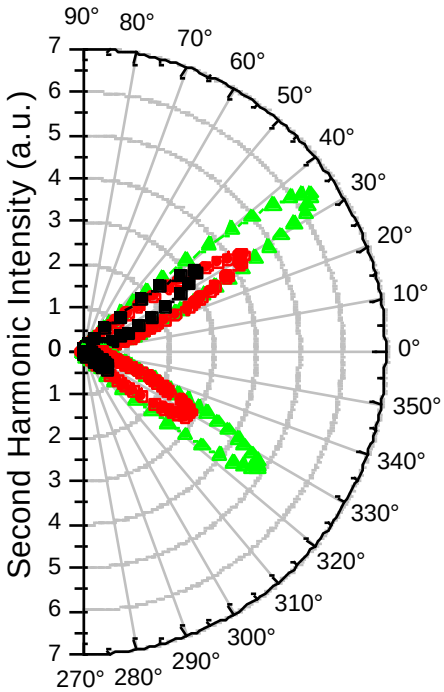

In contrast with linear spectroscopy,
deposition of biotin and then streptavidin enhances considerably the intensity of the second harmonic signal
Signal is further increased by resonant geometry

Molecular adsorption measured as non-linear signal

→ Femtomolar detection

Evanescent wave sensing

Optical waveguide lightmode spectroscopy

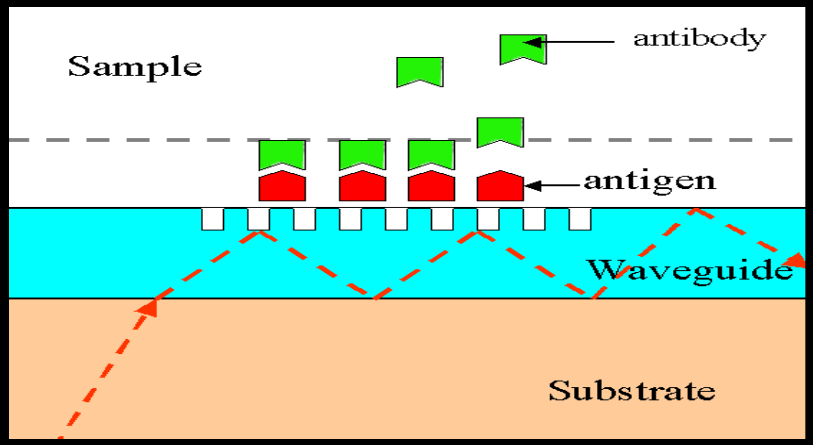

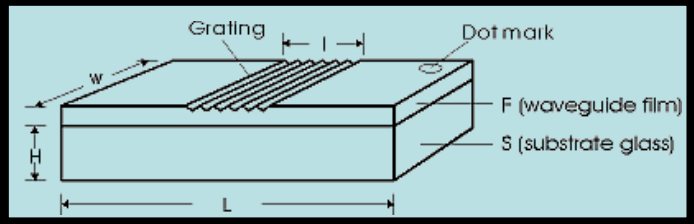

Input grating sensor: **waveguide** (SiO_2-TiO_2, n=1.8) Microvacuum Ltd

Coupling equation

$$N = n\sin\alpha + \frac{l\lambda}{\Lambda}$$

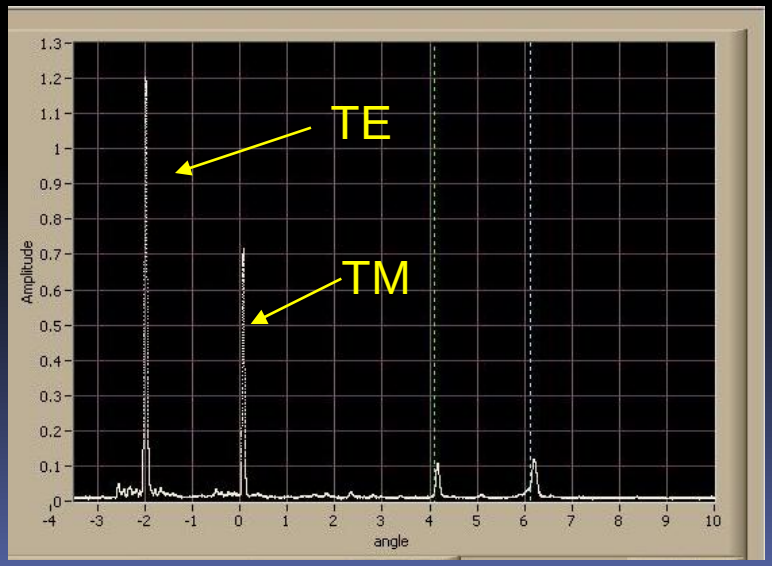

Tiefenthaler and Lukosz, 1982

4 layer mode equation:

$$2k_{z,F} + \Phi_{S,F} + \Phi_{F,A} = 2\pi m$$

The phase shifts at interfaces:

$$\Phi_{F,S} = -2\arctan\left(\frac{n_F^{2\rho} s}{n_S^{2\rho} f}\right)$$

$$\Phi_{F,A,C} = -2\arctan\left[\frac{n_F^{2\rho} a}{n_A^{2\rho} f} \frac{\frac{c}{n_C^{2\rho}} + \frac{a}{n_A^{2\rho}}\tanh(k_0 a d_A)}{\frac{a}{n_A^{2\rho}} + \frac{c}{n_C^{2\rho}}\tanh(k_0 a d_A)}\right]$$

Solutions:

(for thin and thick layers)

n_A ; d_A - refractive index, thickness of the adlayers

$\Gamma = (dn/dc)^{-1} (n_A - n_C) d_A$
– adsorbed quantity in μg/cm²

C. Gergely et al. 2004 Langmuir, 20, 557

In situ monitoring adsorption of molecules on surfaces by OWLS

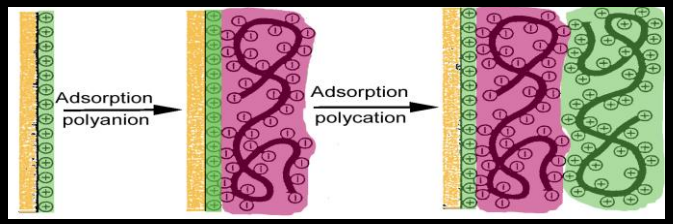

+

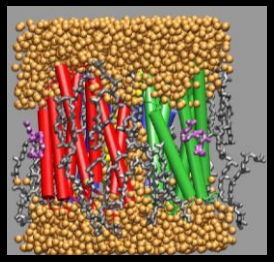

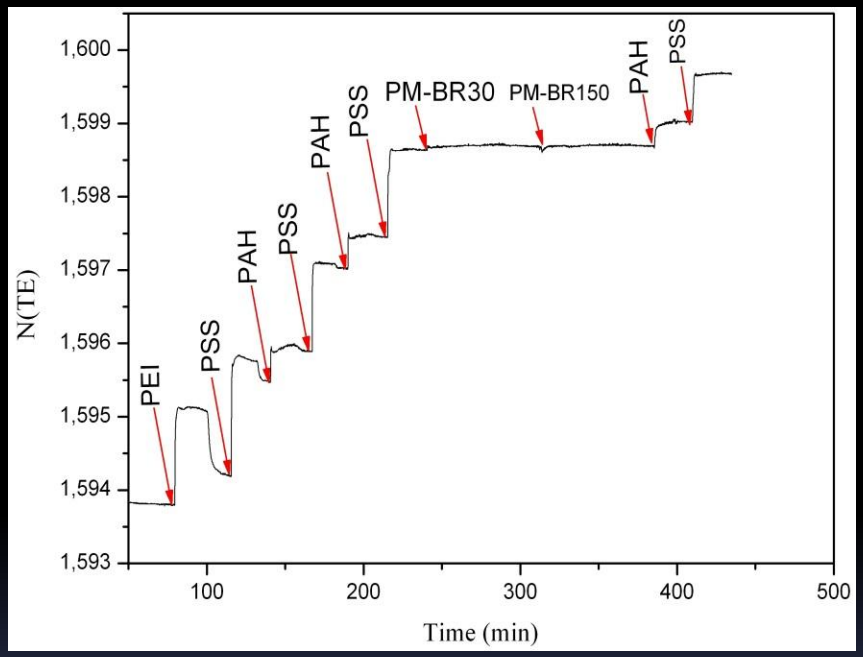

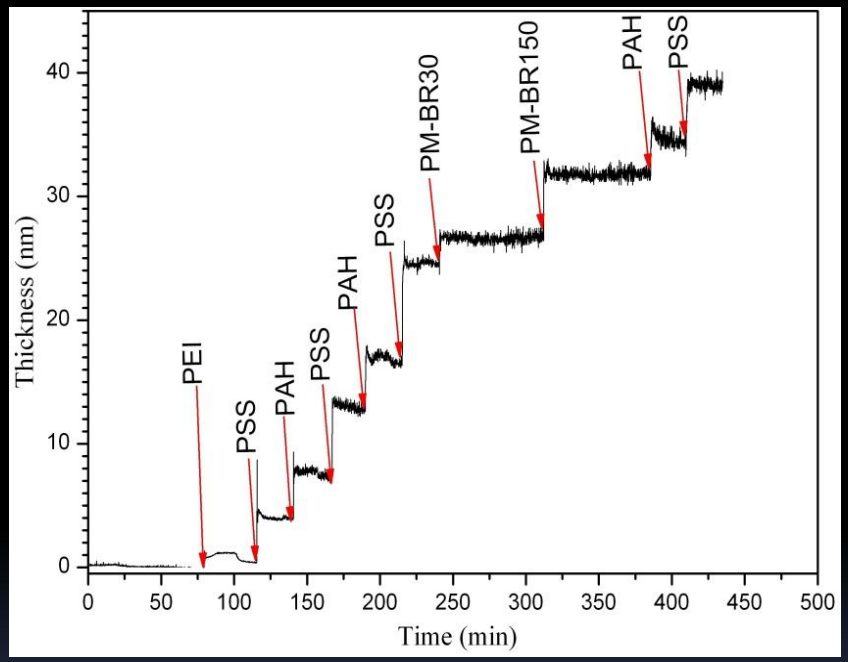

Changes of the effective refractive index of the transverse electric mode (N_{TE}) and the corresponding layer thicknesses upon buildup of PEI-(PSS-PAH)$_2$-PSS-PMBR$_{30}$-PMBR$_{150}$-PAH-PSS matrix

C. Gergely et al 2007 Biomacromolecules 8, 2228

OWLS studies in function of BR concentration and ionic strength

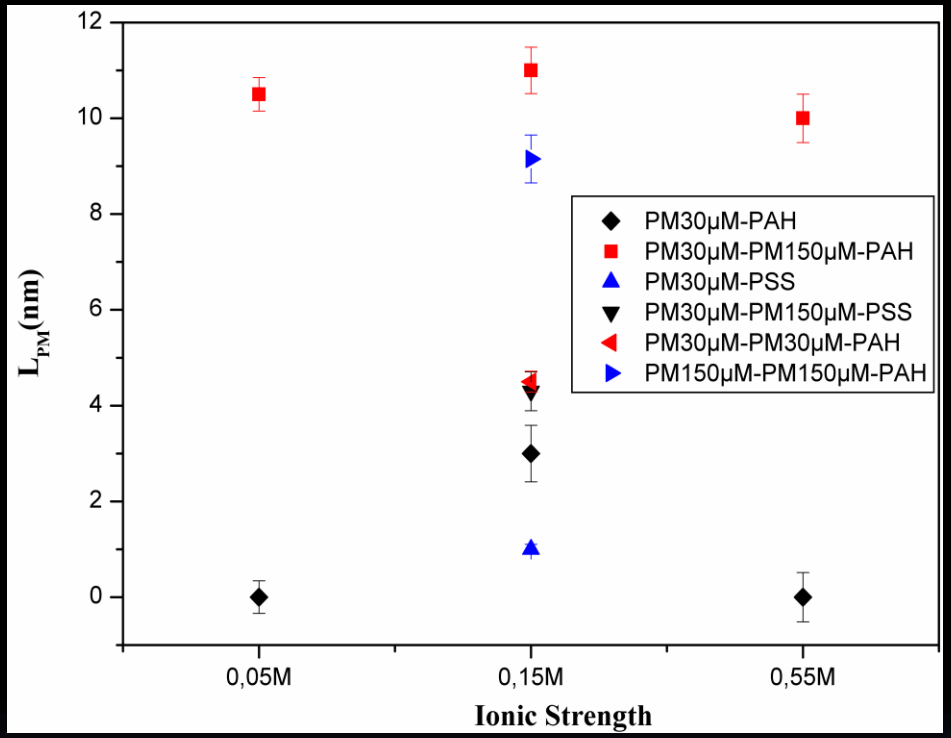

BR containing PM's adsorb in an oriented way in a double (on PAH^+) or a single layer (on PSS^-)

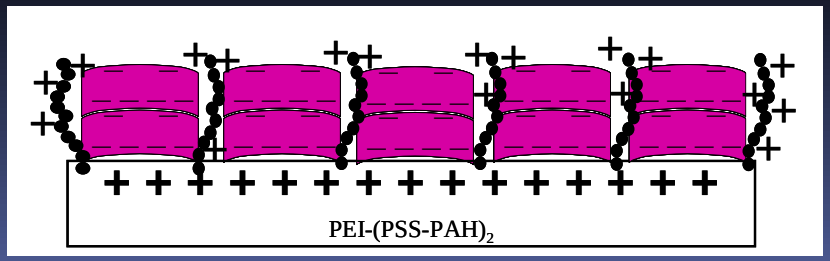

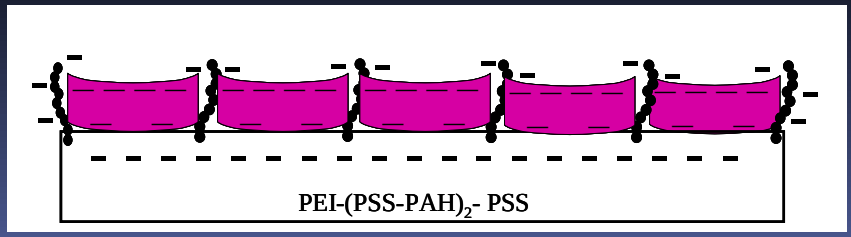

M.b. Saab et al, Langmuir 25, 2009

Reversed symmetry waveguides

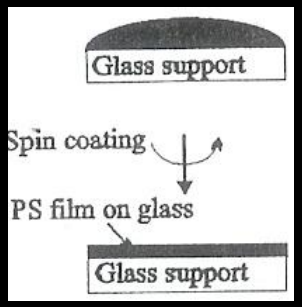

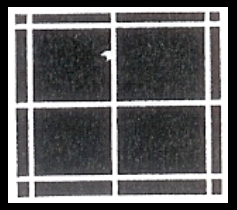

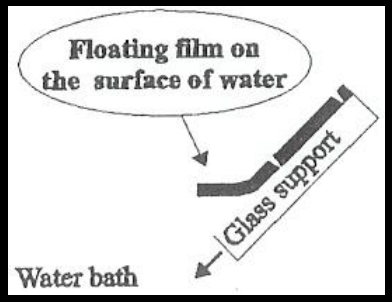

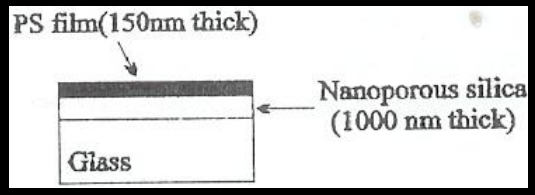

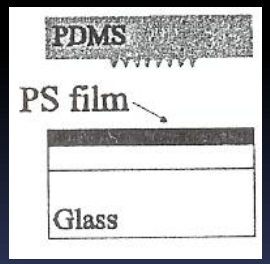

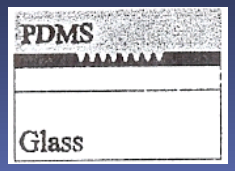

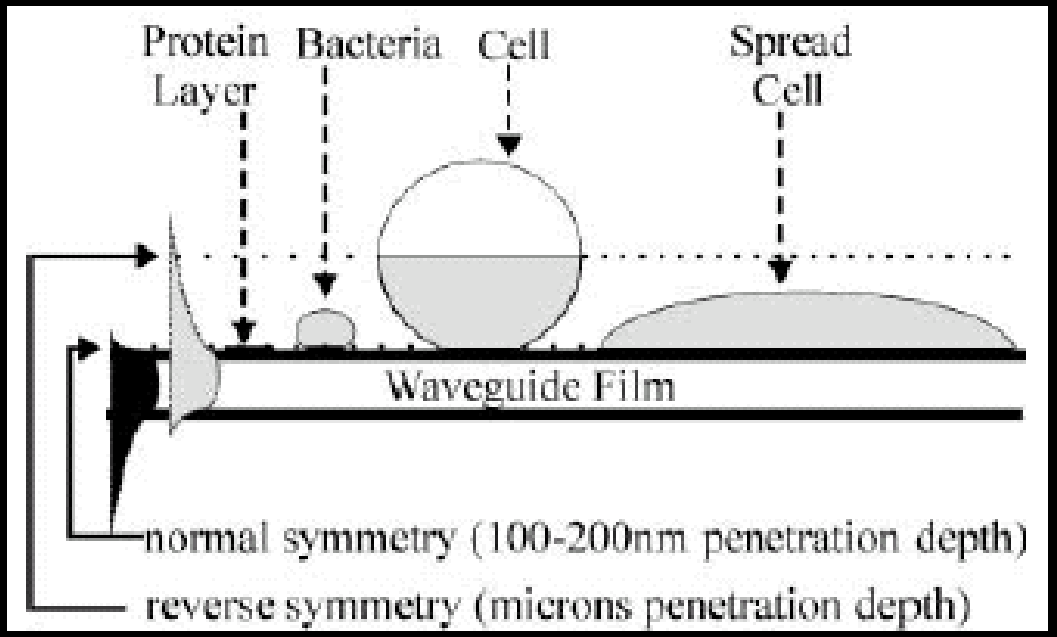

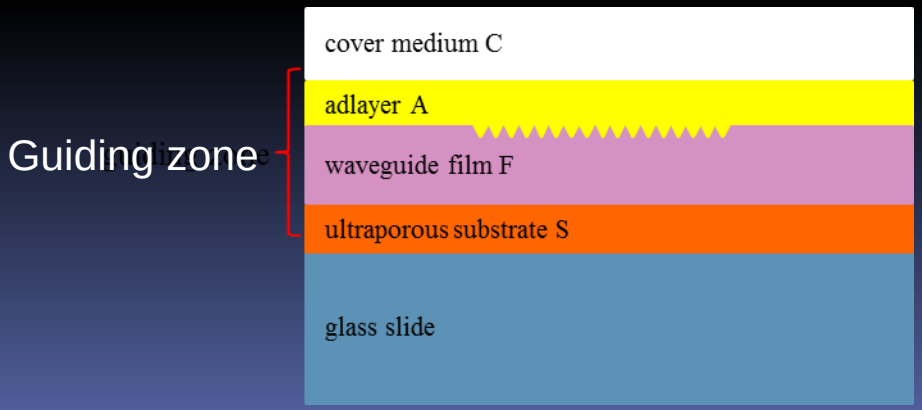

R. Horvath, APL 2005

Towards hybrid photonic devices

SHG in bare Porous Silicon microcavity

MPM monitors at different focal depths within the PSiMc

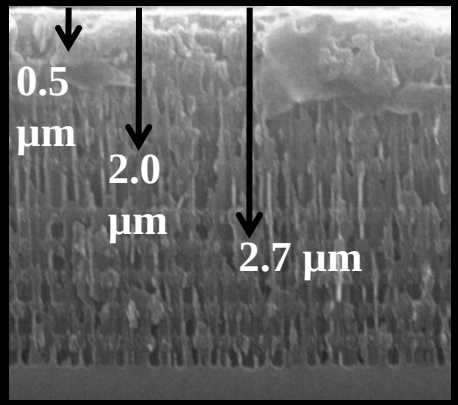

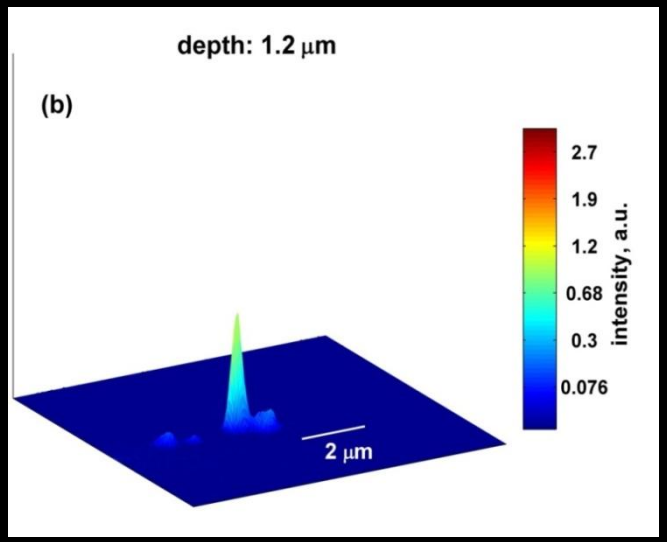

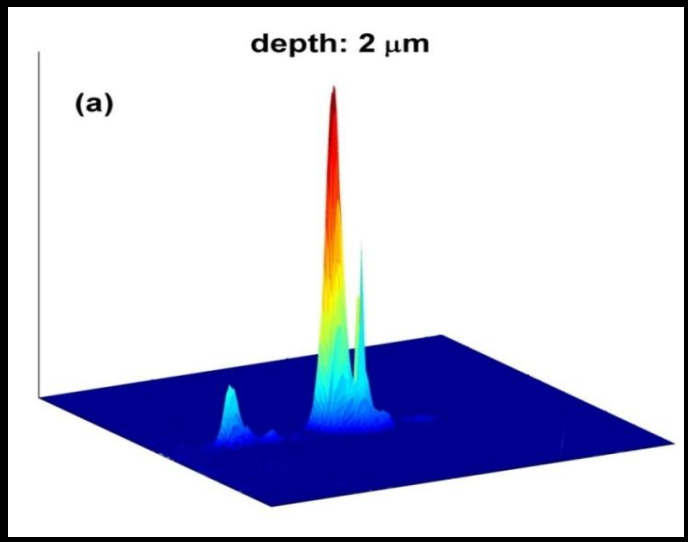

SHG enhancement in PSi (**centrosymmetric material**): fundamental field confinement in the cavity combined with the phase matching in the periodic MC structure

Necessary condition : **fundamental wave resonance with the cavity mode**

Reflectance spectra of PSiMc vs. SHG and GOX fluo.

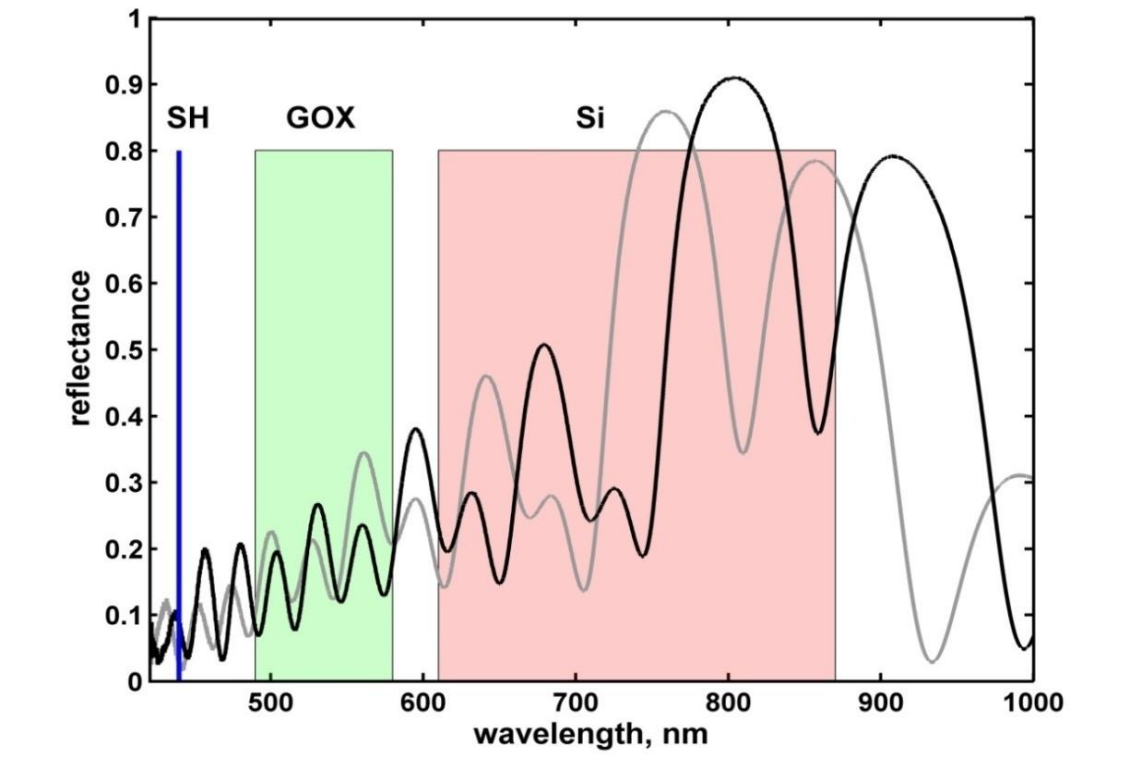

The PSiMc structure is transparent for the SHG and the GOX photoluminescence

Hybrid organic/inorganic photonic devices

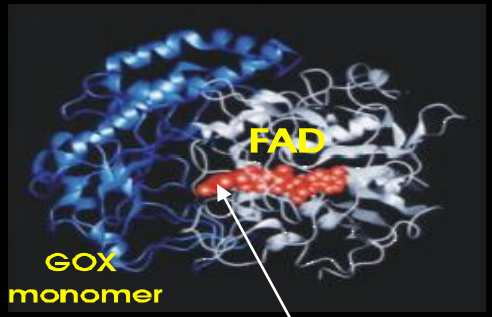

GOX → SHG

PSi microcavity

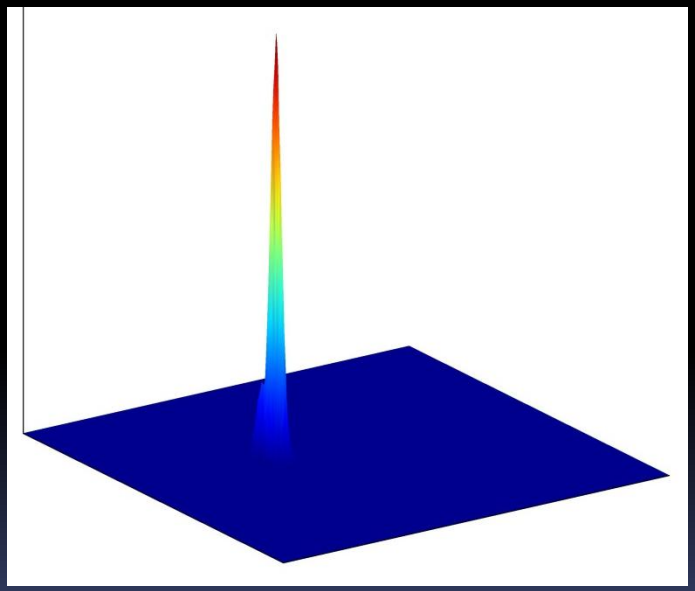

PSi microcavity + GOX

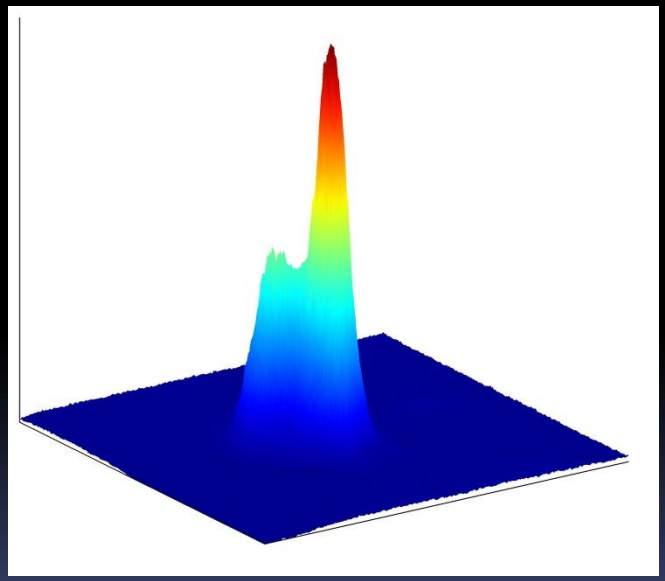

Enhanced 2PEF and SHG emission

-ndividual pores, thus better detection limit

PSiMc infiltrated with GOX at different focal depths as monitored by multiphoton microscope

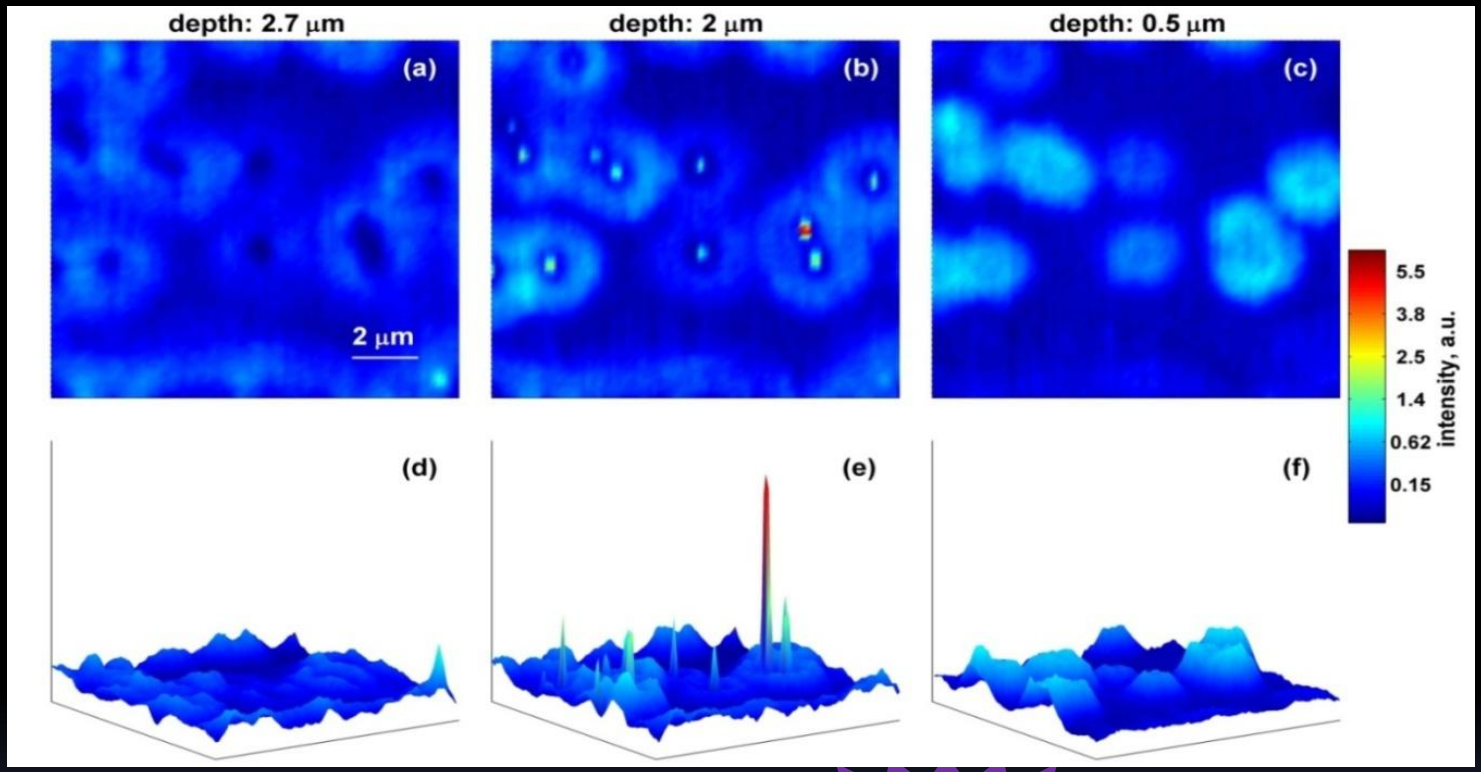

The components of the emission

Ti-sapphire laser (880 nm)

Second Harmonic Generation 440 nm

2Photon FAD emission 525 nm

APPLIED PHYSICS LETTERS 94, 223313 (2009)

Three-dimensional spatial resolution of the nonlinear photoemission from biofunctionalized porous silicon microcavity

M. Martin,[1] G. Palestino,[1,2] T. Cloitre,[1] V. Agarwal,[3] L. Zimányi,[4] and C. Gergely[1,a)]
[1]*Groupe d'Etudes des Semiconducteurs, UMR 5650 CNRS, Université Montpellier II, 34095 Montpellier Cedex 5, France*

PSi microcavity

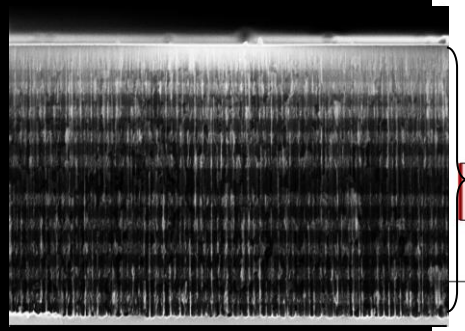

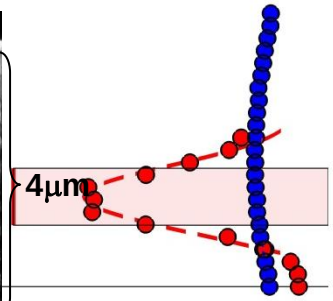

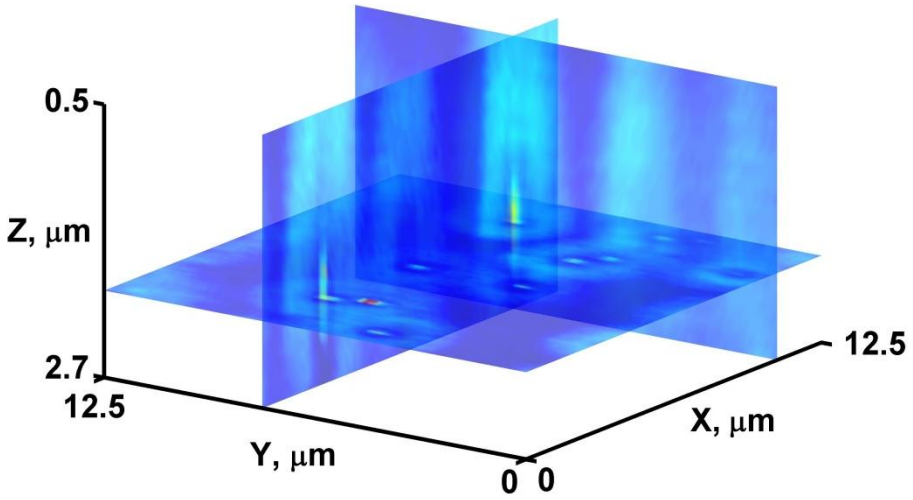

emission intensity averaged over the rings and spots in the center rings

the source of the intense center emission identified within the cavity

M. Martin et al. Appl.Phys.Lett. 94 (2009)